Droughts in western Central Europe and associated atmospheric circulation patterns since 1844

Emile Neimry[1], Hugues Goosse[1], Mathieu Jonard[1]

[1] Earth and Life Institute, Université catholique de Louvain, Louvain-la-Neuve, Belgium

Correspondence to: Emile Neimry (emile.neimry@uclouvain.be)

Abstract. Droughts in western Central Europe have major impacts on agriculture, ecosystems, and society, yet their long-term variability and drivers remain poorly understood. This study investigates drought variability over the past 180 years and its link to atmospheric circulation to identify their dynamic drivers.. Three reanalysis datasets (ERA5, 20CRv3, and ModE-RA)), evaluated against long weather station observations, are used to detectidentify meteorological drought events via the 3-month Standardized Precipitation (Evapotranspiration) Indexes (SPI-3 & SPEI-3)), and to connectrelate them to atmospheric circulation patterns through k-means clustering. Dataset reliability is assessed over western Central Europe, providing consistent coverage from 70 to 165 years. of 500 hPa geopotential height anomalies. Results show that recent severe and successive droughts, such as the 2018 drought, have historical precedents and display strongoccur within pronounced multidecadal variability. Diverging trends between SPI-3 and SPEI-3 over the last decades indicate an Yet the 2010s emerge as the driest decade when assessed with SPEI-3, a feature that disappears when only precipitation is considered, highlighting the increasing rolecontribution of atmospheric evaporative demand (AED). Summer dryness has intensified over the past 180 years) to drought severity. Although annual SPEI-3 exhibits no long-term trend, increasing AED has progressively offset increasing precipitation, leading to contrasting seasonal responses with autumn and winter becoming wetter, whereas winter dryness has declined. Regionalsummer and seasonal contrasts further emphasize the complexity of drought dynamics., more recently, spring becoming drier. Four distinctrecurrent circulation patterns associated with droughts in western Central Europe are identified: the Baltic High, British Isles High, North–South Dipole, and European High. Over time, droughtsDroughts have become increasingly linked toassociated with the European High, a pattern characterizedcharacterised by strong anticyclonic anomalies, large positive AED anomalies, and intense droughts, and this had a central role in the recent spring drying. The findings highlightproviding a dynamical explanation for the recent emergence of circulation patterns that enhance AED, marking a shift in the dynamic drivers of regional droughts under climate changespring drying.

a mis en forme : Correspondence, Espace Après : 0 pt

a mis en forme : Couleur de police : Automatique

a mis en forme : Couleur de police : Automatique

1 Introduction

Drought is a recurring climate phenomenon worldwide, with growing concern in Europe due to the increase in drought events observed over recent decades (Spinoni et al., 2019; Ionita et al., 2020, 2021). Droughts are the most significant environmental hazard in terms of both economic losses (Spinoni et al., 2016; Stahl et al., 2016; Cammalleri et al., 2020; Mens et al., 2022), and human fatalities through famine and disease (Bruce, 1994; Obasi, 1994; Guha-Sapir et al., 2004; Maslin et al., 2025). Both urban and rural environments are highly vulnerable, with particularly severe impacts on agriculture and forest ecosystems (e.g. Choat et al., 2012; Tapia et al., 2017; Vogel et al., 2019).

Despite extensive research, substantial uncertainties remain regarding long-term drought trends. At the global scale, meteorological droughts showed limited evidence of long-term changes since the early to mid-20th century (Sheffield et al., 2012; Spinoni et al., 2014; Vicente-Serrano et al., 2022). Across Europe, drought trends remain difficult to assess because strong multidecadal precipitation variability can obscure long-term signals (Hänsel et al., 2019; Oikonomou et al., 2020). Central Europe represents a particularly uncertain region. Some studies describe this region as a transition zone between drying trends in Southern Europe and wetting trends in Northern Europe since the mid-20th century (Spinoni et al., 2015, 2017, 2018), while others identify Central Europe as part of a broader drying trend (Ionita and Nagavciuc, 2021). While part of the disagreement arises from the differences in spatiotemporal coverage and drought metrics employed (e.g. Freund et al., 2023; compared with Bebchuk et al., 2025), another part originates from the contrasting seasonal responses. While seasonal trends remain sensitive to the definition of the seasons (Hänsel et al., 2019), there is broad agreement that drought conditions intensified during spring and summer across much of Central Europe over the last three to four decades (e.g. Ionita et al., 2020; Philip et al., 2020; Hänsel et al., 2022). In contrast, drought conditions generally weakened during autumn and particularly in winter (e.g. Moberg and Jones, 2005; Hänsel et al., 2009; Spinoni et al., 2017).

Drought variability in Central Europe results from complex interactions between dynamic and thermodynamic processes, whose relative contributions remain uncertain and vary across seasons (van Haren et al., 2013; Suarez-Gutierrez et al., 2020; Hoffmann and Spekat, 2021; Brönnimann et al., 2025). During winter, atmospheric circulation dynamics are hypothesised to dominate, whereas in summer, land–atmosphere feedbacks may play a larger role (Haslinger et al., 2019; Haslinger and Mayer, 2023). Dry conditions over Central Europe are commonly associated with anticyclonic circulation, south-to-easterly winds, and reduced inflow of moist air from the Atlantic (Trnka et al., 2009; Lhotka et al., 2020; Bešťáková et al., 2024). In addition, drought variability has been linked to large-scale circulation features such as the jet stream and teleconnection patterns (e.g. Van Oldenborgh et al., 2000; Brönnimann, 2007; Svensson and Hannaford, 2019; Kim et al., 2023), particularly the North Atlantic Oscillation (NAO) (Hurrell and Van Loon, 1997; Vicente-Serrano and López-Moreno, 2008), even during summer months (Folland et al., 2009; Simpson et al., 2024). Because persistent high-pressure systems simultaneously promote reduced precipitation (Fleig et al., 2011; Kingston et al., 2015; Bakke et al., 2023) and warm extremes (Stefanon et al., 2012; Kautz et al., 2022), the region represents one of the main European hotspots of compound hot and dry events (Ionita et al., 2021), whose impacts exceed those of either hazard occurring in isolation (Zscheischler et al., 2020). Drought is a recurring climate phenomenon worldwide, with Central Europe – the region roughly delineated by the North Sea, the Alps, the Carpathians, and the Baltic Sea – raising particular concern due to the increase in droughts that has been observed over the last decades (Spinoni et al., 2019; Ionita et al., 2020, 2021). As demonstrated in the analysis of continuous global impact databases initiated in the 1960s, droughts have been identified as the most significant environmental hazard in terms of both human fatalities - by driving famine and disease (Maslin et al., 2025) - and economic losses (Bruce, 1994; Obasi, 1994; Guha-Sapir et al., 2004; Delforge et al., 2025). In Europe, the impact of drought on agriculture, public water supply, energy sector, shipping, construction, and tourism result in several € billion annual losses (Corti et al., 2009; Spinoni et al., 2016; Stahl et al., 2016; Cammalleri et al., 2020). Both urban and rural areas are affected by droughts. While Western and Central European cities are highly vulnerable in term of water management (Tapia et al., 2017), agricultural lands and forests are the most impacted components in the environment, which have raised a lot of concern (e.g. Rouault et al., 2006; Allen et al., 2010; Choat et al., 2012; Vicente-Serrano et al., 2012; Manise and Vincke, 2014; Lüttger and Feike, 2018; Netherer et al., 2019; Vogel et al., 2019; Buras et al., 2020; Webber et al., 2020; Senf and Seidl, 2021).

Given those considerable impacts of droughts, numerous studies have been conducted to investigate their past trends and future projections. However, substantial uncertainties remain. At the global scale, although meteorological droughts did not show any substantial changes since the beginning (Vicente-Serrano et al., 2022) or the half (Sheffield et al., 2012; Spinoni et al., 2014) of the 20th century, recent research (Gebrechorkos et al., 2025) has instead indicated an increase in global drought severity due to enhanced atmospheric evaporative demand (AED). Across Europe, there have been little change over the past 50 years (Oikonomou et al., 2020). The elevated multidecadal variability of precipitation renders trends unstable (Hänsel et al., 2019), even for the Mediterranean region (Vicente-Serrano et al., 2025), which has nonetheless been identified as a drought hotspot in recent decades (e.g. Spinoni et al., 2019; Ionita and Nagavciuc, 2021). Furthermore, studies on Central Europe yielded divergent conclusions (e.g. Freund et al., 2023; in comparison to Bebchuk et al., 2025) rendering trends unclear, mainly attributable to variations in spatial and temporal coverage as well as the utilisation of different drought metrics (Vicente-Serrano et al., 2021). More specifically, it has been argued that this region acts as a transition zone between the drying of Southern Europe and the wetting of Northern Europe since the mid-20th century (Spinoni et al., 2015, 2017, 2018) as well as for future projections (Rossi et al., 2023). However, some authors have shown that Central Europe is actually within a drying trend (Ionita and Nagavciuc, 2021), expected to continue in the future (Lehner et al., 2017). The other underlying cause of the divergent trends between studies over extended periods is attributable to divergent seasonal responses. Although seasonal trends are sensitive to shifts in seasonal definitions (Hänsel et al., 2019), there is a consensus that, over the last three to four decades, dryness in summer and, especially, spring has increased across most of Central Europe (Hänsel et al., 2009, 2019; Spinoni et al., 2017, 2018, 2019; Ionita et al., 2020; Ionita and Nagavciuc, 2021; Bešťáková et al., 2024). Conversely, dryness in autumn and, especially, winter has been decreasing (Moberg and Jones, 2005; Hänsel et al., 2009; Spinoni et al., 2017), a trend expected to continue in the future (Spinoni et al., 2018; Böhnisch et al., 2021; de Vries et al., 2022; Herrera-Lormendez et al., 2023).

The mechanisms driving the drought phenomenon in Central Europe and their past and future evolution in the context of anthropogenic warming are rather complex. As demonstrated in the literature (Lhotka et al., 2020; Suarez-Gutierrez et al., 2020; Hoffmann and Spekat, 2021; Brönnimann et al., 2025), the quantification of contributions from dynamic and thermodynamic processes remains unclear. The respective contributions are found to be potentially dependent of the season and the region. During winter, the circulation dynamic would prevail (Haslinger et al., 2019; Haslinger and Mayer, 2023; Savary et al., 2025), while during summer, the land-atmosphere feedbacks could dominate (Haslinger et al., 2019). In addition, more than in any other European region, dynamic patterns have been identified as contributing factors to dry conditions in Western Europe (Savary et al., 2025), which includes western Central Europe from the definition provided in Section 2.

Specifically, the dry circulation types over Central Europe are predominantly characterised as anticyclonic, south-to-easterly winds, and reduced inflow of moist air from the Atlantic, according for instance to Trnka et al. (2009), Lhotka et al. (2020) and Bešťáková et al. (2024). They also identified a rise in the frequency of those types since the mid-20th century during the vegetation period (April - September) and connected it to the increase in spring and summer dryness. Moreover, Central Europe is one of the three preferred centres of action of compound hot and dry events (CHDs) within Europe, and these centres are generally associated with a persistent high-pressure system (Ionita et al., 2021; Kautz et al., 2022). Indeed, precipitation deficits (Fleig et al., 2011; Kingston et al., 2015; Haslinger et al., 2019; Bakke et al., 2023) and temperature (Stefanon et al., 2012) are both consistently linked with high geopotential height and anticyclonic circulation types. Temperature remains one of the drivers of drought via enhanced AED, and its role is becoming increasingly pronounced in a warming world (Briffa et al., 2009; Gebrechorkos et al., 2025), particularly during the summer months. Furthermore, dryness variability in Europe has been linked to the jet stream characteristics (Simpson et al., 2024; Brönnimann et al., 2025) in addition to teleconnection patterns (e.g. Hurrell and Van Loon, 1997; Van Oldenborgh et al., 2000; Brönnimann, 2007; Vicente-Serrano and López-Moreno, 2008; Helama et al., 2009; Shaman, 2014; Svensson and Hannaford, 2019; Simpson et al., 2024). Even though the combined effect of the different modes of variability in the North Atlantic sector, mostly the North Atlantic Oscillation (NAO), over the European climate is more pronounced during winter (Hurrell, 1995; Topál et al., 2025), the link is still substantial during the other seasons (Folland et al., 2009; Simpson et al., 2024; Hernandez and Comas-Bru, 2025). Local thermodynamics might also play a significant role in driving droughts via land-atmosphere feedbacks (Seneviratne et al., 2010; Miralles et al., 2019). A lack of precipitation, in conjunction with enhanced AED, could self-intensify by triggering land desiccation. Nonetheless, a comprehensive verification of land-atmosphere feedbacks remains unaccomplished for both global observations and models (Miralles et al., 2019). Whilst there is a greater degree of consensus on the positive feedback on temperature (Mueller and Seneviratne, 2012; Miralles et al., 2014; Teuling, 2018; Suarez-Gutierrez et al., 2020; Sutanto et al., 2020), the positive feedback on precipitation remains the subject of debate due to the possible opposite effects (Guillod et al., 2015).

Numerous studies have been conducted on meteorological drought variability in Central Europe (Hänsel et al., 2009, 2019, 2022; Spinoni et al., 2015, 2017, 2018, 2019; Ionita et al., 2020; Ionita and Nagavciuc, 2021) and its dynamical drivers (Trnka et al., 2009; Lhotka et al., 2020; Bešťáková et al., 2024), with a particular focus on winter and summer timescales. The western part of Central Europe has been the subject of only a limited amount or research within the context of this theme. Given the spatial variability of drought changes, particularly in terms of seasonality (Vicente-Serrano et al., 2021), and the high instability of trends due to multidecadal variability (Hänsel et al., 2019), a regional assessment of meteorological droughts in western Central Europe on a long-term perspective, incorporating a seasonal analysis, is absent. This is necessary for understanding regional drought changes and optimising local management. To establish a robust foundation for future projections, it is imperative to enhance the comprehension of drought trends, variability, and drivers over a period that extends much further than the last few decades. Furthermore, many studies have linked dry conditions in Central Europe with specific daily weather types. However, there is a lack of research examining the general atmospheric circulation associated with droughts, especially over a long period.

Consequently, the following objectives are pursued in western Central Europe:

1) Place recent meteorological droughts in a historical perspective;
2) Examine the long-term spatiotemporal variability of dryness;
3) Identify and characterise atmospheric circulation patterns associated with seasonal meteorological droughts;
4) Analyse the temporal change of drought-related atmospheric circulation patterns in connection with dryness trends.

Firstly, the present study aims to provide a long-term analysis of drought events (Section 6.1) and dryness variability (Section 6.2) over western Central Europe through the employment of reanalysis datasets, which are evaluated to ensure reliability (Section 5). Secondly, it seeks to establish a consistent link between drought events in western Central Europe and seasonal atmospheric circulation during these periods (Section 6.3). The results are then discussed, in comparison with the existing literature, providing a long-term perspective on recent events (Section 7.1), an analysis of the related atmospheric circulation (Section 7.2), a synthesis of the drivers of dryness trends on a seasonal framework (Section 7.3), and the overall challenges involved (Section 7.4).

2 Study area

The study area encompasses the land region including Belgium, the Netherlands, Luxembourg, northern France, and western Germany. The region is bounded by a latitude extending from 48°N to 54°N and a longitude from 2°E to 10°E. Although van der Wiel et al. (2023) has defined a similar region as north-western Europe, the present study opted to refer to western Central Europe as it intersects both a part of Western Europe and Central Europe. Furthermore, the term north-western Europe may imply the British Isles in some definitions. The objective was to select an area that was neither excessively large, to present climate homogeneity and avoid in particular the direct influence of the Alps, nor excessively small to reduce the influence of microclimate features. The region is characterized by a mild temperate climate, devoid of dry season, and a warm summer according to the Köppen-Geiger classification for the period 1980-2016 (Beck et al., 2018). According to Savary et al. (2025), droughts concur simultaneously within this region in general. The region receives an average of 889 mm of precipitation annually (1991-2020) using ERA5-Land data (Muñoz-Sabater et al., 2021), with minimum values of less than 700 mm in relatively low and flat areas, and maximum values above 1450 mm in some area within the Vosges and Black Forest mountains (Fig. 1). Western Central Europe is predominantly forested (36.8% of tree cover), with croplands (31.6%), and grassland (22.6%) (Zanaga et al., 2022) also present. This geographical distribution renders the region susceptible to the impacts of droughts on both ecosystems and agriculture. The region is also vulnerable to the impacts on society, as it is home to more than 97 million inhabitants in 2020 (WorldPop, 2018), with 6.74% of built-up areas (Zanaga et al., 2022).

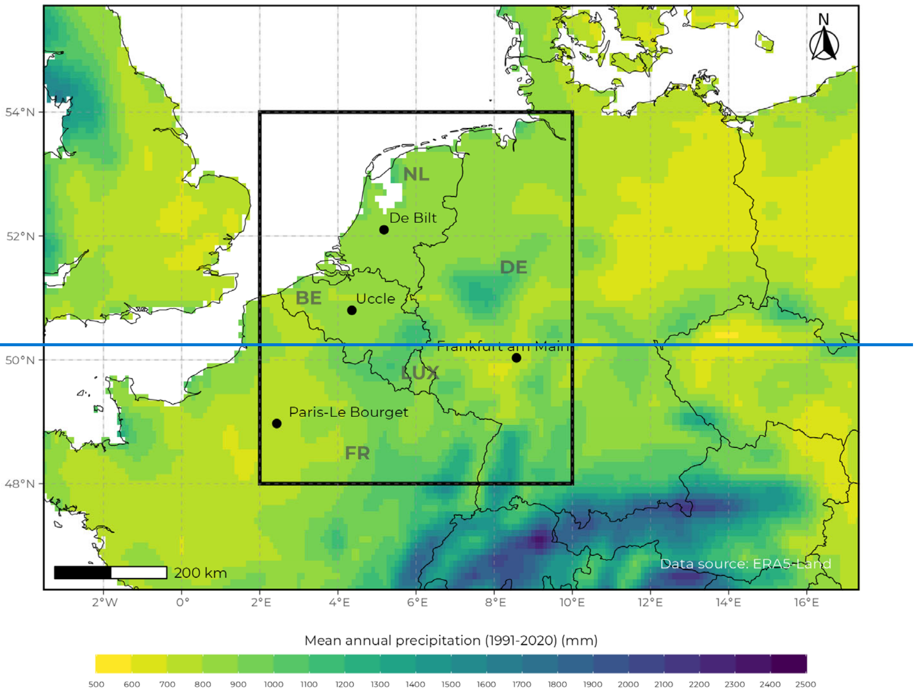

Figure 1: Mean annual precipitation (reference period: 1991-2020) (data source: ERA5-Land; Muñoz-Sabater et al., 2021). The western Central Europe region is delineated by the black box. The dots represent the locations of weather stations that have been utilized for the data evaluation (see Section 5). Acronyms represent the countries that fall within the study area.

3 Data

In addition to the identification of droughts, an objective is to connect them to atmospheric circulation. Consequently, reanalyses are pivotal datasets for this study. A reanalysis is a combination of historical weather observations and weather forecasting models, using a method called data assimilation (Slivinski et al., 2019; Valler et al., 2024). This approach provides a comprehensive dataset that represents fields consistent with each other through the application of physical laws within the model and the elimination of spatial and temporal gaps. Specifically, three complementary reanalyses were employed, which demonstrate a wide range of data assimilated, length-time coverage, and spatial resolutions (see Table 1 for a summary):

- ERA5: The European Centre of Medium-range Weather Forecasts Reanalysis v.5 (ERA5) (Hersbach et al., 2020; Bell et al., 2021; Soci et al., 2024) is a full-input reanalysis that assimilates a wide range of observational data, including satellite, aircraft, buoy, ship, surface, and upper-air station data. It provides high-resolution data (0.25°) from 1940 to the present, with updates available in near-real-time. ERA5 is recognised for its high accuracy and extensive variable coverage; however, it has a relatively shorter time span in comparison to the other reanalyses.
- 20CRv3: Developed by the NOAA, CIRES, and DOE, the Twentieth Century Reanalysis version 3 (20CRv3) (Slivinski et al., 2019) is a surface-input reanalysis that primarily assimilates surface pressure observations. The time span covered extends from 1836 to 2015 with an original resolution of 1°. 20CRv3 offers consistency over time due to its exclusive reliance on surface pressure data, thereby ensuring its suitability for long-term climate studies. However, its accuracy may be inferior to full-input reanalyses.
- ModE-RA: The Modern Era Reanalysis (ModE-RA) (Valler et al., 2024) is a paleo-reanalysis that extends from 1421 to 2008, providing data at a resolution of approximately 1.8°. The assimilation of proxy records, documentary data, and early instrumental measurements renders it an optimal resource for the study of multi-decadal climate variability and past extreme events. The main strength of ModE-RA lies in its extensive temporal coverage; however, it possesses fewer variables and lower spatial resolution than ERA5 and 20CRv3.

Table 1: Summary of reanalyses used in this study.

Dataset	References	Type of reanalysis	Period covered		Spatiotemporal resolution	
			Original	After evaluation	Original	Modified
ERA5	Hersbach et al. (2020) Bell et al. (2021) Soci et al. (2024)	Full input	1940-2023	1947-2023	0.25° Hourly	0.25° Monthly
20CRv3	Slivinski et al. (2019)	Surface input	1836-2015	1918-2015	1° 3-hourly	
ModE-RA	Valler et al. (2024)	Paleo	1421-2008	1844-2008	~1.8° Monthly	

Cross-validation of multiple reanalysis datasets, as proposed by Slivinski et al. (2019), has the potential to enhance the reliability of the conclusions drawn. In order to facilitate spatial comparability, 20CRv3 and ModE-RA have undergone a bilinear downscaling to the resolution of ERA5, i.e. the dataset with the finest resolution (0.25°x0.25°), and anomalies have been adjusted to the 1979-2008 ERA5 climatology, without compromising their inherent variability. In order to proceed with a more in-depth analysis of confidence and to address the varying reliability of reanalyses, an evaluation of the error of the drought indexes and the quality of drought identification is conducted, based on a comparison with point-based observations (see Section 5). The most reliable periods for each reanalysis are retained, i.e. 1844-2008, 1918-2015 and 1947-2023, for ModE-RA, 20CRv3, and ERA5 respectively. Therefore, it enables the analysis of periods of time extending back to the pre-industrial era (1850-1900), as defined by the IPCC (2013).

4Moreover, in a warming climate, the contribution of atmospheric evaporative demand (AED) has become an increasingly important driver of drought severity (Briffa et al., 2009; Gebrechorkos et al., 2025).

Although numerous studies investigated drought variability in Central Europe and its dynamical drivers, western Central Europe—defined here as Belgium, the Netherlands, Luxembourg, northern France, and western Germany—received comparatively limited attention. Yet, this region constitutes one of the major socio-economic centres of Europe (Brunet, 2002), home to approximately 100 million inhabitants in 2020 (WorldPop, 2018), and supports vulnerable ecosystems, including croplands, grasslands, and forests (Zanaga et al., 2022). Given the strong spatial and seasonal variability of drought trends and the influence of multidecadal variability (Hänsel et al., 2019; Vicente-Serrano et al., 2021), this study investigates the evolution of drought conditions and their hydroclimatic drivers in western Central Europe since the pre-industrial era, placing recent droughts in a historical perspective. Moreover, atmospheric circulation has been shown to play a particularly important role in drought variability in western Central Europe compared with many other European regions (Savary et al., 2026; Xue et al., 2026). This study therefore characterises seasonal atmospheric circulation patterns associated with droughts over long time periods, complementing previous work that has mainly focused on specific daily weather types.

2 Methods

42.1 Drought definition

The presentThis study focuses on meteorological droughtdroughts, given its aimobjective of establishing a connectionlinking drought events to atmospheric circulation. The definition employed was based onDrought conditions are characterised using the Standardised Precipitation Index (SPI) (McKee et al., 1993)(SPI, McKee et al., 1993), as recommended by the World Meteorological Organization (WMO, 2012), and the Standardised Precipitation Evapotranspiration Index (SPEI) (Vicente-Serrano et al., 2010). The employment of multiple drought indicators fosters a comprehensive understanding of the multifaceted nature of the drought phenomenon (Lloyd-Hughes, 2014). The two indexes are based on the same principle: the transformation of a fitted distribution of a variable accumulated over a certain period (in months) into a normal standardized (μ=0, sd=1) distribution (Fig. 2). For the SPEI, the accumulated variable is the climate water balance, i.e. precipitation minus potential evapotranspiration (PET), while for the SPI, precipitation is the only considered variable. Although SPEI is predominantly influenced by precipitation in the western Central Europe region (see Fig. 2 in Tomas-Burguera et al., 2020), the role of atmosphere evaporative demand (AED) on the SPEI is pronounced during very dry periods. Consequently, discrepancies between the SPI and the SPEI are expected to be minor, except during very dry periods.

The three-month accumulation period (SPEI-3 and SPI-3) has been utilised as the length of time is sufficiently long to induce a substantial hydrological imbalance, thereby leading to the onset of a drought (IPCC, 2013), and yet sufficiently brief to be directly associated with meteorological drivers. As these are standardised indexes, they are inherently comparable across different geographical locations and temporal periods. Furthermore, they can be easily understood. The onset of the drought is characterised by a decline in the index to a value below -1 (McKee et al., 1993). The drought is considered to have ended when the index recovers over -1. The mean intensity and severity of the drought are defined as the average and the sum of the absolute value of the index during the drought, respectively. The duration is measured in months and is defined as the number of consecutive months in which the index is below -1. The computation of both the SPEI-3 and SPI-3 has been facilitated by the R Package developed by Beguería et al. (2014). The Gamma distribution was selected to fit the observed values for SPI-3 (Fig. 2), a choice that aligns with the recommendations put forth by Vicente-Serrano et al. (2010) and Stagge et al. , and the Standardised Precipitation Evapotranspiration Index (SPEI, Vicente-Serrano et al., 2010). Both indices transform a fitted distribution of a variable accumulated over a given time scale into a standardised normal distribution ($\mu = 0$, $\sigma = 1$). For SPI, the accumulated variable is precipitation, whereas SPEI is based on the climatic water balance, defined as precipitation minus atmospheric evaporative demand (AED).

AED represents the maximum combined evaporation from soil and transpiration from vegetation under given climatic conditions, assuming no soil water limitation. Although AED is often used interchangeably with potential evapotranspiration (PET), from which the index derives its name, this terminology can be ambiguous and is therefore not recommended (Katerji and Rana, 2011; DeJonge et al., 2025). AED is estimated using the Thornthwaite equation (1948), which does not explicitly parameterise a specific reference surface or vegetation type and requires only temperature and latitude, thereby ensuring methodological consistency across the three datasets. In western Central Europe, this method agrees closely with the more physically-based Penman–Monteith approach (1948). The influence of this approximation on the results is evaluated in the Supplementary Material (Supplementary Evaluation), and its implications are discussed in Section 5.4.

A three-month accumulation period (SPEI-3 and SPI-3) is selected as it is sufficiently long to capture a substantial hydrological imbalance, while remaining short enough to be directly linked to dynamic drivers. The three-month accumulation is calculated using a rolling monthly window, resulting in 12 index values per year. Drought onset occurs when the index falls below -1 (McKee et al., 1993), and drought termination when it rises above this threshold. Drought severity and mean intensity are defined as the sum and mean of the absolute index values during an event, respectively. Drought duration corresponds to the number of consecutive months with index values below -1.

SPI-3 and SPEI-3 are computed using the *SPEI* R package (Beguería et al., 2014). Following Vicente-Serrano et al. (2010) and Stagge et al. (2015). In the case of the SPEI-3, the log-logistic distribution was selected to maintain coherence over the entire spectrum of values, including those of low values (Vicente-Serrano et al., 2010). The indexes are computed based on the 1947-2008 reference period, thereby enabling the comparability of the datasets (1947-2008 being the common period between the post-evaluation reanalyses). Indexes have been computed locally for each grid cell. In order to obtain the SPI-3 and SPEI-3 values for the entire western Central Europe region, precipitation and PET values for all land cells have been averaged over the study area. The values have been weighted by the cosine of their latitude, prior to the computation of the index, so as to ensure proper consideration of the whole region, as described in Spinoni et al. (2016). For each month, the area involved by the drought has also been calculated, representing the proportion of cells that are below the threshold within the area. The mean and peak area involved have also been computed and represent the mean and the maximum drought area involved over a drought event defined at the scale of the whole region.

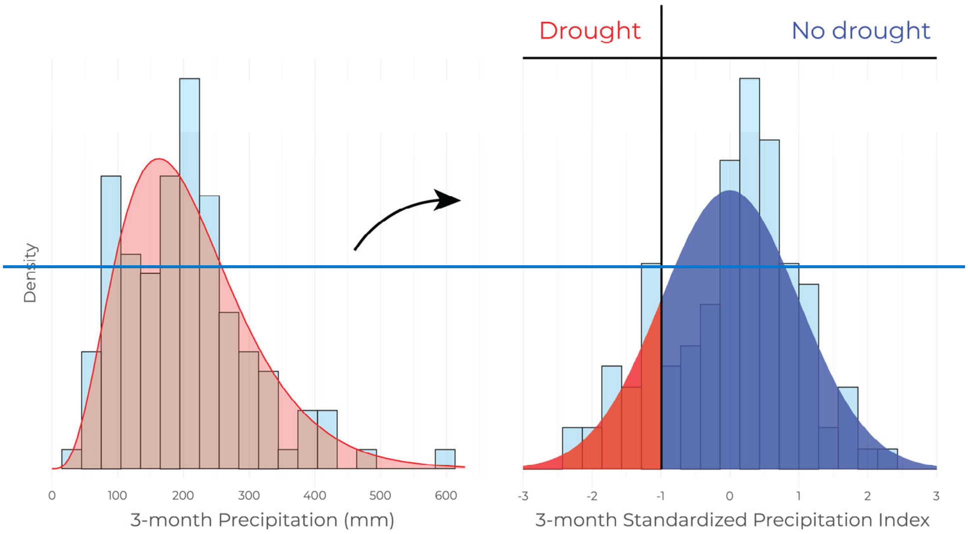

Figure 2: Conceptualisation of the Standardized Precipitation Index (SPI-3) computation. The blue bars represent an example of probability densities of 3-month precipitation. These are fitted to a Gamma distribution that is subsequently transformed into a standard normal distribution to obtain the SPI-3 (density function plot, right side). The SPI-3 value for a specific month is classified as a drought month if it is less than -1, and otherwise classified as a non-drought month. The computation of the Standardized Precipitation Evapotranspiration Index employs a similar principle, with the exception that the blue bars represent the difference between precipitation and potential evapotranspiration values and that these are fitted to a log-logistic distribution.

The SPEI was computed by estimating PET using the Thornthwaite equation (1948). The method is based exclusively on temperature and latitude, thereby ensuring consistent PET estimation across the three datasets. The Thornthwaite equation has been demonstrated to be reliable using ERA5 and 20CRv3 in the western Central European region, as evidenced by the excellent agreement with the more physically-based Penman-Monteith equation (1948) (Fig. S1).

4, a Gamma distribution is fitted for SPI-3, and a log-logistic distribution for SPEI-3. The indices are computed relative to the 1947–2008 reference period, corresponding to the common period shared by all post-evaluation reanalyses. The indices are computed at both the grid-cell and regional scales. At the regional scale (48°N–54°N, 2°E–10°E), precipitation and AED are aggregated and area-weighted across all land grid cells before the computation of the index to ensure a consistent regional representation, as described in Spinoni et al. (2016). For each month, the drought area involved is also calculated as the proportion of grid cells with index values below -1.

2.2 Atmospheric circulation classification

As meteorological drivers must demonstrate sufficient longevity to engender a drought (IPCC, 2013; Raposo et al., 2023), the aim here is to associate drought events in western Central Europe to the low-frequency atmospheric circulation over the Euro-Atlantic. Many methodologies for daily analyses have been employed in the literature (see Huth et al., 2008 for a review) and can also be utilised for monthly analyses. In this study, the k-means clustering method from Hartigan and Wong (1979) was selected for its performance in synoptic classification of atmospheric circulation patterns over Europe (Huth et al., 2016). This method has been shown to exhibit very good separability and stability (Huth et al., 2008).

The clustering was performed based on 500hPa monthly geopotential height (Z500) anomaly, with the data being averaged over the month of the drought onset and the two preceding months. This approach was adopted since three months of imbalance are accumulated in the drought index. The clustering was based on seasonal droughts, defined as periods of dryness that occurred in February, May, August and November, referred to later as winter, spring, summer and autumn droughts. The consideration of seasonal droughts is evidently subject to certain limitations. Firstly, it is unable to capture short inter-seasonal droughts. Secondly, it divides single prolonged inter-seasonal droughts into multiple ones, which tend to affect more drought during the warm seasons, as they are generally longer than during the cold season (Banfi et al., 2024). However, it permits consideration of the primordial non-stationarity of the atmospheric circulation variability (Comas-Bru and Hernández, 2018).

The Z500 anomalies are based on the 1979-2008 reference period, thus ensuring the comparability of outputs from the datasets. The spatial extent of the input is defined as the Euro-Atlantic sector (30°N-70°N, 35°W-35°E, approximately 5000 km from west to east at 50°N). Indeed, general atmospheric circulations are set from continental to hemispheric scale to accommodate the recurrent and persistent low-frequency atmospheric dynamics (Huth et al., 2008). The clustering is temporal-based, with each cell grid constituting a variable and each Z500 anomaly mean representing an observation. As the k-means clustering algorithm is intended to minimise the intra-cluster variance, the calculation of the Euclidian distance must be weighted by the cosine of the latitude. In order to ensure the stability of the clustering process and prevent the occurrence of local optima, which can be an issue in the context of large datasets with k-means clustering (Philipp et al., 2007), the process has been iterated one thousand times for each K cluster from 2 to 20. All iterations demonstrate the presence of the same K clusters up to six clusters, thus indicating that the initial position of the centroid locations does not exert a strong influence on the dominant clusters.

In order to define the K groups prior to the k-means clustering, four clusters were chosen for the purposes of analysis. This approach is consistent with the finding that atmospheric circulation patterns are often characterised by a small number of general patterns (Huth et al., 2008). While numerous indexes (e.g. AIC, BIC, Silhouette, CH, Davies-Bouldin) did not objectively agree on the optimal number of clusters for the present analysis (see Fig. S2), it was deemed more appropriate to choose the K clusters based on the subjective separability of the patterns regarding their spatial composition.

In addition, the first three empirical orthogonal functions (EOFs) were computed in the Euro-Atlantic sector for the entire period, for each season, in order to gain insight into the modes associated with each cluster. They are hereafter presented in descending order of explained variance: the North Atlantic Oscillation (NAO), the East Atlantic (EA) pattern, and the Scandinavia (SCA) pattern (Barnston and Livezey, 1987). The EOFS have been computed based on Z500 seasonally means and area-weighted by the square root of the cosine of theBecause meteorological drivers must persist long enough to trigger drought onset (IPCC, 2013; Raposo et al., 2023), the aim is to relate drought events in western Central Europe to low-frequency atmospheric circulation over the Euro-Atlantic sector (30°N-70°N, 35°W-35°E). The clustering is performed on 500 hPa geopotential height (Z500) anomalies computed relative to the 1947–2008 reference period and focuses on seasonal drought events occurring in February, May, August, and November, corresponding to winter, spring, summer, and autumn, respectively. For each event identified in one of these four months, Z500 anomalies are averaged over that month and the two preceding months (i.e. December–February, March–May, June–August, and September–November, respectively) to match the three-month accumulation period of SPI-3 or SPEI-3. The k-means clustering algorithm of Hartigan and Wong (1979) is then applied to these composites to identify recurrent circulation patterns associated with drought. Separate analyses are performed for SPI-3 and SPEI-3 drought events.

Clustering is performed in the temporal dimension, with grid cells treated as variables and drought-event Z500 composites as observations. As the k-means clustering algorithm minimises the intra-cluster variance, Euclidean distances are weighted by the cosine of the latitude. To assess clustering stability and reduce sensitivity to centroid initialisation (Philipp et al., 2007), the algorithm was repeated 1000 times for each number of clusters between 2 and 20. The dominant patterns remained stable up to six clusters, indicating limited sensitivity to the initial centroid positions.

Prior to clustering, the number of clusters was fixed to four. Monthly-to-seasonal atmospheric circulation is generally characterised by a few broad-scale recurrent patterns (Huth et al., 2008), unlike daily weather-type classifications that typically require more clusters (e.g. Schwander et al., 2017; Pfister et al., 2025). In addition, only drought-related circulation states are considered here, reducing the expected diversity of patterns. Common clustering diagnostics (Fig. S1) suggested between two and six clusters, providing no unique optimum. Four clusters were ultimately selected based on the spatial separability of the resulting patterns.

To characterise the dominant modes of variability and compare them with the different clusters, the first three empirical orthogonal functions (EOFs) are computed from the complete record of seasonal Z500 over the Euro-Atlantic sector, rather than from drought events only. The EOF analysis is performed on seasonal mean Z500 fields weighted by the square root of the cosine of latitude (Chung and Nigam, 1999).

42.3 Trend detection

The modified Mann-Kendall test, incorporating a variance correction approach from Hamed and Rao (1998), was employed utilising the R package developed by Patakamuri & O'Brien (2017) for the purpose of detecting temporal trends. The Mann-Kendall (MK) trendTemporal trends are detected using the modified Mann–Kendall (MK) test (Mann, 1945; Kendall, 1948)(Mann, 1945; Kendall, 1948) is non-parametric and depends on the ranks of the observations instead of their values. This reduces its vulnerability to the effects of tails and outliers, rendering it more appropriate for identifying trends in climatological and hydrological time series than parametric trend testswith the variance correction proposed by Hamed and Rao (1998) (hereafter MMKH), implemented through the R package by Patakamuri and O'Brien (2017). The MK test is a non-parametric rank-based method that is widely used for climatological and hydrological time series (Hamed, 2008). The MK test assumes that the dataBecause SPI-3 and SPEI-3 are randomly and independently distributed. Evidently, this is not the case for drought indexes based on three-monthly accumulated variables, which are strongly auto-correlated. In order to remove thismonth accumulations, they exhibit serial correlation, violating the independence assumption of the MK test. This effect, a is accounted for using the variance correction approach is applied, as described byof Hamed and Rao (1998), which also accounts for the multiple lags in theconsiders serial correlation across multiple lags (Khaliq et al., 2009). This approach and has been demonstratedshown to be especially statistically powerfulprovide good statistical power (Blain, 2013). The magnitude of the trends is quantified by the Sen's slope estimator (Sen, 1968). This is defined as the median value of the slopes between all possible pairs of points within the specified time series. This approach is also non-parametric and less sensitive to tails and outliers than parametric estimators. Trend magnitude is estimated using Sen's slope (Sen, 1968), a non-parametric estimator defined as the median slope between all pairs of observations.

a mis en forme : Espace Après : 10 pt

a mis en forme : Police :Gras, Couleur de police : Noir, Crénage 16 pt

a mis en forme : Police :Gras, Couleur de police : Noir, Crénage 16 pt

a mis en forme : Police :Gras, Couleur de police : Noir, Crénage 16 pt

a mis en forme : Police :Gras, Couleur de police : Noir, Crénage 16 pt

5 Data Evaluation

Reanalyses datasets represent a valuable tool for the analysis of past climate variability and extreme events (Slivinski, 2018). However, it is imperative to assess their reliability, which is contingent upon three factors: the quality and quantity of observations, the performance of the model, and the data assimilation method. Whilst the aforementioned two variables are hypothesised to remain constant across time for each reanalysis, this is not the case for the former. In consideration of the exponentially increasing temporal extent of the observational framework, it is anticipated that earlier periods will engender reduced reliability. In order to achieve a "meta-confidence" (Slivinski et al., 2019), three reanalyses are employed, each of which possesses a common temporal period, and are thus used to cross-validate one another. Furthermore, a comparison is made between the drought indexes (SPEI-3 and SPI-3) estimated from long weather station observations within the area and those from the three reanalyses at the same location. In order to ensure that the evaluation was not overly sensitive to resolution, the ERA5-Land dataset (Muñoz-Sabater et al., 2021) was also examined. This is a downscaled land product of ERA5 with a resolution of 0.1°x0.1°, spanning from 1950 to 2023 in this study.

To compute SPI-3 and SPEI-3 using Thornthwaite estimation, a selection of weather stations available on the KNMI Climate Explorer dataset (Trouet and Van Oldenborgh, 2013) that covered a minimum of 150 years for temperature and precipitation was made. From the initial pool, a further selection was made of weather stations that covered a minimum of 100 years continuously (in this context, 'continuous' is defined as no gap longer than one year) for both temperature and precipitation at the same time. As outlined in Table 2, the locations under discussion are Uccle, De Bilt, Frankfurt-am-Main, and Paris-Le Bourget. The most recent years absent from the KNMI Climate Explorer dataset were addressed by utilising updated data (until 2023) for the Uccle weather station, which was obtained from the Royal Meteorological Institute of Belgium (RMI). Furthermore, the RMI facilitated the acquisition of potential evapotranspiration data estimated with Penman-Monteith for the Uccle weather station. This data supported the investigation of the differences between potential evapotranspiration estimation methods for this study (see Fig. S1).

Table 2: Summary of weather stations selected for data evaluation. The maximum continuous years within the specified period are indicated in bold.

Weather Stations	Period covered for temperature (T)	Period covered for precipitation (P)	Commun period for both T and P	Latitude	Longitude	Altitude	Sources
Uccle (BE)	1833 - 2023 **(191)**	1833 - 2023 **(191)**	1833 - 2023 **(191)**	50.80° N	4.40° E	100 m	RMI
De Bilt (NL)	1706 - 2018 **(313)**	1849 - 2018 **(170)**	1849 - 2018 **(170)**	52.10° N	5.18° E	2 m	KNMI Climate Explorer
Frankfurt am Main (DE)	1757 - 1961 **(205)**	1826 - 2000 **(175)**	1826 - 1960 **(135)**	50.10° N	8.70° E	109 m	
Paris-Le Bourget (FR)	1757 - 2000 **(244)**	1770 - 2004 **(235)**	1770 - 2000 **(231)**	48.80° N	2.50° E	50 m	

Firstly, the general behaviour of the drought indexes was investigated (Fig. 3a). Secondly, the identification of drought was specifically evaluated (Fig. 3b). For both cases, the reanalyses are compared to each weather station as a reference point. For a period of the reanalysis to be considered reliable and thus included in the analysis, it is essential that it respects both concurrently for all the weather stations. For the former, the Mean Absolute Error (MAE) was utilised, while for the latter, the Matthew's Correlation Coefficient

3 Reanalysis datasets and evaluation

Three complementary atmospheric reanalyses are used at monthly resolution, covering different periods, spatial resolutions, and data-assimilation strategies (Table 1). The European Centre of Medium-range Weather Forecasts Reanalysis v.5 (**ERA5**) (Soci et al., 2024) assimilates a broad range of observations, including satellite, aircraft, buoy, ship, surface, and upper-air station data. It provides high-resolution data and extensive variable coverage, although over a shorter period than the other reanalyses. The Twentieth Century Reanalysis version 3 (**20CRv3**) (Slivinski et al., 2019) primarily assimilates surface pressure observations. Its more limited data assimilation provides temporal consistency for long-term climate studies, although with lower accuracy than full-input reanalyses. The Modern Era Reanalysis (**ModE-RA**) (Valler et al., 2024) assimilates proxy records, documentary data, and early instrumental measurements, rendering it particularly useful for analysing multidecadal variability and historical extremes, despite its lower spatial resolution and more limited variable availability.

Table 1: Summary of reanalyses used in this study.

Dataset	References	Type of reanalysis	Data assimilation method	Period covered		Spatiotemporal resolution	
				Original	After evaluation	Original	Resampled
ERA5	Soci et al. (2024)	Full input	4D-Var	1940-2023	1947–2023	0.25° Hourly	0.25° Monthly
20CRv3	Slivinski et al. (2019)	Surface input	Ensemble Kalman Filter	1836-2015	1918–2015	1° 3-hourly	0.25° Monthly
ModE-RA	Valler et al. (2024)	Paleo	Ensemble Square Root Filter	1421-2008	1844–2008	~1.8° Monthly	0.25° Monthly

For spatial comparability, 20CRv3 and ModE-RA were bilinearly interpolated to the ERA5 resolution (0.25° × 0.25°). This interpolation does not introduce additional spatial information but ensures a consistent grid for comparison while preserving the native ERA5 resolution. Therefore, spatial analyses focus on mid- to large-scale structures, as differences below approximately 200 km remain uncertain because of differences in native resolution. At the aggregated regional scale, this resampling has no significant impact on the conclusions. In addition, monthly anomalies from 20CRv3 and ModE-RA were computed relative to their respective climatologies and then multiplied by the corresponding 1979–2008 ERA5 climatology. This adjustment harmonises the datasets while preserving their relative temporal variability. The 1979–2008

ERA5 climatology is used only for this step, as ERA5 is considered the most reliable reanalysis during the recent overlapping period.

Reanalysis reliability depends on model performance, the data assimilation method, and the density and quality of assimilated observations, which generally decrease further back in time. The datasets were therefore evaluated before further analysis. The evaluation compares SPI-3 and SPEI-3 from the reanalyses with long-term station observations at Uccle, De Bilt, Frankfurt am Main, and Paris-Le Bourget (Table S1). These stations were selected from the KNMI Climate Explorer dataset (2022) based on the availability of long, near-continuous temperature and precipitation records. Updated Uccle observations until 2023 and Penman–Monteith AED estimates were obtained from the Royal Meteorological Institute of Belgium. The latter were used to assess the sensitivity of AED estimates to the Thornthwaite method.

The evaluation considers both the general behaviour of the drought indices and the identification of drought events. Index behaviour is assessed using the 10-year left-moving mean absolute error (MAE) between each reanalysis and station record. Drought-event identification is evaluated using the 20-year left-moving Matthews correlation coefficient (MCC, Matthews, 1975) ~~was employed. Specifically, it was subjectively determined that the 10-year left moving MAE of reanalyses must remain continuously below a threshold of 0.5, i.e. the half of the standard deviation, during the reliable period (Fig. 3a). MCC has been shown to be an excellent index with which to measure the~~, which provides an excellent measure of agreement between binary classifications (Chicco and Jurman, 2020). ~~It is considered that the 20-year left moving MCC of reanalyses must be lower than 0.4 is to be regarded as not reliable (Fig. 3b). The 20-year timeframe was selected over a 10-year period for the MAE due to the necessity for binary classification indexes to comprise a substantial number of observations in order to be both representative and robust (e.g. Tractenberg et al., 2010).~~A period is retained only when both criteria are satisfied across the station network. Specifically, reliable periods require the moving MAE to remain below 0.5 and the moving MCC to remain above 0.4.

a mis en forme : Retrait : Première ligne : 0,63 cm

a mis en forme : Couleur de police : Automatique

~~The evaluation of data for SPI-3 is shown in Fig. 3, as it has been found to be a more decisive metric than SPEI-3 for determining the reliability periods. However, it should be noted that SPEI-3 exhibits a generally similar behaviour for both moving MAE and MCC (Fig.~~ SPI-3 provides the clearest constraints on reliable periods and is therefore shown in Fig. 1, while SPEI-3 shows broadly similar behaviour (Fig. S2). After the early 1960s, all reanalyses closely follow the station-based SPI-3 and SPEI-3 variability, and drought-event agreement is generally good, especially at Uccle and De Bilt. Before the 1960s, larger discrepancies appear between datasets. ERA5 shows excessive dryness during the first years of its record, particularly at Frankfurt, likely related to the limited availability of upper-air temperature observations before 1946 (Soci et al., 2024) and therefore their influence on atmospheric water vapour and precipitation over land. 20CRv3 shows excessive wetness before the late 1910s, consistent with the sharp increase in assimilated Northern Hemisphere observations in the early 1920s (Slivinski et al., 2021). ModE-RA performs reliably from 1844 onward, while its lower reliability before the 1840s likely reflects the limited number of assimilated observations.

The retained periods are therefore 1947–2023 for ERA5, 1918–2015 for 20CRv3, and 1844–2008 for ModE-RA, extending the analysis back to the pre-industrial era (IPCC, 2013). In addition, reanalyses show good agreement between themselves in identifying regional drought events, especially between ERA5 and ModE-RA. Over the common reference period, MCC values are 0.46 for ERA5–20CRv3, 0.44 for 20CRv3–ModE-RA, and 0.79 for ERA5–ModE-RA for SPEI-3, with similar values for SPI-3 (0.45, 0.41, and 0.78, respectively).

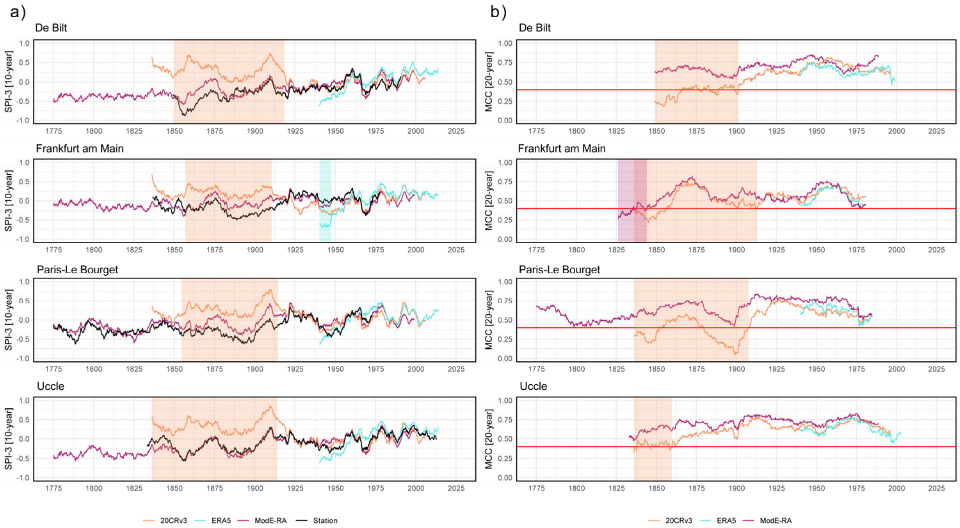

Figure 1: Data evaluation based on (a) the 10-year left-moving average of SPI-3, , calculated using the 1940–2000 evaluation reference period, for each reference station and reanalysis, and (b) the 20-year Matthews correlation coefficient (MCC) for drought classification between each reference station and the reanalyses. For each reanalysis–station pair in (a), the shaded period begins when the 10-year left-moving mean absolute error exceeds 0.5 and extends until it subsequently decreases below 0.5 and remains below this threshold. In (b), the shaded period begins when the 20-year left-moving MCC falls below 0.4 and extends until it subsequently rises above 0.4 and remains above this threshold. In both panels, shaded areas are coloured according to the dataset considered unreliable during the corresponding periods.

4 Results

4.1 Drought events

Regional drought indices (Fig. 2a and Fig. S3a) are strongly correlated with the spatial extent of drought (r = 0.77–0.81 for SPEI-3 and 0.81–0.84 for SPI-3), indicating that they provide a representative measure of regional drought conditions. The most severe droughts (Fig. 2a), defined as those exceeding the 90th percentile of drought severity over the 1947–2008 reference period for each reanalysis, affected the entire region at their peak (Fig. 2b and Fig. S3b), demonstrating high spatial coherence across western Central Europe. Among them, the 1921 drought stands out because of its exceptional duration (14 months in ModE-RA), resulting in a severity exceeding twice the 90th percentile threshold for SPEI-3.

S4). After the early 1960s, the 10-year left moving average of SPI-3 and SPEI-3 for all the reanalyses are very close to the observations. Furthermore, the agreement for drought identification between the two data sources is good, especially at the De Bilt and Uccle locations. Prior to the 1960s, there is a divergence between reanalyses. The subsequent paragraph delineates the limits identified in each reanalysis.

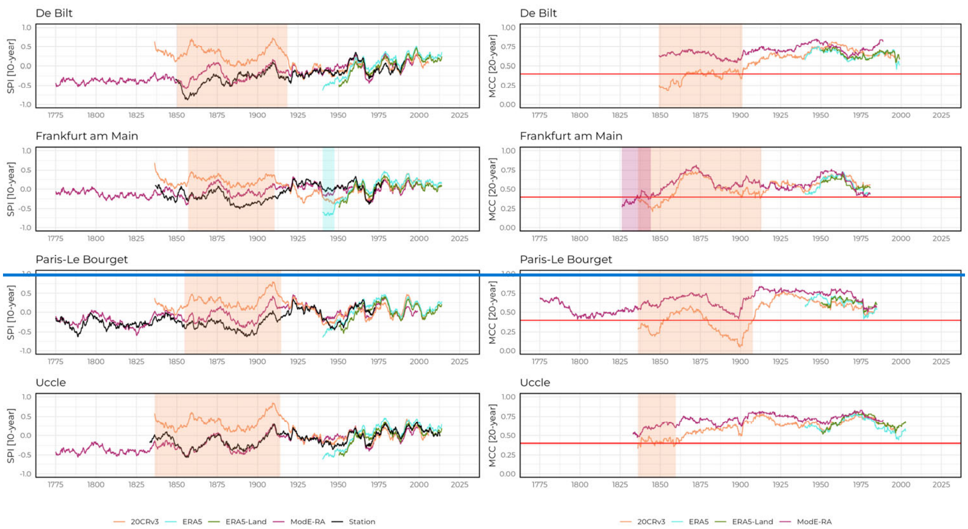

Figure 3: (a) 10-year left moving average of SPI-3 (reference period: 1950-2008) for each reference station and the reanalyses. The shaded area of a reanalysis extends when the 10-year left moving mean absolute error with the reference station is greater than 0.5 until it becomes lower than 0.5 in the rest of the time series. (b) 20-year left moving Matthew's Correlation Coefficient (MCC) of the classification of droughts between each reference station and the reanalyses. The shaded areas extend when the 20-year left

moving MCC is strictly below until it is not in the whole time series. Shaded areas in both (a) and (b) represent periods considered as not reliable for related reanalyses.

ERA5 demonstrates excessive dryness, especially at Frankfurt location, for the first seven years of its timespan (Fig. 3a). This is presumably attributable to the paucity of upper air temperature observations prior to 1946 (Soci et al., 2024), which influences the total column of water vapour and precipitation over land. As demonstrated in Fig. 3a, 20CRv3 exhibits excessive wetness for all four weather station comparisons prior to the late 1910s. As indicated by Slivinski et al. (2021), there was a significant increase in the number of observations assimilated in the Northern Hemisphere in 20CRv3 at the beginning of the early 1920s, which subsequently led to a substantial decrease in error. ModE-RA achieved a sufficient level of agreement with the Frankfurt weather station after 1844, while it proved sufficiently reliable prior to that date for the other reference stations. Prior to the 1840s, the number of observations assimilated was very low, which may explain its lack of performance for this period in the data evaluation (Fig. 3b). The subsequent consistency exhibited by ModE-RA may be attributable to the quantity of observations assimilated, which exhibits relative stability in comparison with the two other reanalyses. This quantity is subject to variation, though not exponential, with the exception of the period from the 1860s to the 1890s, during which it attains its maximum. Consequently, it is considered that ERA5, 20CRv3, and ModE-RA are reliable over 1947-2023, 1918-2015, and 1844-2008 respectively.

6 Results

6.1 Drought events

Overall, reanalyses demonstrate a high degree of agreement in identifying drought events for the western Central Europe region, especially between ERA5 and ModE-RA, whether for SPEI-3 (Fig. 3 - over the reference period: $MCC_{ERA5\text{-}20CRv3}$ = 0.46, $MCC_{20CRv3\text{-}ModE\text{-}Ra}$ = 0.44, $MCC_{ERA5\text{-}ModE\text{-}RA}$ = 0.79) or SPI-3 (Fig. S5 – over the reference period: $MCC_{ERA5\text{-}20CRv3}$ = 0.45, $MCC_{20CRv3\text{-}ModE\text{-}Ra}$ = 0.41, $MCC_{ERA5\text{-}ModE\text{-}RA}$ = 0.78). The most severe droughts highlighted on Fig. 4 have been defined as the droughts that show a severity above the 90th percentile of severity of the reference period (1947-2008) proper to each reanalysis. They are not ranked since reanalyses exhibit slight discrepancies between them. However, many droughts were of large severity and extent in all reanalyses. Here are the most severe droughts appearing at least in one reanalysis (chronologically): 1857, 1921, 1947, 1948, 1953, 1959, 1971, 1976, 1995, and 2018 for both drought indexes; 2003 and 2011 for SPEI-3 alone; 1853, 1870, 1873, 1893, 1908, 1911, and 1929 for SPI-3 alone. Specifically, the 1921 drought is very severe (more than twice of the 90th percentile of severity of the reference period for SPEI-3 in ModE-RA) due to its exceptional duration (14 months for SPEI-3 in ModE-RA). However, it is not considered as extreme in 20CRv3 because the event is identified as two distinct droughts. For both SPEI-6 and SPI-6, 1921 drought is one single drought for 20CRv3 and is categorised as the most severe, by far, as it is for SPEI-3 and SPI-3 for ModE-RA.

A drought identified with SPI-3 is also identified with SPEI-3 in most cases and vice versa (Fig. 4 vs Fig. S5 – over the reference period: MCC_{ERA5} = 0.76, MCC_{20CRv3} = 0.81, $MCC_{ModE-RA}$ = 0.74). However, their intensity and severity vary between drought indexes. For instance, the 1976-drought is more intense with SPI-3 than with SPEI-3, and inversely for 2018-drought. Overall, droughts after the 1990s were more numerous, lasted longer and were slightly more intense at their peak with SPEI-3 than SPI-3 (over 1990-2023 for ERA5: 33 events with an average of 2.61 months duration and a mean peak intensity of 1.48 for SPEI-3, 25 events with an average of 2.08 months duration and a mean peak intensity of 1.44 for SPI-3). Conversely, the most severe droughts highlighted on Fig. 4 and Fig. S5 are more numerous and generally occurring at an earlier point in time for SPI-3 than for SPEI-3. These are consequences of the increase of both precipitation and AED since the industrial period (see section 6.2).

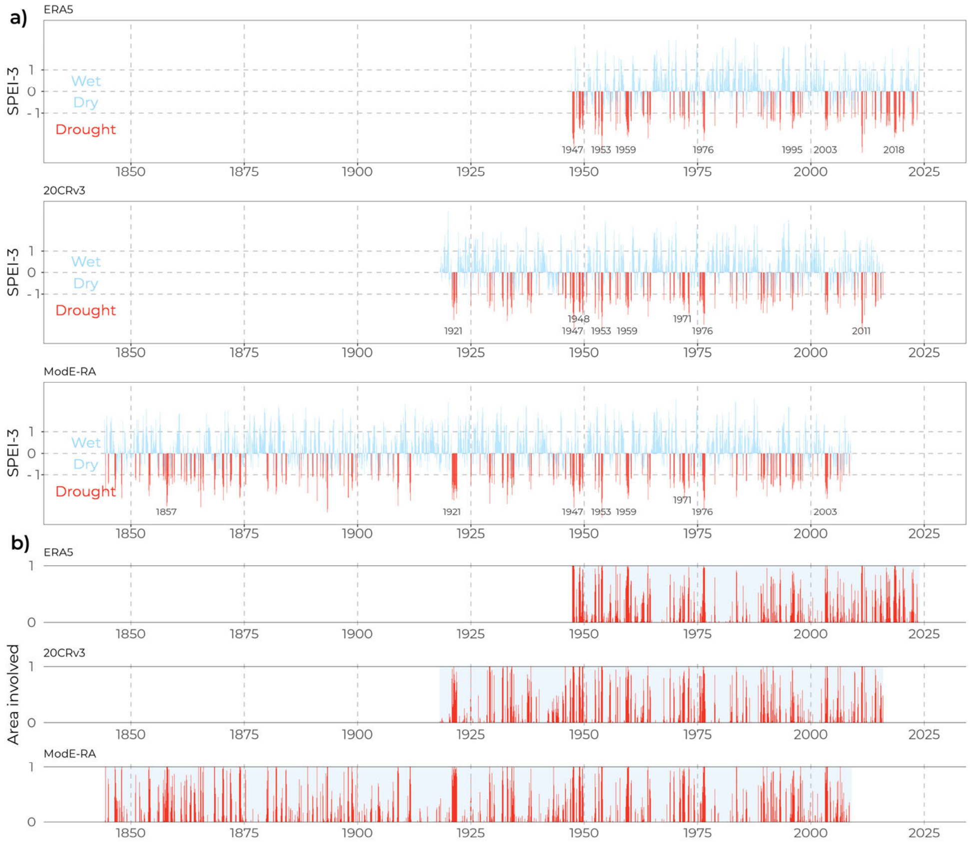

Figure 42: (a) 3-month Standardized Precipitation Evapotranspiration Index time series for the aggregate western Central Europe region for each reanalysis dataset (each row) (reference period: 1947–2008). The red bars indicate drought months (SPEI-3 < -1), and the most severe drought events are highlighted. (b) Time series of the proportion of the western Central Europe region under drought (illustrated in red) according to the SPEI-3 values of the grid cells.

a mis en forme : Police :10 pt, Non Gras

SPI-3 and SPEI-3 identify largely the same drought events (Fig. 2; Fig. S3), with MCC values of 0.76 (ERA5), 0.81 (20CRv3), and 0.74 (ModE-RA) over the common reference period. However, their intensity and severity differ. For example, the well-documented 1976 drought is more intense according to SPI-3, whereas the recent 2018 drought is more intense according to SPEI-3. Since the 1990s, SPEI-3 identifies more droughts, with longer durations than SPI-3 (ERA5, 1990–2023: 33 vs. 25 events, mean duration 2.61 vs. 2.08 months), while mean peak intensity is only slightly higher (1.48 vs. 1.44). Conversely, the most severe droughts are more numerous and generally occur earlier in the record according to SPI-3. In addition to the most severe droughts common to both indices (Fig. 2a and Fig. S3a), the 2003 and 2011 droughts appear for SPEI-3 only, whereas the 1853, 1870, 1873, 1893, 1908, 1911, and 1929 droughts appear only with SPI-3.

The recent period 2011–2023 was characterised by frequent droughts, particularly according to SPEI-3 (29.2 drought months per decade in ERA5). Similar periods also occurred during 1857–1874 (31.7 drought months per decade in ModE-RA) and 1947–1960 (29.3–34.3 drought months per decade depending on the reanalysis). In contrast, drought frequency was particularly low during 1912–1920 (1.6 drought months per decade in ModE-RA) and 1977–1988 (6.7–8.3 drought months per decade).

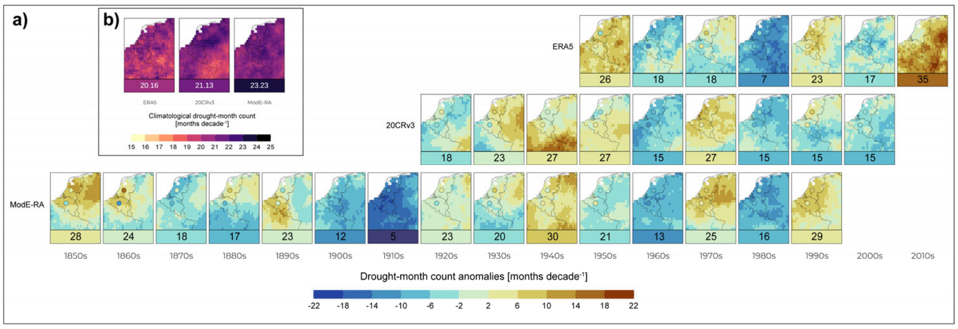

Figure 3: (a) Anomalies in decadal SPEI-3 drought-month counts for each dataset (rows) and complete decade (columns), relative to (b) the mean number of SPEI-3 drought months per decade over the 1947–2008 reference period. Positive values in (a) indicate more drought months than the climatological decadal mean, whereas negative values indicate fewer. The absolute number of drought months computed at the regional scale is shown below each corresponding map. Discs represent anomalies at weather stations that fully cover both the corresponding decade and the reference period.

Decadal drought-month count (Fig. 3a) further highlights the pronounced multidecadal variability of drought occurrence. According to SPEI-3, the 2010s experienced the highest drought-month frequency since the beginning of the pre-industrial period, with 35 drought months (29% of the decade) in ERA5. Western Germany was particularly affected, locally exceeding 40 drought months during the decade. Conversely, the 1910s experienced only five drought months (4%) according to ModE-RA. These values contrast with the climatological frequency of approximately 20–23 drought months per decade (Fig. 3b), close to the 16% expected from the standardised drought threshold (SPI/SPEI < -1). The SPI-3 perspective differs substantially (Fig. S4). In particular, the 2010s no longer emerge as an exceptionally dry decade, exhibiting the largest differences between SPI-3 and SPEI-3.

4.2 Hydroclimatic trends

Year-round SPI-3 and SPEI-3 exhibit contrasting long-term trends (Fig. S5). SPI-3 indicates a long-term wetting over the past 180 years, consistent with increasing 3-month precipitation in all reanalyses (Fig. 4a), with high statistical confidence for ModE-RA and ERA5. In contrast, SPEI-3 exhibits no significant long-term trend, indicating that increasing AED has offset much of the precipitation increase. The strongest increases in both precipitation and AED occur during the most recent period, consistent with accelerated warming. Indeed, their increases per degree of warming are consistent across the three reanalyses (Table S2), despite their different temporal coverage. Warming itself accelerated over time, reaching 0.42 K per decade during 1990–2023 in ERA5.

Seasonal trends reveal a marked contrast between winter and summer. Winter exhibits widespread wetting in both indices, particularly over 1844–2008 (ModE-RA) and 1947–2023 (ERA5), driven by increasing precipitation that outweighs the comparatively small increase in AED, despite substantial warming (Fig. 4a). Conversely, summer shows the strongest increase in AED, which largely offsets increasing precipitation in ERA5 and 20CRv3, resulting in SPEI-3 drying (low statistical confidence, Fig. S5). Over 1844–2008, ModE-RA indicates summer drying because of both increasing AED and decreasing precipitation. However, this pattern is not reproduced by ERA5 or 20CRv3 over their common period with ModE-RA (Fig. S6), nor by the station observations (Fig. S7).

Spring and autumn generally exhibit intermediate behaviour between the winter and summer extremes (Fig. 4a). Over 1844–2008 and 1918–2015, increasing AED offsets precipitation increases, producing little change in SPEI-3. During 1947–2023, spring is more similar to summer, with SPI-3 wetting but SPEI-3 drying (low statistical confidence), whereas autumn closely resembles winter, with wetting in both indices (high statistical confidence for SPI-3, moderate for SPEI-3). However, station observations do not support the autumn wetting, except at De Bilt, while Uccle shows a statistically significant SPEI-3 drying trend (Fig. S8). The seasonal divergence between SPI-3 and SPEI-3 is greatest in spring over 1844–2008, followed by autumn (Fig. S5), indicating a comparatively strong influence of AED despite smaller absolute increases than in summer.

While the previous results describe aggregated regional trends, local analyses reveal spatial variability (Fig. 4b–c). Agreement between reanalyses is lower locally than regionally (Fig. S8), and correspondence with station observations is less consistent. Nevertheless, several spatial features emerge. Year-round local trends broadly follow the regional signal, except for a significant SPEI-3 wetting along the Dutch coast during 1947–2023. Winter exhibits widespread wetting across the region, in agreement with the station observations. In contrast, spring and summer drying patterns vary spatially and reflect both decreasing precipitation and increasing AED, whereas autumn displays relatively homogeneous wetting despite slight SPEI-3 drying at Uccle.

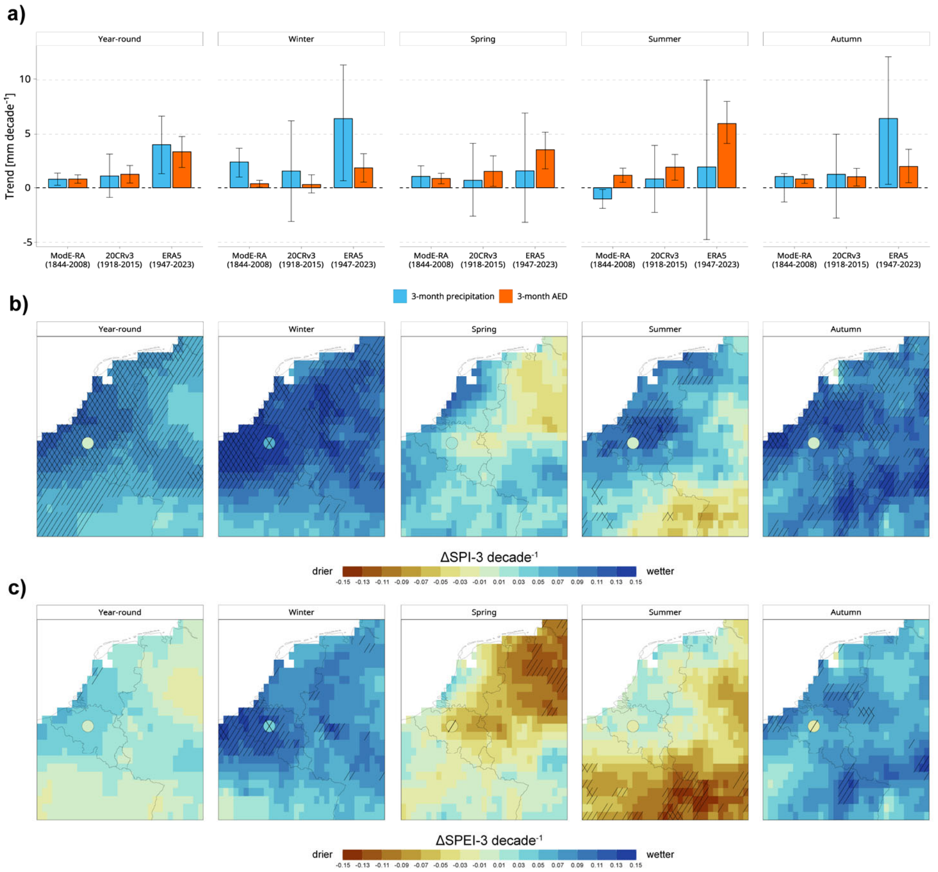

Figure 4: (a) Year-round and seasonal trends per decade in 3-month precipitation and AED for each period–reanalysis combination, estimated using Sen's slope. Error bars indicate the 95% confidence interval of Sen's slope, accounting for the variance correction proposed by Hamed and Rao (2008). Sen's slope maps of year-round and seasonal SPI-3 (b) and SPEI-3 (c) per decade over 1947–2023 (ERA5). Discs represent the Sen's slope of SPEI-3 at the Uccle weather station over the same period, the only station in the datasets used in this study with a continuous record spanning 1947–2023. A single diagonal line indicates a modified Mann–Kendall test *p*-value < 0.05, whereas two crossing diagonal lines indicate $p < 0.001$.

4.3 Atmospheric circulation patterns

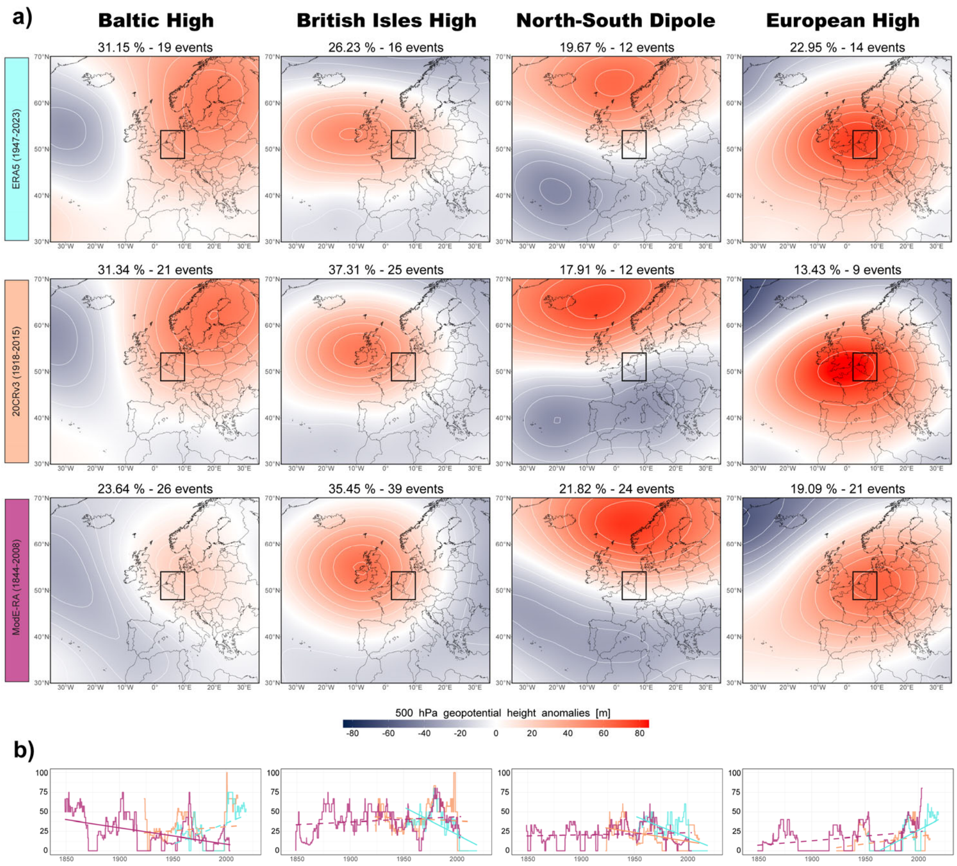

Figure 5: Atmospheric circulation patterns identified from SPEI-3 drought-based clustering (a) and associated drought occurrence trends (b). (a) Cluster centroids of 500 hPa geopotential height anomalies (reference period: 1947–2008) for each period–reanalysis combination. The numbers above each map indicate the percentage and number of drought events assigned to the corresponding cluster within each period–reanalysis combination. The western Central Europe region is delineated by the black box. The interval spanning from 2011 to 2023 was marked by successive periods of droughts in western Central Europe, as evidenced by the ERA5 dataset, particularly regarding SPEI-3 droughts (29.23 SPEI-3 drought months per

decade). Thanks to the consideration of long-term datasets, similar periods have been observed, for both drought types, in the last 180 years: 1857-1874 (31.67 SPEI-3 drought months per decade for ModE-RA) and 1947-1960 (29.29 to 34.29 SPEI-3 drought months per decade depending on the reanalysis). Conversely, periods of relatively low number of droughts (both types) occurred: over 1912-1920 (1.56 SPEI-3 drought months per decade for ModE-RA) and 1977-1988 (6.67 to 8.33 drought months per decade depending on the reanalysis). To evaluate the evolution of drought more consistently, a comparison of the drought-month frequency across decades was also conducted (Fig. 5). This analysis reveals the high multidecadal variability of the droughts over western Central Europe. Considering SPEI-3, the 2010s has been identified as the decade with the highest frequency of drought months since the pre-industrial period (1850). This finding is supported by ERA5, which shows that 35 months (29 % of the decade) of drought accumulated over the entire region (Fig. 5a). Western Germany was particularly impacted, with areas experiencing more than 40 months of drought. Conversely, the 1910s exhibited an exceptionally low frequency of droughts, with only 5 months (4 %) of droughts according to ModE-RA. These decades are particularly extreme in comparison to the climatology (Fig. 5b), which shows approximately 17 to 19 % of months per decade characterised by drought. This is close to the 16th driest conditions assumed by the definition of the drought indexes (Section 4.1).

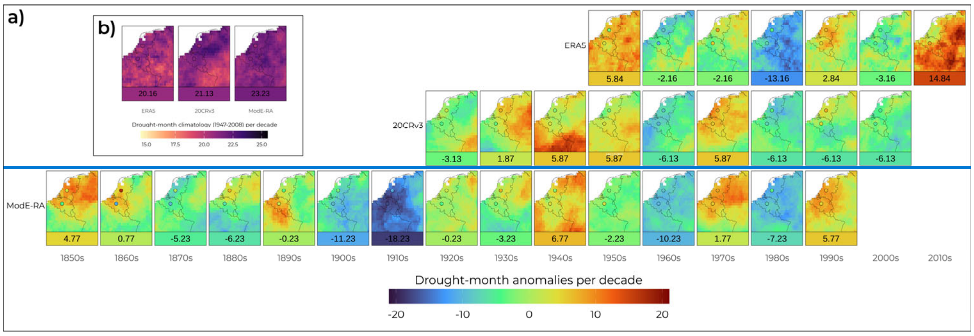

Figure 5: (a) Cumulative SPEI-3 drought-month anomalies for each dataset (row) for each complete decade (column). The anomalies refer to the (b) SPEI-3 drought-month climatology (1947-2008). The values for the aggregated region are displayed below the related maps. The discs represent the values at the weather stations that fully cover both the related decade and the reference period.

To gain insight into the homogeneity of the drought phenomenon, the correlation between the mean dryness in western Central Europe and the drought area involved was examined. The correlation was found to be strong, with values ranging from 0.77 to 0.81 for SPEI-3 and from 0.81 to 0.84 for SPI-3. It is noteworthy that SPI-3 demonstrates a stronger correlation compared to SPEI-3 across all datasets. Most of the extreme droughts affected the whole area at their peak (area involved =

1). More generally, the spatial variability of the drought indexes within the study area is rather small (e.g. mean standard deviations of SPEI-3 and SPI-3 values within the area for ERA5 are 0.45 and 0.47 respectively) and exhibits small variations over time, which verifies the homogeneity of the climate of the region as originally supposed in Section 2. Nevertheless, it is noteworthy that the nature of the drought index has an impact on the changes in variance. When drought periods are only considered, the mean standard deviations of SPEI-3 and SPI-3 within the area for ERA5 are found to be 0.36 and 0.53, respectively. In fact, for all SPEI-3 values, the wetter, the larger the variance within the area, which is the opposite for SPI-3 values (correlation of 0.14 for SPEI-3 and -0.21 for SPI-3 with standard deviation values for ERA5).

6.2 Dryness trends

A divergence of trends in dryness is observed between different drought indexes. On the one hand, SPI-3 has exhibited a decrease in year-round dryness over the past 180 years, as evidenced by the increasing trend of the index across the three datasets. This result is achieved with very high confidence during the period 1844-2008 (ModE-RA, p-val < 0.001) and 1947-2023 (ERA5, p-val = 0.009), and medium confidence during the interval 1918-2015 (20CRv3, p-val = 0.227) (Fig. 6a). The Sen's slopes over the full period covered by the reanalyses are almost equal for the periods 1844–2008 and 1918–2015 (ModE-RA and 20CRv3), with an increase in the index of 0.018 and 0.02 per decade, respectively. The increase in the SPI-3 was found to be 0.074 per decade over the period 1947-2023 (ERA5), which indicates that it increased by more than 0.57 standard deviations. This is substantially higher than the values observed in the periods 1918-2015 (0.20 – 20CRv3) and 1844-2008 (0.30 – ModE-RA). However, the differences observed between these periods may stem from the reanalyses utilised, given that over the common period (1947-2008): the trends for SPI-3 are approximately 0.116/decade, 0.077/decade and 0.011/decade for ERA5, 20CRv3 and ModE-RA, respectively (Fig. S6). Given the superior performance of the 20CRv3 and ModE-RA rates at the Uccle and De Bilt weather stations over the 1947-2008 period (Fig. S3), it can be deduced that the SPI-3 increase over the 1947-2023 period (ERA5) is likely to be overestimated. The observed decrease in dryness corresponds to increases in year-round three-month precipitation anomalies of 34.24 mm over 1947-2023 (ERA5, likely overestimated), 10.88 mm over 1918-2015 (20CRv3) and 13.58 mm over 1844-2008 (ModE-RA). From 1990 onwards, the year-round warming over the area is of particular importance. For instance, the ERA5 dataset demonstrates an increase of up to 0.40°C/decade until 2023, larger than 0.22°C/decade when assessed over the entire time span of 1947 to 2023. Precipitation have increased at a rate of 9.1 % per degree Celsius of warming (hereafter % $°C^{-1}$) over 1947-2023 (ERA5), 5.9 % $°C^{-1}$ over 1918-2015 (20CRv3) and 6.2 % $°C^{-1}$ over 1844-2008 (ModE-RA). However, the reanalyses do not reach a consensus over the common period (19 % $°C^{-1}$, 13.7 % $°C^{-1}$, 2.1 % $°C^{-1}$).

On the other hand, year-round dryness for SPEI-3 exhibited no changes for the corresponding periods (Fig. 6a), except for a slight decrease over 1947-2023 (ERA5) with very low confidence (p-val = 0.64). This finding indicates that AED has been counteracting the rise in precipitation over time. This is further evidenced by the difference between the two indexes (SPI-3 – SPEI-3) that has been increasing (Fig. 6a). For all three datasets, this difference is especially increasing since 1990, with rates between 0.071 and 0.117 per decade (instead of 0.045 to 0.057 per decade over 1947-2008), coinciding with the intensification of warming.

Behind the year-round behaviour, dryness at the seasonal scale shows strong divergences. The most pronounced contrast is observed between the winter and summer dryness. Winter dryness for both indexes has been strongly decreasing with medium to high confidence over 1947-2023 (ERA5) and 1844-2008 (ModE-RA) and slightly decreasing with low confidence over 1918-2015 (20CRv3) (Fig. 6). However, the confidence in these trends is diminished as winter slopes diverge between reanalyses over the common period (1947-2008) (Fig. S6). Furthermore, winter dryness trend magnitude is larger than the year-round behaviour over the three respective periods. Additionally, the trend of the difference between both indexes (SPI-3 – SPEI-3) for winter is very small despite a strong increase in winter PET across all datasets over time. For instance, for the ERA5 dataset (1947-2023), the increase in winter PET has been of 33.6% °C^{-1} but this represents only 14.65 mm of 3-month precipitation anomaly increase, while the increase in winter precipitation has been 49.99 mm with 12.6% °C^{-1}. Spatially, the decrease occurs across the entire region (as shown over 1947-2023, Fig. 6b), a finding that aligns with the four weather station records utilised in the data evaluation. Nevertheless, the decrease in dryness has been more pronounced in the north-western part of the region during the 1947-2023 (Fig. 6b) and 1844-2008 periods. In contrast, the 1918-2015 period exhibits an opposing spatial gradient. Nonetheless, spatial differences for seasonal and year-round trends between periods should be considered with a low confidence level, as evidenced by inconsistencies that emerge between reanalyses over the common period, particularly with the ModE-RA dataset (Fig. S6).

Conversely, there has been an increase in summer dryness for both indexes over 1844-2008 (-0.023 and -0.044 per decade for SPI-3 and SPEI-3, respectively). However, the reliability of this finding may be questionable. Over the common period (1947-2008), ModE-RA dryness increased by -0.091 and -0.153 per decade for SPI-3 and SPEI-3, respectively. These increases are considerably higher than the two other reanalyses (0.051 and -0.017 for ERA5, 0.008 and -0.057 for 20CRv3) that spatially fit with the Uccle and De Bilt weather stations. Furthermore, SPEI-3 dryness has increased over the 1918-2015 and 1947-2023 periods, albeit with low confidence over the entire region. This is attributable to diverging spatial differences within the area. For instance, over 1947-2023 (Fig. 6b), dryness decreased in the north to north-western part of the region, while it has been increasing in the southern and eastern. In the contrary, summer dryness exhibited by SPI-3 has shown a decline of 0.016/decade and 0.035/decade, with a low confidence level, over the periods 1918-2015 and 1947-2023. The opposite trend directions exhibited by SPEI-3 and SPI-3 over 1918-2015 and 1947-2023 may be attributable to the fact that the time span under consideration is more recent and therefore underwent a pronounced warming. This is evidenced by the increase in summer temperature per decade, which has been recorded to be 0.06°C, 0.09°C, and 0.275°C (1844-2008, 1918-2015, and 1947-2023, respectively). This is also evident in the summer PET trend per decade, with 1.18, 1.925, and 6.305 mm, in comparison to -6.94, 3.82, and 5.24 mm per decade for summer precipitation (-6.93, 3.82, and 5.24% °C^{-1}).

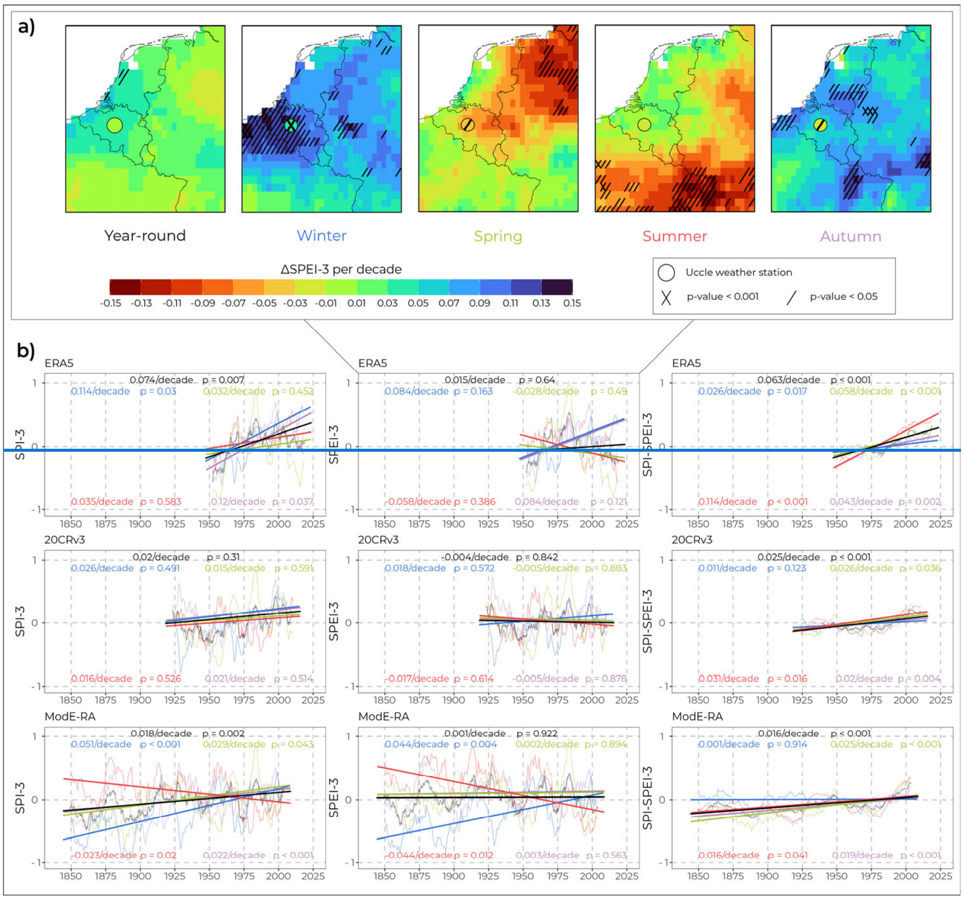

Figure 6: (a) Sen's slope maps of year-round and season SPEI-3 values per decade over 1947-2023 (ERA5). The discs represent the Sen's Slope for SPEI-3 values for Uccle weather station over the same period. Cross and diagonals represent the MMKH p-values. (b) 10-year moving average time series of year-round and seasonal SPI-3 values (first column), SPEI-3 values (second column), and the difference between SPI-3 values and SPEI-3 values (third column) in western Central Europe for each dataset (each row). The colours refer to the timeframe indicated in (a). Sen's slopes of raw values of each drought index (not 10-year moving average) are illustrated with straight lines and p-value of each MMKH trend test of raw values of each drought index is written for year-round and seasons in the corresponding colour.

Both autumn and spring dryness exhibited a similar trend to that of the year-round over 1844-2008 and 1918-2015, situated between the summer and winter trend extremes (Fig. 6). Over the period 1947-2023, spring trend magnitudes (0.032 per decade for SPI-3) have exhibited a greater similarity to those of summer trends. In a similar manner, the magnitude of autumn trends (0.12 per decade for SPI-3) is comparable to or equivalent to that of winter trends. SPEI-3 spring dryness has been marginally increasing over the 1947-2023 (low confidence) as well as over 1918-2015 (very low confidence). However, the increase in spring dryness in the north-eastern part of the region over 1947-2023 is particularly large (high confidence). The areas exhibiting increased spring dryness are not congruent with those identified in the summer. Likewise, the spatial patterns exhibited by autumn dryness trends deviate from those observed in winter trends. Consequently, year-round dryness is more spatially homogeneous than at the seasonal scale. Ultimately, spring followed by autumn have the largest seasonal increasing difference between SPI-3 and SPEI-3 over 1844-2008 (more than summer) (high confidence).

6.3 Atmospheric circulation patterns

(b) Ten-year moving fraction (%) of drought events associated with each cluster, using the same colours as in (a). Straight lines represent linear regressions fitted to the moving fractions. Solid lines indicate statistically significant trends according to the modified Mann–Kendall test ($p < 0.05$), whereas dashed lines indicate non-significant trends ($p \geq 0.05$).

Four atmospheric circulation patterns have been identified as being associated withfrom the clustering of Z500 anomalies during drought events defined by SPEI-3 (Fig. 7)(Fig. 5a) and SPI-3 (Fig. S7) seasonal drought events:S9a): a high Z500 anomaly centred over the Baltic region; a high Z500 anomaly centred over the British Isles; a dipole of a high Z500 anomaly over Northern Europe and a low Z500 anomaly over Southern Europe; and a high Z500 anomaly centred over the European continent. Henceforth theseThese patterns are hereafter referred to as Baltic High, British Isles High, North-–South Dipole, and European High, respectively. The circulation patterns exhibited by each period are consistent for both clustering, with some minor exceptions. RegardingFor SPEI-3 clustering, the Baltic High over the period 1844-2008 (ModE-RA), is less clearly defined in ModE-RA (1844–2008) than over 1918-2015 (in 20CRv3 (1918–2015) and ERA5 (1947-–2023 (ERA5). With regard to). For SPI-3 clustering, the centre of the European High is slightly shifted towards the British Isles over 1844-2008 (in ModE-RA) and 1918-2015 (20CRv3).. The consistency exhibited is not as robustcirculation patterns identified over the common reference period (1947-2008), which may be attributable to an insufficient number of 2008) exhibit lower spatial agreement between reanalyses than those identified over their respective full periods, likely because fewer drought events to ensure representativeness and the potential repetition of thoseare available to robustly characterise the patterns.

In general, droughts have been associated more frequently with the The British Isles High (26.23% to –37.31% for% of SPEI-3 clusteringdroughts depending on the reanalyses) and the Baltic High (23.64% to 24–31.34%), and less frequently%) are the most frequent circulation patterns associated with drought, whereas the North-–South Dipole (17.91% to 21.82%) and the European High (13.43% to 22.95%) (Fig. 7). Also, theoccur less frequently. The Baltic High is more often associated with SPEI-3 droughts than with SPI-3 droughts. Conversely, , whereas the opposite is true for the British Isles High is more associated with SPI-3 droughts than SPEI-3 droughts. SPEI-3 seasonal droughts have been increasingly associated with the European High over 1947-2023 and 1948-2015 (high confidence), and 1844-2008 (medium confidence). SPI-3 seasonal droughts have also been(Fig. 5a; Fig. S9a). Over time, droughts have become increasingly associated with the European High over 1947-2023 (in all reanalyses for both indices (moderate to high statistical confidence) and). An increase in association with the Baltic High (medium confidence). Conversely, droughts for both indices over 1947-2023 have been decreasingly associatedis also observed over 1947–2023. Conversely, associations with the British Isles High and the North-–South Dipole (high confidence).

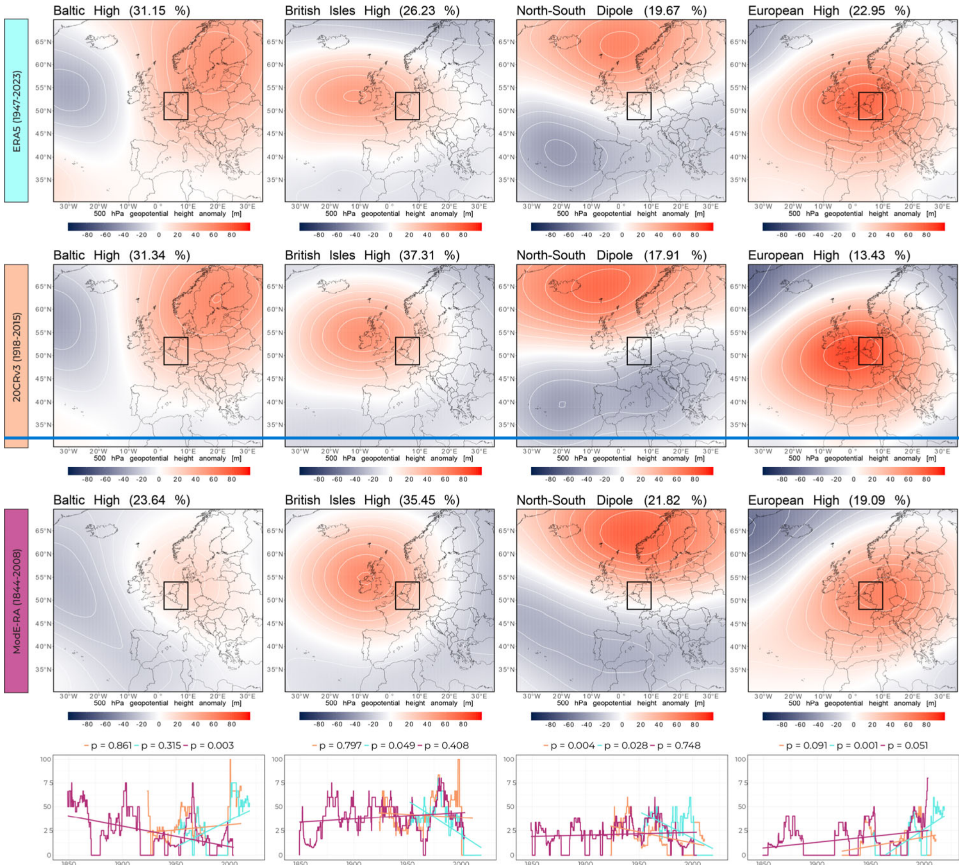

Figure 7: Atmospheric circulation patterns and associated drought occurrence trends. The three upper rows indicate the 500 hPa geopotential height anomalies (reference period: 1947-2008) of the centroids from the clustering for each period-reanalysis. The proportion of each cluster within the related period-reanalysis is shown in brackets. The final row indicates the 10-year moving fraction of the droughts associated with the related cluster (column). The straight lines in the graphs represent related linear regressions, whilst the p-values correspond to related MMKH trend tests. The colours refer to the related period-reanalysis indicated in the three first rows. The western Central Europe region is delineated by the black box.

In addition to the k-means clustering, the atmospheric circulation has been averaged over seasons characterized by drought events for the three reanalyses, which demonstrate highly similar results. The mean pattern for winter exhibits characteristics akin to a dipole, reminiscent of the North-South Dipole, albeit shifted towards the south. In contrast, the mean patterns for spring, summer, and autumn manifest as a monopole, exhibiting high similarities between each other. Specifically, the mean pattern for spring is in close proximity to the European High, albeit with the high shifted towards the North Sea; the mean pattern for summer is in close proximity to both the British Isles High and the European High, with the latter centred on the east coast of the British Isles; and the mean pattern for autumn is very close to the British Isles High. This can be attributed to the occurrence of droughts associated with the North-South Dipole, which primarily manifestdeclined during winter months. Winter droughts have been identified as a primary feature of the North-South Dipole (Fig. 8c and 1947–2023 in ERA5 (high statistical confidence) (Fig. S8c and5b; Fig. S9c). Droughts associated with the European High, in particular, have been observed to occur during the spring months, while the Baltic High and the British Isles High have been linked to drought conditions throughout the year. Also, autumn droughts have been shown to be almost exclusively associated with the Baltic High and the British Isles High, especially over 1918-2015 (20CRv3) and 1947-2023 (ERA5S9b).

a mis en forme : Retrait : Première ligne : 0,75 cm

The link between the three first natural modes of variability (North Atlantic Oscillation, NAO; East Atlantic pattern, EA; Scandinavian pattern, SCA) and the atmospheric circulation patterns associated with the seasonal droughts are presented in Fig. 8a, Fig S8a, and Fig. S9a for SPEI-3. The Baltic High has been found to be strongly associated with the positive phase of SCA (SCA+) over the period 1918-2015 (mean indexes are 0.09 for both SPEI-3 and SPI-3) and 1947-2023 (mean indexes are 0.14 and 0.12 for SPEI-3 and SPI-3, respectively), and EA+ over 1947-2023 (mean indexes are 0.14 and 0.12 for SPEI-3 and SPI-3, respectively); the British Isles High is associated with the negative phase of EA (EA-) for both indexes and across all periods (mean indexes are within the range from -0.03 to -0.09); the North-South Dipole with NAO- over 1918-2015 (mean indexes are -0.10 for both SPEI-3 and SPI-3) and strongly with SCA+ for both indexes and across all periods (mean indexes are within the range from 0.09 to 0.14); the European High is associated with NAO+ over 1844-2008 (mean indexes are 0.07 for both SPEI-3 and SPI-3), and especially over 1918-2015 (mean indexes are 0.2 and 0.19 for SPEI-3 and SPI-3, respectively). With regard to the three first natural modes of variability in relation to all drought events at the seasonal scale (see Fig. S10), for both drought indexes across all periods: winter droughts are associated with the EA- (-0.05 to -0.06), and SCA+ (0.07 to 0.14); spring droughts have weak associations; summer droughts are associated with NAO+ (0.04 to 0.11); autumn droughts are associated with NAO+ (0.03 to 0.12).

In general, during each period, droughts associated with the Baltic High and the European High exhibited higher PET anomalies compared to the other two groups, particularly the European High, which consistently demonstrated positive values (Fig. 6b, Fig. S8b and Fig. S9b). Conversely, droughts associated with the North-South Dipole have almost systematically negative PET anomaly values. It is evident that the absolute magnitude of precipitation anomalies associated with all drought events is significantly higher than that of PET anomalies. This indicates that precipitation has been the predominant factor contributing to drought conditions in the water balance in western Central Europe, rather than AED. However, an examination of the evolution of anomalies in droughts over time (Fig. S11) reveals that for both indexes over the periods 1918-2015 and 1947-2023, while PET have increased, precipitation deficit has decreased (high confidence). Consequently, the role of AED has been increasing in comparison to precipitation deficit, which has been decreasing.

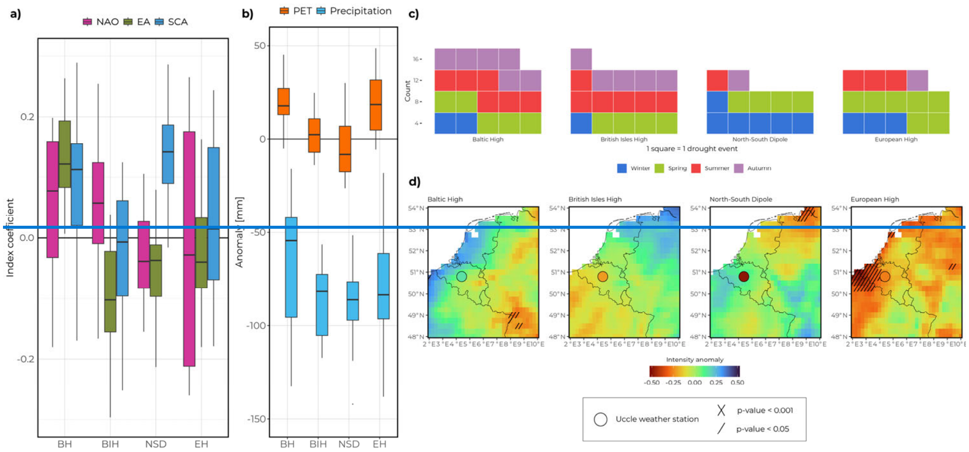

Figure 8: Atmospheric circulation pattern characteristics for SPEI-3 drought-based clustering over 1947-2023 (ERA5). (a) Boxplot of seasonal EOFs indexes values. (b) Boxplot of 3-month- potential evapotranspiration (PET) and -precipitation anomalies (reference period: 1979-2008). (c) Waffle chart of season occurrence. (d) Maps of SPEI-3 mean drought intensity anomalies: difference of the mean cluster-related SPEI-3 of drought with the mean SPEI-3 of droughts over 1947-2008. The discs represent the SPEI-3 mean drought intensity anomaly for Uccle weather station over the same period. Cross and diagonals represent the t-test p-values between those two groups. BH, BIH, NSD, and EH stand for the Baltic High, the British Isles High, the North-South Dipole, and the European High.

Droughts associated with the North-South Dipole exhibited reduced intensity for both drought indexes, particularly in the middle and southern regions of western Central Europe (Fig. 8d), across all the periods (Fig. S8d and Fig. S9d). The intensity gradient of the drought is observed where the most intense parts coincide with the high Z500 anomaly in atmospheric circulation; thus, indicating a higher drought intensity in the eastern regions of the study area for the Baltic High, whilst the opposite is true in the western regions for the British Isles High. It is evident that SPEI-3 droughts associated with the European High over 1947-2023 (ERA5) and 1918-2015 (20CRv3) are more intense than with the other patterns. Particularly, a high degree of intensity is being observed over the western part of Belgium and the northernmost part of France. The principal factor responsible for this discrepancy in intensity when compared to other circulation patterns

~~is the elevated AED anomalies associated with the European High, given that this pattern is no longer as pronounced when assessed through SPI-3 droughts.~~

~~7~~The first three dominant modes of variability identified from the EOF analysis correspond to the North Atlantic Oscillation (NAO), the East Atlantic (EA) pattern, and the Scandinavia (SCA) pattern (Barnston and Livezey, 1987; Hernandez and Comas-Bru, 2025; Topál et al., 2025) (Fig. S10). The Baltic High is primarily associated with SCA+ and, to a lesser extent, EA+, whereas the British Isles High is associated with EA−. The North–South Dipole combines SCA+ with NAO−, while the European High is mainly associated with NAO+ over 1844–2008 and 1918–2015 (Fig. 6a; Figs. S11a–S12a).

Winter droughts occur predominantly under the North–South Dipole, spring droughts under the European High, whereas the Baltic High and British Isles High occur throughout the year (Fig. 6b; Figs. S11b–S12b). Autumn droughts are almost exclusively associated with these latter two patterns. In terms of the dominant modes of variability, winter droughts are characterised by EA− and SCA+, summer and autumn droughts by NAO+, whereas spring shows only weak relationships with the dominant modes (Fig. S13).

Droughts associated with the Baltic High and especially the European High exhibit the largest positive AED anomalies, whereas the North–South Dipole is generally characterised by negative AED anomalies (Fig. 6c; Figs. S11c–S12c). Although the magnitude of precipitation anomalies remains substantially larger than that of AED anomalies, AED anomalies associated with droughts increased over time, whereas precipitation anomalies weakened across all periods, particularly over 1947–2023 (Fig. S14).

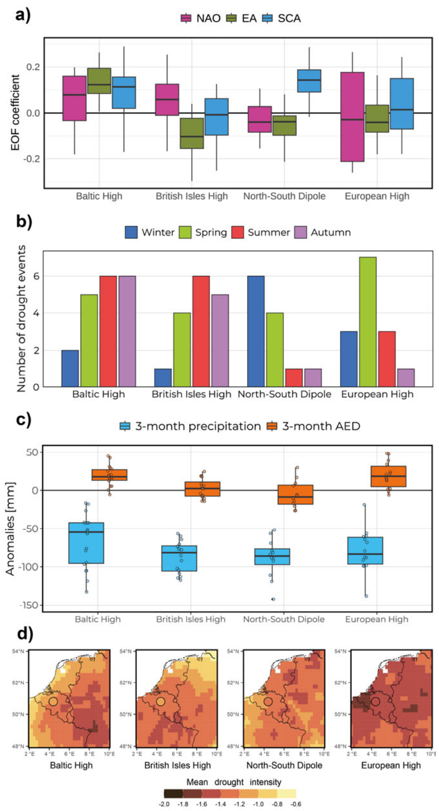

Figure 6: Atmospheric circulation pattern characteristics associated with SPEI-3 drought-based clustering over 1947–2023 (ERA5). (a) Boxplots of EOF coefficients from seasonal EOF analyses of the full Euro-Atlantic record for drought events associated with each circulation pattern (all seasons pooled). (b) Seasonal distribution of drought events for each circulation pattern. (c) Boxplots of 3-month atmospheric evaporative demand (AED) and precipitation anomalies for each cluster, with individual events shown as jittered points. For (a) and (c), the black line indicates the median, the box boundaries represent the first and third quartiles, and the whiskers extend to the most extreme values within 1.5 times the interquartile range (IQR). Values beyond the whiskers are shown as individual outliers. (d) Maps of the mean SPEI-3 drought intensity for each cluster. Discs represent the mean SPEI-3 drought intensity at the Uccle weather station over the same period, the only station in the datasets used in this study with a continuous record spanning 1947–2023.

Drought intensity also varies with the associated circulation pattern (Fig. 6d; Figs. S11d–S12d). The North–South Dipole is associated with the weakest droughts, particularly over the central and southern parts of western Central Europe. Baltic High events are associated with stronger droughts over the southeastern part of the region, whereas British Isles High events are associated with stronger droughts over the western part. The European High is associated with the most intense SPEI-3 droughts over 1918–2015 and 1947–2023, especially over western Belgium and northern France. This enhancement is much less pronounced for SPI-3 (not shown), consistent with the larger positive AED anomalies associated with the European High.

5 Discussion

75.1 Long perspective on recent events

Recent severe droughts, such as the 2018 drought, have attracted considerable attention in the literature (e.g. Bakke et al., 2020). The findings of the present study indicate that these droughts have historical precedents in western Central Europe, in agreement with other studies (Vicente-Serrano et al., 2021), such as that in 1857 (Hanel et al., 2018), 1921 (Bonacina, 1923; Briffa et al., 1994; Hanel et al., 2018; Bertrand et al., 2021; van der Schrier et al., 2021), 1947 (Lhotka et al., 2020), 1953 (Hanel et al., 2018; Hänsel et al., 2019), 1976 (Feyen and Dankers, 2009; Hanel et al., 2018; Hänsel et al., 2019), 2011 (Hänsel et al., 2019). While the present analysis enables long retrospective investigations, it does not extend sufficiently to encompass certain historical droughts, such as that experienced in 1842 (Brázdil et al., 2019). However, it does allow for the inclusion of the particularly severe drought that occurred in 1921. This was the most severe in the whole Europe since the beginning of the twentieth century according to van der Schrier et al. (2021), the most severe in Central Europe in the last 250 years according to Hanel et al. (2018), and the most severe of the past 180 years in western Central Europe according to the present study. From the perspective of precipitation alone, it is not unexpected to observe the most extreme drought occurring in the distant past, given that year-round SPI-3 trends have exhibited an upward trajectory over the course of time. In consideration of the AED and the long-term stable trend of the SPEI-3, a more recent occurrence of drought comparable to the severity of that experienced in 1921 would not have been unexpected, given the natural variability. The 1921-drought is notable for its long persistence (van der Schrier et al., 2021) (14 months for ModE-RA for SPEI-3), rather than its peak or intensity. As demonstrated by Hanel et al. (2018), Hänsel (2020), and van der Schrier et al. (2021), when considering solely the vegetation period, the 1921-drought is no longer the most severe, but rather more recent ones (1947, 2003 and 2018).

Similarly, evidence indicates that successive intense drought periods, akin to those experienced in 2011-2023, have occurred in the past, specifically over 1857-1874 and 1947-1960, separated by periods of very low numbers of droughts as seen over 1912-1920 and 1977-1988. This high multi-decadal variability has also been reported in the literature (Hänsel, 2020), with dry and wet decades similar to those previously cited (Briffa et al., 1994; van der Schrier et al., 2006; Haslinger et al., 2019; Hänsel et al., 2019; Bertrand et al., 2021; Lekarkar et al., 2025). Especially, the 2010s have been identified as the worst decade in terms of the frequency of drought months over western Central Europe since the 1850s, extending the findings of Lekarkar et al. (2025) over Belgium. In order to elucidate this high multidecadal variability, teleconnection patterns have also been investigated. No substantial correlation was identified between the low-frequency dryness in western Central Europe and the NAO index or the El Niño–Southern Oscillation (ENSO). However, a correlation was observed with the Atlantic Meridional Oscillation (AMO), particularly in ERA5 (-0.275 and -0.677 with 20-year moving average SPI-3 and SPEI-3, respectively). Precipitation rates in western Central Europe may not be directly linked to the Atlantic Multidecadal Oscillation (AMO), however, as the correlation with low-frequency SPI-3 dryness is much weaker than that of SPEI-3. This may be indicative of a relationship between high Atlantic sea surface temperature (SST) and high temperature in Western Central Europe, thereby driving SPEI-3 towards low values. Some studies have been linking Atlantic SST with Central Europe drying (e.g. Haslinger et al., 2019; Tuel and Eltahir, 2021; Haslinger and Mayer, 2023) but uncertainties remain. Furthermore, van der Wiel et al. (2023) found that multi-year droughts in a region analogous to western Central Europe were actually the coincidence of successive typical meteorological forcing, i.e. low precipitation and high AED, but found no evidence for multi-year processes. Given that multi-year droughts have been shown to have a greater impact than isolated events (Chen et al., 2025; Hoover and Smith, 2025), the underlying drivers should be a subject of interest. The highlighted decades may be considered relevant study cases for further investigation.

Furthermore, a robust correlation has been identified between the mean dryness in western Central Europe and the drought area concerned. This finding is in accordance with the expected relationship between these variables, with the former being dependent on the latter. This further underscores the strong homogeneity of the drought phenomenon within the region. In addition, when considering AED, the dryness variance within the region is smaller during drought periods than during the entire period, meaning that the spatial homogeneity of the dryness is greater when a drought is occurring. Conversely, when precipitation is only considered, the dryness variance within the region is larger for drought periods than for the whole period, indicating that the spatial homogeneity of the dryness is reduced during drought. This might be attributable to the temperature, which exhibit greater homogeneity in comparison to the precipitation fields. Consequently, this would result in the spatial smoothing of the contribution of precipitation deficit differences within the drought index. Furthermore, the mean and peak drought area have exhibited a slight decrease for SPEI-3 droughts for all the periods (low confidence, not shown). However, in the absence of a change in year-round SPEI-3 dryness trends, this suggests that the heterogeneity of increasing precipitation may be taking precedence over the homogeneity of increasing AED over time. It is therefore hypothesised that spatial variations in drought conditions have increased, resulting in a greater prevalence of dry and wet spots. Consequently, it can be posited that mitigation strategies should encompass this growing spatial heterogeneity of dryness by implementing measures at the local scale, in addition to the regional scale, which remains important to consider, especially in the case of intense droughts, which are inherently more extensive, as has been demonstrated.

7.2 Dynamics behind the droughts

Four dominant atmospheric circulation patterns – the Baltic High, the British Isles High, the North-South Dipole, and the European High – were found to be consistently associated with seasonal drought occurrence over the past 180 years. The following paragraphs provide an overview of each atmospheric circulation pattern.

The **Baltic High** is associated with south-eastern wind anomalies over the region studied. Lhotka et al. (2020) showed that the southeasterly circulation type is conductive to drought in Central Europe. Conversely, the opposite direction of winds has been shown to be associated with wet and extreme precipitation events in Belgium (Brisson et al., 2011; Schoofs et al., 2025). Also, during summer in Belgium, continental air masses result in warmer days than with oceanic air masses (Serras et al., 2024). This is consistent with the above-average AED of droughts associated with this pattern. Likewise, continental air masses are typically characterised by drier conditions than oceanic air masses. The Baltic High is more associated with SPEI-3 droughts than with SPI-3 droughts, and this is connected to the non-negligible role of AED for those droughts. The drought intensity gradient within the region is likely attributable to the spatial proximity to the Z500 high. Indeed, Z500 anomalies and SPEI- exhibit a strong negative correlation across Europe (Kingston et al., 2015; Bakke et al., 2023). This is due to positive Z500 anomalies that diminish upward movement, thereby reducing cloud cover, which in turn decreases precipitation and increases incoming shortwave radiation, thus raising AED.

The droughts associated with the **British Isles High** are more precipitation-deficit driven than the Baltic High. This may be attributable to the fact that northerly wind anomalies are not especially linked with warmer conditions (Serras et al., 2024), which is consistent with the meridional temperature gradient. Moreover, the British Isles High is associated with EA- (in contrast to the Baltic High, which is associated with EA+). The EA pattern has been shown to exhibit a stronger correlation with temperature than with other climate variables (Hernandez and Comas-Bru, 2025), which would therefore explain the AED differences between those two patterns. Indeed, the British Isles High is more associated with SPI-3 droughts than with SPEI-3 droughts, which is consistent with the near-zero AED anomalies. Pauling et al. (2006) suggest that a very similar pattern to the British Isles High brings moist air over the Scandinavian mountains while the subsequent regions are left dry. They also linked this pattern to dry anomalies over Central Europe in winter for the past half millennium. Moreover, the observed pattern is comparable to the British Isles high (16 – HB) weather type from the European "Grosswetterlagen" classification system (Hess and Brezowsky, 1969), that has been associated with streamflow drought in Southern Germany (1962-1992) (Stahl and Demuth, 1999). Just as the Baltic High, the proximity of the Z500 high also explains the observed drought intensity gradient in western Central Europe with the British Isles High exhibiting a more pronounced intensity over Northern France compared to Western Germany.

The **North-South Dipole** is associated with easterly wind anomalies, and its influence being attributed to the difference in moisture content between air masses originating from inland regions and those from the ocean. Droughts associated with the North-South Dipole mostly manifest during winter, thereby explaining the negative anomalies of AED, as continental air masses are colder than oceanic air masses during this season due to the ocean heat capacity. Winter streamflow droughts were associated with eastern cold flow in Southern Germany (Stahl and Demuth, 1999). Also, winter SCA+, which is associated with the North-South dipole, is negatively correlated to both temperature and precipitation levels in Central Europe (Bladé et al., 2012; Simpson et al., 2024; Hernandez and Comas-Bru, 2025). Consequently, the overall less intense nature of the drought phenomenon associated with this pattern is explained by precipitation deficits being the sole driving factor. This also explains the greater association with SPI-3 droughts than with SPEI-3 droughts over 1918-2015 and 1947-2023.

The association with the **European High** pattern is unsurprising, given that a high anticyclonic circulation over Europe has been repeatedly associated with Western (Savary et al., 2025) and Central European droughts (Lhotka et al., 2020). A very similar pattern is also associated with European heatwaves in Stefanon et al. (2012), which is consistent with the substantial AED anomalies associated with the European High. During atmospheric blocking, this pattern gives rise to droughts and heatwaves, consequent to large-scale subsidence that results in cloud-free skies (Kautz et al., 2022). The strongly increasing association of droughts with the European High suggest that it may be an emerging and recurring pattern for CHDs, typical of warm spring droughts. Moreover, its increase is of relative importance for both SPI-3 and SPEI-, indicating that it is not solely heat-related but also associated with strong precipitation deficits as measured by the SPI-3. The observed association of this pattern with more intense droughts than those associated with other patterns may be consequently explained by the influence of both precipitation deficits and temperature.

7.3 Drivers of dryness trends

The present study shows that year-round precipitation in western Central Europe has increased at a rate of 6 to 9% C-1, depending on the period and dataset used. This rate is very close to the Clausius-Clapeyron rate (CC), which gives an increase in water vapour pressure at saturation of approximately 7% per degree. Drought events in western Central Europe are, in general, consistent with the prevailing trends of dryness. In addition, future projections in Belgium for extreme precipitation events also follow CC (Brajkovic et al., 2025), suggesting that the entire spectrum of year-round precipitation in the region is following CC over time. Concurrently, the highly temperature-dependent AED has been increasing, evidenced by the increase in the difference between SPI-3 and SPI-3, by an amount akin to the precipitation increase. This finding would indicate that the year-round water supply and demand trends have been predominantly influenced by warming in western Central Europe, with these trends compensating each other, thereby maintaining a constant SPEI-3 dryness over time. Thermodynamics alone could therefore be sufficient to explain the year-round dryness trends for both SPI-3 and SPEI-3. However, the year-round trend is actually a combination of divergent seasonal trends that cannot be explained by thermodynamics alone. Long-term annual and seasonal changes in rainfall patterns are primarily driven by dynamical changes, while their contribution to temperature changes is secondary (Hoffmann and Spekat, 2021; Dong and Sutton, 2025).

In this section will be addressed the role of changes in atmospheric circulation patterns, in addition to other drivers identified in the literature, in explaining the spatial and temporal trends in dryness for each season.

The decline in dryness has been more pronounced in **winter** (Moberg and Jones, 2005; Bertrand et al., 2021). Precipitation increased at higher rate than the CC, e.g. at 12.6% $°C^{-1}$ over 1947-2023. A decline in the association of drought events with the North-South dipole, the predominant drought pattern during winter, was observed. This could offer a possible explanation for the observed winter dryness trend, although this was only evident over 1947-2023, when the winter trend was particularly pronounced. Additionally, the drivers of this stronger rate may also be associate with dynamic changes that are not necessarily linked to droughts, but rather to the other tail of the distribution. For instance, the NAO has been identified as the predominant factor of winter precipitation trends in Northern and Southern Europe (Matti et al., 2009). The NAO winter series have exhibited an upward trend, at least since the mid-20th century (Visbeck et al., 2001; Hasanean et al., 2023), which might explain the observed increase in winter precipitation in western Central Europe, as the NAO has been demonstrated to be positively correlated to precipitation in north-west Europe during winter (Simpson et al., 2024). Anthropogenic forcing has also been detected in observed (Christidis and Stott, 2022). A further particularity of winter is that it demonstrates the smallest increasing difference between SPEI-3 and SPI-3. During the cold season, AED might still have a minimal effect on western Central Europe droughts in comparison to precipitation. This aligns with Tomas-Burguera et al. (2020), who argue that the utilisation of SPI-3 or SPEI-3 is approximately equivalent in humid regions during winter.

Spring dryness, for both types of indexes, has been roughly following the year-round dryness trends over 1844-2008 and 1918-2015, with precipitation rates following closely CC. However, over 1947-2023, SPEI-3 dryness has been increasing (middle confidence). As spatial disparities are demonstrated within the Western Central European region, a comparison with existing literature is not straightforward. For western Germany, in Hänsel et al. (2019), the trends observed over 1951-2015 align closely with those presented in this study over 1947-2023. Overall, spring dryness increase appears to be substantial in western Central Europe since the mid-20th century (Spinoni et al., 2018), especially over the last three to four decades (Spinoni et al., 2017; Baudewyn, 2023; Bešťáková et al., 2024; Douville et al., 2025), and particularly in April (Ionita et al., 2020). The recent shift in spring can be explained by changes in dynamics (Douville et al., 2025). Indeed, droughts have been increasingly associated with the European High pattern, especially in the last decades. This pattern associated with droughts, mostly manifest during spring. This finding aligns with the literature that has demonstrated the role of anticyclonic atmospheric circulation (Trnka et al., 2009; Lhotka et al., 2020; Bešťáková et al., 2024) during spring, especially the increase of blocking events coinciding with the presedfence of persistent anticyclonic pressure system over western Central Europe region. These systems are the main driver of the recent spring droughts (Ionita et al., 2015; Bakke et al., 2023). Trnka et al. (2009) demonstrated that circulation types conductive to drought remained stable until the 1940s (from 1881) and increased steadily afterwards, which is in accordance with the findings of the present study.

A marked increase in **summer** SPEI-3 dryness has been observed across all periods. Indeed, there has been an increase in summer dryness in most parts of Europe since the start of the 20th century, especially since the mid-20th century (Hänsel et al., 2022) and especially in Central Europe (Spinoni et al., 2019). However, precipitation rates are not consistent with CC, even in the opposite direction for 1844-2008 (-6.9 % °C^{-1}) (low confidence due to inconsistencies). A range of mechanisms have been posited to explain the observed increase in dryness during summer. The relative association of drought with atmospheric circulation patterns does not provide a comprehensive explanation of the evolution of the circulation patterns alone. Changes in summer drought geopotential heights (Fig. S12) do not correspond with specific patterns that have been associated with drought events. However, the changes indicate an increase in geopotential height anomalies across Europe during the three periods, particularly over the 1947-2023 interval. This finding aligns with the literature (Jacobeit et al., 2003; Trnka et al., 2009; Lhotka et al., 2020; Bešťáková et al., 2024), which has documented a persistent rise in anticyclonic conditions over Central Europe during summer, strengthening in the latter half of the 20th century and corresponding to the dryness trends. Furthermore, the role of AED, and thus temperature, is essential in driving SPEI-3 droughts, especially in summer where the strongest increase has been documented in the present study over 1947-2023. As posited by Vautard et al. (2023), the marked increase in temperature during summer in Central Europe can be attributed to an enhanced advection of warm air from Southern Europe. Atmospheric blocking systems have also been related to drivers of strong summer warming (Suarez-Gutierrez et al., 2020; Kautz et al., 2022) and increased dryness in Central Europe (Ionita et al., 2015). The persistent conditions during the summer months across Central Europe have been associated with the occurrence of an amplified hemisphere-wide wavenumber 7 circulation pattern – linked with a strongly meandering jet stream (Coumou et al., 2014; Kornhuber et al., 2020), that have increased over recent decades (Kornhuber et al., 2019), to a sufficient degree to emerge from the natural variability (Mann et al., 2017). It has also been proposed that Arctic amplification (see Coumou et al., 2014, 2015, 2018; Kornhuber et al., 2017) and the weakening of the Atlantic Meridional Overturning Circulation (AMOC, see Rousi et al., 2021; Ionita et al., 2022) might play a significant role in the interconnected processes that contribute to the increase in the persistence of anticyclonic conditions in Central Europe during the warm season. Finally, a pivotal mechanism that connects summer warming and drying in western Central Europe is the land-atmosphere feedbacks (e.g. Suarez-Gutierrez et al., 2020). These feedbacks would mainly occur during summer season in this region because the system needs to be soil-moisture limited. Conversely, the system in the other seasons would remain energy-limited due to excessive wetness, which hinders its capacity to influence evapotranspiration variability (Miralles et al., 2019). In response to warming, there is a northward shift of summer soil-moisture limited systems from the Mediterranean region (Seneviratne et al., 2006a). Consequently, soil moisture and temperature in western Central Europe are becoming increasingly coupled. In addition, climate model studies found that the drying occurring in spring triggers soil-moisture feedbacks (Stegehuis et al., 2021), which, in turn, exacerbate the circulation-driven warming (Douville et al., 2025) and drying (Tuel and Eltahir, 2021) during summer. For instance, during the dry decades of the 1860s and 1940s, substantial precipitation deficits in spring resulted in enhanced feedbacks in the subsequent summer (Haslinger et al., 2019).

Autumn dryness has followed the year-round dryness trends over 1844-2008 and 1918-2015, aligning closely with CC. Over 1947-2023, dryness trends are closer to the strong increase of the winter trends, which is in accordance with the literature (Spinoni et al., 2018). According to Ionita et al. (2015), autumn dryness variability in Central Europe is strongly related to the NAO, as further evidenced by the association of atmospheric circulation during autumn drought with NAO+ in the findings of the present study. However, no significant changes in NAO have been documented since the mid-20th century (Bladé et al., 2012; Hasanean et al., 2023). Cahynová and Huth (Cahynová and Huth, 2009) indicates a heightened frequency of westerly and north-westerly winds became more frequent in autumn in Central Europe during the latter half of the 20th century. This could provide a coherent explanation for the pronounced decrease in dryness observed since 1947. The drivers of autumn dryness have received less attention in the literature, as autumn is a transitional season without many impactful droughts to attract interest. However, given its contribution to the year-round dryness, further studies may be warranted to investigate the mechanisms and temporality of the shift between the drying of summer and the wetting of winter.

7.4 Challenges

A prevailing trend that is evident across all seasons and periods is the increasing role of AED. Concurrently, droughts have been marked by elevated temperatures, yet increased precipitation (Fig. S11). Even though precipitation remains the primary driver of the water balance in the western Central Europe region, the role of AED has evolved substantially, particularly since the 1990s. This is consistent with the role of AED in the recent global increase of drought severity, including in some humid regions (Gebrechorkos et al., 2025). Since 1990, western Central Europe has been a warming hotspot with a rate of 0.4°C/decade (ERA5). This rate is higher than the global mean (e.g. Dong et al., 2017; Yin et al., 2024; Douville et al., 2025) and thus western Central Europe is one of the regions displaying heightened sensitivity to AED (Wang et al., 2025). Therefore, recent droughts have been amplified by warming, while precipitation deficits have played a more significant role in earlier periods. Moreover, warming renders the probability of occurrence of CHDs increasing throughout Europe (Manning et al., 2019; Schumacher et al., 2024). This suggests the potential for heat-related atmospheric circulation patterns to emerge in association with droughts, as evidenced by the European High that was only scarcely associated with droughts prior to the second half of the twentieth century. However, this does not imply that other precipitation deficit-only patterns, such as the British Isles High, will progressively disappear in the association with drought in western Central Europe with warming. This is because precipitation deficits is a necessary condition for the onset of droughts. For instance, Tuel and Eltahir (2021) as well as Rousi et al. (2021), have demonstrated an increase of a similar pattern to the British Isles High in a warmer climate.

The increasing spring and summer dryness, concomitant with increased frequency of CHDs, is a matter of concern from an impact perspective. Indeed, spring and summer droughts are the most likely to be the most impactful, especially on the ecological aspect as it spans the growing vegetation period. Moreover, CHDs have been found to exert an even more significant impact than remote events in isolation (Zscheischler et al., 2020). Furthermore, an increase in spring and summer dryness does not exclude an increase in the opposite hydroclimate extreme. Indeed, the concurrence of drought and heavy precipitation events has increased since the second half of the 20th century, particularly in the western part of Central Europe during spring (Hänsel et al., 2022). Projections indicate an increase in both droughts (Lehner et al., 2017) and extreme precipitation events (Brajkovic et al., 2025) within the region. Consequently, the projected increase in climate variability (Rossi et al., 2023) must be a consideration in management strategies, encouraging mitigation effective for both droughts and heavy precipitation events, such as nature-based solutions offering a "sponge function" (e.g. Yimer et al., 2024).

Projections indicate a strengthening of seasonal divergence, characterised by a decline in summer precipitation (Böhnisch et al., 2021; de Vries et al., 2022) and a reduction in winter droughts (Böhnisch et al., 2021) in Central Europe. Land-atmosphere feedbacks may well amplify their role in modulating summer precipitation (Seneviratne et al., 2006b), 2006b) and temperature (Suarez-Gutierrez et al., 2020) variability in Central Europe during the 21st century. It is projected that dynamic changes will continue to play a role, but uncertainties remain on their relative importance. During summer, there may be a decline in the frequency of westerlies and an increase in the frequency of easterlies over Central Europe (Herrera-Lormendez et al., 2023). In addition, there may be an increase in anomalously high-pressure systems (Bakke et al., 2023). These would favour more continental, dry and warm air masses over the western Central Europe region. Nevertheless, CMIP6 models struggle to reproduce the spatial heterogeneity of the circulation changes (Bakke et al., 2023). Additionally, there is a paucity of models that can adequately predict the self-intensification of CHDs via the land-atmosphere coupling (Miralles et al., 2019). The present study, in conjunction with extant literature regarding historical trends, suggests that circulation changes have been the main driver of droughts. The literature suggests that land-atmosphere feedbacks may also have a significant role to play, albeit with a certain degree of uncertainty. Consequently, there is a necessity to enhance the reproduction of both processes in the models in order to more effectively anticipate future droughts that may be currently underestimated.

8Recent severe droughts, particularly the 2018 event, have attracted considerable attention (e.g. Bakke et al., 2020; Zscheischler and Fischer, 2020; Huang et al., 2021). However, the present results show that comparable events have occurred previously in western Central Europe, consistent with earlier studies (e.g. Vicente-Serrano et al., 2021). Notably, the 1921 drought (Bonacina, 1923; Briffa et al., 1994; Bertrand et al., 2021) emerges as the most severe event in western Central Europe over 1844–2023 and has likewise been identified among the most severe European droughts of the past centuries (Hanel et al., 2018; van der Schrier et al., 2021). This conclusion nevertheless depends on the metric considered. Based on precipitation alone (SPI-3), the most severe droughts occur predominantly during the earlier part of the record, in agreement with the long-term increase in precipitation. When AED is included (SPEI-3), recent droughts exhibit an increasing potential to reach comparable severity because of the growing contribution of AED to drought severity (Gebrechorkos et al., 2025). In the future, droughts similar to that of 2018 are expected to become even more severe, partly owing to increasing AED (van der Wiel et al., 2021; Aalbers et al., 2023). Moreover, the exceptional severity of the 1921 drought primarily reflects its persistence (14 months in ModE-RA) rather than its peak or mean intensity. During the growing season, more recent droughts (1947, 2003, and 2018) exceed the 1921 event in severity (Hanel et al., 2018; Hänsel, 2020; van der Schrier et al., 2021). Overall, these findings show that recent droughts are not unprecedented but differ from historical events in both their characteristics and underlying drivers, highlighting the importance of combining multiple drought indices (Lloyd-Hughes, 2014).

Beyond individual events, successive dry periods comparable to 2011–2023 occurred during 1857–1874 and 1947–1960, separated by relatively wet intervals during 1912–1920 and 1977–1988. This pronounced multidecadal variability agrees with previous studies (Briffa et al., 1994; van der Schrier et al., 2006; Haslinger et al., 2019; Hänsel et al., 2019; Bertrand et al., 2021). In particular, the 2010s constitute the decade with the highest drought-month frequency over western Central Europe since the 1850s, extending the findings of Lekarkar et al. (2026) for Belgium over the 1970–2020 period. To investigate the drivers of this multidecadal variability, teleconnection indices were examined, but no substantial relationship was found with the NAO, the El Niño–Southern Oscillation, or the Atlantic Multidecadal Oscillation. Although Atlantic SST variability has been linked to Central European drying (e.g. Haslinger et al., 2019; Tuel and Eltahir, 2021; Haslinger and Mayer, 2023), the associated mechanisms remain uncertain. Likewise, although prolonged periods of reduced precipitation and enhanced AED have been shown to favour multi-year droughts over western Central Europe, the underlying processes remain poorly understood (van der Wiel et al., 2023; van Mourik et al., 2025). Given the greater impacts of multi-year droughts compared with shorter droughts (Chen et al., 2025; Hoover and Smith, 2025; Ruijsch et al., 2025) and their expected increase under warmer climate conditions in western Central Europe (van der Wiel et al., 2023), the successive dry periods identified here provide useful case studies for future research.

5.2 Changing contribution of atmospheric evaporative demand

Because precipitation predominantly influences SPEI-3 in the relatively humid climate of western Central Europe (Raible et al., 2017; Tomas-Burguera et al., 2020), the contribution of AED to drought events was expected to be minor. However, although increasing AED has been offset by increasing precipitation, resulting in no long-term trend in SPEI-3, drought events have become increasingly characterised by larger AED anomalies relative to precipitation anomalies. In ERA5, this is reflected in seasonal drought events since 1990, which exhibit larger mean AED anomalies (24.3 vs. 7.3 mm) and less negative mean precipitation anomalies (−59.7 vs. −81.2 mm) than those during 1947–1989. Consequently, although negative precipitation anomalies remain the primary driver of droughts, the contribution of AED has increased markedly over time, making AED a substantial contributor to drought severity. This increasing contribution of AED reflects both the reduction in negative precipitation anomalies caused by increasing precipitation and the intensification of AED anomalies under warming. Since the 1990s, western Central Europe has warmed at 0.42 K per decade (ERA5), exceeding the global mean warming rate (e.g. Dong et al., 2017; Yin et al., 2024; Douville et al., 2025) and making the region particularly sensitive to AED (Huang et al., 2021; Wang et al., 2025). Recent droughts have therefore been increasingly amplified by warming, whereas earlier droughts were primarily associated with larger negative precipitation anomalies. This shift is illustrated by the 2010s, which no longer emerge as an exceptionally dry decade when AED is neglected. These findings therefore highlight the importance of systematically accounting for AED in drought monitoring, particularly from the 1990s onwards.

The relative influence of precipitation and AED differs when considering background hydroclimatic trends rather than individual drought events. At the annual scale, the opposing effects of precipitation and AED on the climatic water balance remain broadly balanced because both variables have increased by comparable magnitudes. Seasonally, however, contrasting responses emerge. The growing divergence between SPI-3 and SPEI-3 reflects the increasing contribution of AED but is not solely controlled by absolute AED trends. Because both indices are standardised, it also depends on the seasonal variability of the climatic water balance. Consequently, despite smaller absolute increases in AED than in summer, spring and autumn exhibit the largest increase in the relative contribution of AED over 1844–2008 (3-month AED increase: 14.5 and 13.8 mm in spring and autumn, respectively, compared with 19.5 mm in summer; SPI-3 − SPEI-3 divergence: 0.41 and 0.31, compared with 0.26 in summer). During the more recent periods, however, the much larger increase in AED made summer the season with the largest contribution of AED to SPEI-3 trends, whereas winter showed the smallest because of lower temperatures. Nevertheless, winter displays the largest proportional increase in AED (33% K^{-1} in ERA5), reflecting the strong energy limitation of winter evapotranspiration. Accordingly, winter and autumn became wetter because large precipitation increases exceeded those in AED, whereas summer and, during recent decades, spring experienced drying because large warming-driven increases in AED outweighed the more limited precipitation gains.

5.3 Atmospheric circulation and drought evolution

The four circulation patterns identified in this study represent distinct hydroclimatic environments over western Central Europe. The Baltic High and the European High are associated with the largest positive AED anomalies, whereas the British Isles High is characterised primarily by negative precipitation anomalies and the North–South Dipole by winter precipitation anomalies combined with negative AED anomalies. These differences reflect the associated flow. The Baltic High induces southeasterly circulation, transporting warm continental air (Serras et al., 2024) that enhances AED, explaining why droughts associated with this pattern are more frequently identified by SPEI-3 than SPI-3. Conversely, the British Isles High favours cooler northerly flow, in line with its association with EA− and the positive relationship between the EA pattern and temperature (Hernandez and Comas-Bru, 2025), resulting in near-zero AED anomalies. The large negative precipitation anomalies associated with this pattern may arise because moist air precipitates over the Scandinavian mountains, leaving western Central Europe in the rain shadow (Pauling et al., 2006). The North–South Dipole occurs predominantly during winter and is associated with SCA+ and NAO−, both linked with cold and dry winter conditions (Bladé et al., 2012; Simpson et al., 2024; Hernandez and Comas-Bru, 2025). This explains its negative AED anomalies, as easterly continental air masses are colder than maritime air masses during winter (Stahl and Demuth, 1999), and consequently why droughts associated with this pattern are generally the weakest. Consistent with the tendency for drought intensity in western Central Europe to increase closest to the largest positive Z500 anomalies (Kingston et al., 2015; Bakke et al., 2023), the European High combines strong negative precipitation anomalies with the largest positive AED anomalies. This agrees with previous studies linking persistent anticyclonic circulation to compound hot (Stefanon et al., 2012; Kautz et al., 2022) and dry (Lhotka et al., 2020; Savary et al., 2026) events through large-scale subsidence, reduced cloud cover and enhanced incoming shortwave radiation.

While the year-round precipitation trends (6–8% K^{-1}, Table S2) are broadly consistent with expected Clausius–Clapeyron thermodynamic scaling (~7% K^{-1}), the contrasting seasonal trends highlight the role of atmospheric circulation. The evolving association of droughts with these circulation patterns provides a coherent interpretation of the seasonal hydroclimatic evolution, particularly during winter and spring. Winter wetting, characterised by particularly large precipitation increases (12–18% K^{-1}), is consistent with the declining association of droughts with the North–South Dipole, the dominant circulation pattern for winter droughts. Because this pattern is closely linked with NAO−, the observed shift towards more positive winter NAO phases since the mid-twentieth century (Visbeck et al., 2001; Hasanean et al., 2023) provides a plausible explanation for the large increase in winter precipitation, in agreement with the established positive relationship between winter NAO and precipitation over the study area (Simpson et al., 2024). Conversely, spring precipitation increased only weakly over 1947–2023 (3.5% K^{-1}), well below the Clausius–Clapeyron scaling, whereas AED increased by more than twice as much. This evolution coincides with the increasing association of droughts with the European High, which predominantly characterises spring droughts. Persistent anticyclonic circulation and blocking have repeatedly been identified as the principal drivers of recent spring droughts in Central Europe (Trnka et al., 2009; Ionita et al., 2015; Lhotka et al., 2020; Bakke et al., 2023; Bešťáková et al., 2024), supporting the circulation changes identified here.

The increasing association of droughts with the European High suggests that compound hot and dry events may become increasingly characteristic feature of droughts in western Central Europe, in agreement with the growing influence of AED identified in this study. This does not imply, however, that circulation patterns primarily associated with negative precipitation anomalies, such as the British Isles High, will become less relevant under a warmer climate, as negative precipitation anomalies remain a necessary condition for drought development and similar circulation patterns have also been projected to become more frequent (Rousi et al., 2021; Tuel and Eltahir, 2021).

5.4 Strengths and limitations

An important strength of this study is the combined use of three independent century-scale reanalyses, each relying on different numerical models, data assimilation systems and assimilated observations. Cross-validation of multiple reanalyses has been recommended to strengthen confidence in analyses of historical climate variability and extreme events (Slivinski, 2018), while reanalyses provide a suitable framework for jointly analysing hydroclimatic variability and atmospheric circulation (Baatz et al., 2021). Evaluation against long weather station observations, together with the comparison over the common reference period, increases confidence in the drought indices. Despite differences between datasets, the principal conclusions regarding drought identification, hydroclimatic trends and atmospheric circulation are consistently reproduced. Remaining discrepancies mainly concern local and seasonal features, reflecting the greater uncertainty of historical precipitation fields and the coarser spatial resolution of reanalyses.

The use of long reanalysis records also highlights the importance of multidecadal variability when interpreting hydroclimatic trends. Sensitivity analyses (not shown) indicate that long-term trends are statistically more robust than trends estimated over recent decades, which are more strongly influenced by the phase of internal climate variability (Hänsel et al., 2019). Consequently, differences between reanalyses primarily reflect their differing temporal coverage rather than contradictory hydroclimatic behaviour. The common reference period provides a practical measure of agreement between datasets, although its relatively short duration is itself influenced by multidecadal variability and should therefore be interpreted with caution. Confidence is highest where datasets converge and lower where agreement across reanalyses or with station observations is limited, such as for the decrease in summer precipitation in ModE-RA and the long-term autumn wetting.

Using both SPI-3 and SPEI-3 additionally strengthens the interpretation by separating the respective roles of precipitation and AED (Lloyd-Hughes, 2014). This interpretation nevertheless depends on the estimation of AED. The temperature-based Thornthwaite formulation can overestimate warming-driven increases in AED (Seneviratne, 2012; Sheffield et al., 2012), consistent with the supplementary evaluation (Supplementary Material). However, these differences do not alter the conclusions regarding drought events, long-term trends, or atmospheric circulation. While Penman–Monteith is more physically based, its homogeneous application across the three reanalyses is precluded by the availability and differing estimation of the required meteorological variables (Córdova et al., 2015), and the additional long-term variables introduce their own uncertainties (Trenberth et al., 2014). More generally, the interpretation of long-term AED changes remains complicated by substantial land-use change and rising atmospheric CO_2 concentrations, which are not explicitly represented by either formulation (Villani et al., 2026). Thus, while AED estimation remains a source of uncertainty, its influence on the regional-scale conclusions appears limited, with the evaluation indicating greater uncertainty in long-term precipitation estimates than that arising from the choice of AED formulation.

The identified seasonal circulation patterns are physically meaningful and consistent with previous classifications of Central European drought weather types at daily timescales (e.g. Stahl and Demuth, 1999; Lhotka et al., 2020; Savary et al., 2026). The seasonal framework adopted here accounts for the pronounced seasonality of atmospheric circulation (Comas-Bru and Hernández, 2018), but splits prolonged droughts spanning multiple seasons into distinct events, particularly during the warm season when droughts are generally longer (Banfi et al., 2024). Seasonal mean circulation patterns may also mask important subseasonal variability. In addition, this approach does not directly quantify changes in the frequency or persistence of circulation patterns, although it successfully captures the recent spring drying, winter wetting, and the associated drought characteristics. However, the circulation patterns alone do not fully explain all aspects of the observed hydroclimatic evolution. In particular, the present framework does not explicitly resolve the respective roles of moisture transport, atmospheric convergence, cloud cover, radiative forcing, and land–atmosphere interactions in drought development. Summer drying and some local features indicate that additional processes may also be important. For example, summer drought evolution is likely influenced by land–atmosphere feedbacks (Seneviratne et al., 2006; Miralles et al., 2019; Suarez-Gutierrez et al., 2020), potentially reinforced by spring drying through soil–moisture preconditioning (Stegehuis et al., 2021; Douville et al., 2025), while the coastal wetting is likely enhanced by increasing North Sea SSTs (Lenderink et al., 2009; Philip et al., 2020). Quantifying the respective contributions of dynamical and thermodynamical processes, particularly during the warm season, remains an important avenue for future research.

6 Conclusion

This study presents ~~a diagnosis~~the evolution of meteorological droughts in western Central Europe and their associated atmospheric circulation from the mid-19th century to the present, using three complementary reanalysis datasets ~~and both~~ evaluated against long weather station observations. The combined analysis of SPI-3 and SPEI-3 ~~drought indices. By cross-validating reanalyses and rigorously evaluating their reliability against long~~provides a long-term ~~weather station records, robust temporal coverage and confidence in the~~ perspective on recent droughts while disentangling the respective roles of precipitation and AED, whereas the characterisation of seasonal atmospheric circulation patterns further places these hydroclimatic changes into a dynamical framework.

The results ~~are ensured. Major historical droughts—including 1921, 1947, 1953, 1959, and 1976—were consistently identified across datasets, although with differing intensities depending on whether SPI-3 or SPEI-3 was applied. The present analysis also confirms~~show that ~~while~~ recent droughts~~—such~~ are not unprecedented in terms of severity, with the 1921 drought emerging as ~~those in 2003 and 2018—are~~ the most severe~~, they are not without historical precedent; multi-year drought clusters and~~ event over 1844–2023 in western Central Europe. The analysis also reveals pronounced ~~wet/dry decades have occurred~~multidecadal variability, with successive dry periods (e.g. 1947–1960) repeatedly alternating with markedly wetter intervals (e.g. 1912–1920) over the last 180 years. Furthermore, while the 2010s represent the driest decade since the mid-nineteenth century when AED is considered, analyses based solely on precipitation no longer identify this decade as exceptional, demonstrating the increasing contribution of AED to drought severity under warming, particularly since the 1990s.

a mis en forme : Retrait : Première ligne : 0,75 cm

~~A key finding is the divergence between SPI-3 and SPEI-3 trends. SPI-3 (precipitation-only) indicates a long-term wetting trend driven by rising precipitation, while SPEI-3 (which incorporates AED) remains flat or shows recent drying, highlighting the increasing role of temperature-driven evaporative demand. This divergence has grown most rapidly since the 1990s, coinciding with accelerated regional warming. Seasonal analyses reveal distinct contrasts: summer dryness has intensified, particularly in the short-term SPEI-3, due to elevated AED, whereas winter dryness has markedly decreased due~~

~~to strong precipitation increases and limited AED influence. Spring and autumn generally mirror the year-round patterns, but since the mid-20th century spring SPEI-3 dryness has increased markedly, especially in northern and eastern parts of the region. This seasonal contrast reflects both a shift in atmospheric circulation and the amplifying effect of higher AED, especially during the warm season.~~

Although annual SPEI-3 exhibits no significant long-term trend, this apparent stability masks substantial hydroclimatic changes. Increasing precipitation has compensated for increasing AED at the annual scale, whereas contrasting seasonal responses have emerged. Winter and autumn became wetter as precipitation increases exceeded those in AED, while summer and, more recently, spring experienced drying because warming-driven increases in AED outweighed comparatively limited precipitation gains.

Through k-means clustering of Euro-Atlantic geopotential height anomalies, four ~~robust~~ atmospheric circulation patterns associated with droughts have been identified: the Baltic High, British Isles High, North–South Dipole, and European High. ~~The~~ Their distinct hydroclimatic signatures explain differences in drought intensity and the relative importance of precipitation and AED. The evolving association of droughts with these patterns also provides a coherent interpretation of the observed seasonal hydroclimatic trends, particularly the decline of winter droughts associated with the North–South Dipole and the emergence of spring droughts associated with the European High~~—characterized~~. This circulation pattern is characterised by strong anticyclonic anomalies over Central Europe and ~~elevated~~particularly large positive AED~~, as well as intense droughts, has~~ anomalies, suggesting that compound hot and dry events may become an increasingly ~~dominant since~~characteristic feature of droughts in western Central Europe.

Overall, these results demonstrate that drought evolution in western Central Europe reflects the ~~1990s and~~ interconnected influences of atmospheric circulation, precipitation, atmospheric evaporative demand, and multidecadal hydroclimatic variability. Considering these processes together is ~~closely tied to the~~therefore essential for placing recent ~~rise in spring dryness. This shift underscores the evolving interplay between dynamics and thermodynamics in drought generation~~droughts into a long-term perspective and for improving drought monitoring and future risk assessment in a warming climate.

a mis en forme : Police :Italique

~~Our approach—integrating long-term, cross-validated reanalyses, multiple drought metrics, and semi-objective circulation pattern analysis—provides a consistent framework for linking regional droughts to large-scale atmospheric drivers. The results emphasize that climate adaptation and drought risk management in western Central Europe must explicitly address the increasing spring and summer dryness, the growing role of AED, and the emergence of new circulation patterns that implies compound hot and dry events. Continued monitoring and improved modelling of both thermodynamics and dynamic processes will be essential for anticipating and mitigating drought impacts in this densely populated, ecologically and agriculturally vital region.~~

~~*Data*~~*Data and code* *availability.* The reanalyses datasets and the weather station data used in this study are all available online: ERA5 from the Copernicus Climate Change Service implemented by the ECMWF at https://cds.climate.copernicus.eu/; 20CRv3 from the NOAA PSL, Boulder, Colorado, USA, at https://psl.noaa.gov; ModE-RA from Valler et al. ~~(2023)~~(2023) at https://doi.org/10.26050/WDCC/ModE-RA_s14203-18501; Paris, De Bilt and Frankfurt am Main weather station data from the KNMI Climate Explorer at https://climexp.knmi.nl/; Uccle weather station data from the Royal Meteorological Institute of Belgium at https://opendata.meteo.be/. The code and the main diagnostics ~~computed~~ from ~~the~~this study will be ~~provided before~~made available upon publication~~:~~, including SPI-3 and SPEI-3 over western Central Europe ~~with~~for ERA5, 20CRv3, and ModE-RA~~;~~, as well as atmospheric circulation patterns associated with ~~droughts~~drought events for ~~ERA5, 20CRv3 and ModE-RA~~the same datasets.

a mis en forme : Espace Avant : 96 pt

Author contribution. EN: conceptualization; data curation; formal analysis; visualization, writing – original draft and editing. HG & MJ: conceptualization; supervision; writing – review and editing.

Competing interests. The authors declare that they have no conflict of interest.

Acknowledgements. Computational resources have been provided by the supercomputing facilities of the Université catholique de Louvain (CISM/UCL) and the Consortium des Équipements de Calcul Intensif en Fédération Wallonie Bruxelles (CÉCI) funded by the F.R.S.-FNRS under convention 2.5020.11 and by the Walloon Region. Specifically, the R software (R Core Team, 2021) ~~has been utilised for the data analysis and the ggplot2 R package (Wickham, 2011) has been used for the visualisation. GitHub Copilot assisted with coding, while DeepL Write~~was utilised for the data analysis. GitHub Copilot assisted with coding, while DeepL Write and OpenAI helped with rephrasing sentences. HG is a Research Director within the F.R.S.-FNRS (Belgium). The authors ~~area~~are grateful to Q. Dalaiden and A. Hoy for the constructive discussions.

References

~~Allen, C. D., Macalady, A. K., Chenchouni, H., Bachelet, D., McDowell, N., Vennetier, M., Kitzberger, T., Rigling, A., Breshears, D. D., Hogg, E. H. (Ted), Gonzalez, P., Fensham, R., Zhang, Z., Castro, J., Demidova, N., Lim, J.-H., Allard, G., Running, S. W., Semerci, A., and Cobb, N.: A global overview of drought and heat-induced tree mortality reveals emerging climate change risks for forests, For. Ecol. Manag., 259, 660–684, https://doi.org/10.1016/j.foreco.2009.09.001, 2010.~~

Aalbers, E. E., van Meijgaard, E., Lenderink, G., de Vries, H., and van den Hurk, B. J. J. M.: The 2018 west-central European drought projected in a warmer climate: how much drier can it get?, Nat. Hazards Earth Syst. Sci., 23, 1921–1946, https://doi.org/10.5194/nhess-23-1921-2023, 2023.

Baatz, R., Hendricks Franssen, H. J., Euskirchen, E., Sihi, D., Dietze, M., Ciavatta, S., Fennel, K., Beck, H., De Lannoy, G., Pauwels, V. R. N., Raiho, A., Montzka, C., Williams, M., Mishra, U., Poppe, C., Zacharias, S., Lausch, A., Samaniego, L., Van Looy, K., Bogena, H., Adamescu, M., Mirtl, M., Fox, A., Goergen, K., Naz, B. S., Zeng, Y., and Vereecken, H.: Reanalysis in Earth System Science: Toward Terrestrial Ecosystem Reanalysis, Rev. Geophys., 59, e2020RG000715, https://doi.org/10.1029/2020RG000715, 2021.

Bakke, S. J., Ionita, M., and Tallaksen, L. M.: The 2018 northern European hydrological drought and its drivers in a historical perspective, Hydrometeorology/Mathematical applications, https://doi.org/10.5194/hess-2020-239, 2020.

Bakke, S. J., ~~Wanders, N., van der Wiel, K~~Ionita, M., and Tallaksen, L. ~~M.: A data-driven model for Fennoscandian wildfire danger, Nat. Hazards Earth Syst.~~M.: Recent European drying and its link to prevailing large-scale atmospheric patterns, Sci~~., 23, 65–89~~ Rep, 13, 21921, https://doi.org/10.~~5194/nhess-23-65-2023~~1038/s41598-023-48861-4, 2023.

Banfi, F., Cammalleri, C., and Michele, C. D.: A joint spatio-temporal characterization of the major meteorological droughts in Europe, Environ. Res. Lett., 19, 094041, https://doi.org/10.1088/1748-9326/ad6ba9, 2024.

Barnston, A. G. and Livezey, R. E.: Classification, Seasonality and Persistence of Low-Frequency Atmospheric Circulation Patterns, Mon. Weather Rev., 115, 1083–1126, https://doi.org/10.1175/1520-0493(1987)115<1083%3C1083;CSAPOL>2%3E2.0.CO;2, 1987.

Baudewyn, M.: Détermination d'un indice de sécheresse atmosphérique des forêts en Belgique, M.S. thesis, Université de Liège, https://matheo.uliege.be/handle/2268.2/20828, 2023.

Bebchuk, T., Moir, A. K., Arosio, T., Kirdyanov, A. V., Torbenson, M. C. A., Krusic, P. J., Hindson, T. R., Howard, H., Buchwal, A., Norman, C. A. P., and Büntgen, U.: Taxus tree-ring chronologies from southern England reveal western European hydroclimate changes over the past three centuries, Clim. Dyn., 63, 108, https://doi.org/10.1007/s00382-025-07601-2, 2025.

Beck, H. E., Zimmermann, N. E., McVicar, T. R., Vergopolan, N., Berg, A., and Wood, E. F.: Present and future Köppen-Geiger climate classification maps at 1-km resolution, Sci. Data, 5, 180214, https://doi.org/10.1038/sdata.2018.214, 2018.

Beguería, S., Vicente-Serrano, S. M., Reig, F., and Latorre, B.: Standardized precipitation evapotranspiration index (SPEI) revisited: parameter fitting, evapotranspiration models, tools, datasets and drought monitoring, Int. J. Climatol., 34, 3001–3023, https://doi.org/10.1002/joc.3887, 2014.

Bell, B., Hersbach, H., Simmons, A., Berrisford, P., Dahlgren, P., Horányi, A., Muñoz-Sabater, J., Nicolas, J., Radu, R., Schepers, D., Soci, C., Villaume, S., Bidlot, J. R., Haimberger, L., Woollen, J., Buontempo, C., and Thépaut, J. N.: The ERA5 global reanalysis: Preliminary extension to 1950, Q. J. R. Meteorol. Soc., 147, 4186-4227, https://doi.org/10.1002/qj.4174, 2021.

Bertrand, C., Ingels, R., and Journée, M.: Homogenization and trends analysis of the Belgian historical precipitation time series, Int. J. Climatol., 41, 5277–5294, https://doi.org/10.1002/joc.7129, 2021.

Bešťáková, Z., Kyselý, J., Lhotka, O., Heilig, M., and Eitzinger, J.: Warm-Season Drying Across Europe and Its Links to Atmospheric Circulation, Earth Space Sci., 11, e2023EA003434, https://doi.org/10.1029/2023EA003434, 2024.

Bladé, I., Liebmann, B., Fortuny, D., and van Oldenborgh, G. J.: Observed and simulated impacts of the summer NAO in Europe: implications for projected drying in the Mediterranean region, Clim. Dyn., 39, 709–727, https://doi.org/10.1007/s00382-011-1195-x, 2012.

Blain, G. C.: The modified Mann-Kendall test: on the performance of three variance correction approaches, Bragantia, 72, 416–425, https://doi.org/10.1590/brag.2013.045, 2013.

Böhnisch, A., Mittermeier, M., Leduc, M., and Ludwig, R.: Hot Spots and Climate Trends of Meteorological Droughts in Europe–Assessing the Percent of Normal Index in a Single-Model Initial-Condition Large Ensemble, Front. Water, 3, https://doi.org/10.3389/frwa.2021.716621, 2021.

Bonacina, L. C. W.: The European Drought of 1921, Nature, 112, 488–489, https://doi.org/10.1038/112488b0, 1923.

Brajkovic, J., Fettweis, X., Noël, B., Vyver, H. V. D., Ghilain, N., Archambeau, P., Pirotton, M., and Doutreloup, S.: Increased intensity and frequency of extreme precipitation events in Belgium as simulated by the regional climate model MAR, J. Hydrol. Reg. Stud., 59, 102399, https://doi.org/10.1016/j.ejrh.2025.102399, 2025.

a mis en forme : Anglais (Royaume-Uni)

a mis en forme : Anglais (Royaume-Uni)

a mis en forme : Anglais (Royaume-Uni)

Brázdil, R., Demarée, G. R., Kiss, A., Dobrovolný, P., Chromá, K., Trnka, M., Dolák, L., Řezníčková, L., Zahradníček, P., Limanowka, D., and Jourdain, S.: The extreme drought of 1842 in Europe as described by both documentary data and instrumental measurements, Clim. Past, 15, 1861–1884, https://doi.org/10.5194/cp-15-1861-2019, 2019.

Briffa, K. R., Jones, P. D., and Hulme, M.: Summer moisture variability across Europe, 1892–1991: An analysis based on the palmer drought severity index, Int. J. Climatol., 14, 475–506, https://doi.org/10.1002/joc.3370140502, 1994.

Briffa, K. R., Van Der Schrier, G., and Jones, P. D.: Wet and dry summers in Europe since 1750: evidence of increasing drought, Int. J. Climatol., 29, 1894–1905, https://doi.org/10.1002/joc.1836, 2009.

Brisson, E., Demuzere, M., Kwakernaak, B., and Van Lipzig, N. P. M.: Relations between atmospheric circulation and precipitation in Belgium, Meteorol. Atmospheric Phys., 111, 27–39, https://doi.org/10.1007/s00703-010-0103-y, 2011.

Brönnimann, S.: Impact of El Niño–Southern Oscillation on European climate, Rev. Geophys., 45, https://doi.org/10.1029/2006RG000199, 2007.

Brönnimann, S., Franke, J., Valler, V., Hand, R., Samakinwa, E., Lundstad, E., Burgdorf, A.-M., Lipfert, L., Pfister, L., Imfeld, N., and Rohrer, M.: Past hydroclimate extremes in Europe driven by Atlantic jet stream and recurrent weather patterns, Nat. Geosci., 18, 246–253, https://doi.org/10.1038/s41561-025-01654-y, 2025.

Bruce, J. P.: Natural Disaster Reduction and Global Change, Bull. Am. Meteorol. Soc., 75, 1831–1836, https://doi.org/10.1175/1520-0477(1994)075<1831%3C1831:NDRAGC>2%3E2.0.CO;2, 1994.

Buras, A., Rammig, A., and Zang, C. S.: Quantifying impacts of the 2018 drought on European ecosystems in comparison to 2003, Biogeosciences, 17, 1655–1672, https://doi.org/10.5194/bg-17-1655-2020, 2020.

Cahynová, M. and Huth, R.: Changes of atmospheric circulation in central Europe and their influence on climatic trends in the Czech Republic, Theor. Appl. Climatol., 96, 57–68, https://doi.org/10.1007/s00704-008-0097-2, 2009.

Brunet, R.: Lignes de force de l'espace européen, https://doi.org/10.3406/mappe.2002.1759, 2002.

Cammalleri, C., Naumann, G., Mentaschi, L., Formetta, G., Forzieri, G., Gosling, S., Bisselink, B., De, R. A., and Feyen, L.: Global warming and drought impacts in the EU, https://doi.org/10.2760/597045, 2020.

Chen, L., Brun, P., Buri, P., Fatichi, S., Gessler, A., McCarthy, M. J., Pellicciotti, F., Stocker, B., and Karger, D. N.: Global increase in the occurrence and impact of multiyear droughts, Science, 387, 278–284, https://doi.org/10.1126/science.ado4245, 2025.

Chicco, D. and Jurman, G.: The advantages of the Matthews correlation coefficient (MCC) over F1 score and accuracy in binary classification evaluation, BMC Genomics, 21, 6, https://doi.org/10.1186/s12864-019-6413-7, 2020.

Choat, B., Jansen, S., Brodribb, T. J., Cochard, H., Delzon, S., Bhaskar, R., Bucci, S. J., Feild, T. S., Gleason, S. M., Hacke, U. G., Jacobsen, A. L., Lens, F., Maherali, H., Martínez-Vilalta, J., Mayr, S., Mencuccini, M., Mitchell, P. J., Nardini, A., Pittermann, J., Pratt, R. B., Sperry, J. S., Westoby, M., Wright, I. J., and Zanne, A. E.: Global convergence in the vulnerability of forests to drought, Nature, 491, 752–755, https://doi.org/10.1038/nature11688, 2012.

Christidis, N. and Stott, P. A.: Human Influence on Seasonal Precipitation in Europe, https://doi.org/10.1175/JCLI-D-21-0637.1, 2022.

a mis en forme : Français (Belgique)

a mis en forme : Français (Belgique)

a mis en forme : Français (Belgique)

Chung, C. and Nigam, S.: Weighting of geophysical data in Principal Component Analysis, J. Geophys. Res. ~~Atmospheres,~~Atmos., 104, 16925–16928, https://doi.org/10.1029/1999JD900234, 1999.

Comas-Bru, L. and Hernández, A.: Reconciling North Atlantic climate modes: revised monthly indices for the East Atlantic and the Scandinavian patterns beyond the 20th century, Earth Syst. Sci. Data, 10, 2329–2344, https://doi.org/10.5194/essd-10-2329-2018, 2018.

~~Corti, T., Muccione, V., Köllner-Heck, P., Bresch, D., and Seneviratne, S. I.: Simulating past droughts and associated building damages in France, Hydrol. Earth Syst. Sci., 13, 1739–1747, https://doi.org/10.5194/hess-13-1739-2009, 2009.~~

~~Coumou, D., Petoukhov, V., Rahmstorf, S., Petri, S., and Schellnhuber, H. J.: Quasi-resonant circulation regimes and hemispheric synchronization of extreme weather in boreal summer, Proc. Natl. Acad. Sci., 111, 12331–12336, https://doi.org/10.1073/pnas.1412797111, 2014.~~

~~Coumou, D., Lehmann, J., and Beckmann, J.: The weakening summer circulation in the Northern Hemisphere mid-latitudes, Science, 348, 324–327, https://doi.org/10.1126/science.1261768, 2015.~~

~~Coumou, D., Di Capua, G., Vavrus, S., Wang, L., and Wang, S.: The influence of Arctic amplification on mid-latitude summer circulation, Nat. Commun., 9, 2959, https://doi.org/10.1038/s41467-018-05256-8, 2018.~~

~~Delforge, D., Wathelet, V., Below, R., Sofia, C. L., Tonnelier, M., van Loenhout, J. A. F., and Speybroeck, N.: EM-DAT: the Emergency Events Database, Int. J. Disaster Risk Reduct., 124, 105509, https://doi.org/10.1016/j.ijdrr.2025.105509, 2025.~~

~~Dong, B. and Sutton, R. T.: Drivers and mechanisms contributing to excess warming in Europe during recent decades, Npj Clim. Atmospheric Sci., 8, 41, https://doi.org/10.1038/s41612-025-00930-3, 2025.~~

Córdova, M., Carrillo-Rojas, G., Crespo, P., Wilcox, B., and Célleri, R.: Evaluation of the Penman-Monteith (FAO 56 PM) Method for Calculating Reference Evapotranspiration Using Limited Data, Mt. Res. Dev., 35, 230–239, https://doi.org/10.1659/MRD-JOURNAL-D-14-0024.1, 2015.

DeJonge, K. E. and W. R., Allen, K., and et al.: Evapotranspiration Terminology and Definitions, J. Irrig. Drain. Eng., 151, 06025003, https://doi.org/10.1061/JIDEDH.IRENG-10491, 2025.

Dong, B., Sutton, R. T., and Shaffrey, L.: Understanding the rapid summer warming and changes in temperature extremes since the mid-1990s over Western Europe, Clim. Dyn., 48, 1537–1554, https://doi.org/10.1007/s00382-016-3158-8, 2017.

Douville, H., Roehrig, R., and Nabat, P.: Contribution of large-scale atmospheric circulation and anthropogenic aerosols to recent summer warming over western Europe, Clim. Dyn., 63, 208, https://doi.org/10.1007/s00382-025-07689-6, 2025.

~~Feyen, L. and Dankers, R.: Impact of global warming on streamflow drought in Europe, J. Geophys. Res. Atmospheres, 114, https://doi.org/10.1029/2008JD011438, 2009.~~

Fleig, A. K., Tallaksen, L. M., Hisdal, H., and Hannah, D. M.: Regional hydrological drought in north-western Europe: linking a new Regional Drought Area Index with weather types, Hydrol. Process., 25, 1163–1179, https://doi.org/10.1002/hyp.7644, 2011.

Folland, C. K., Knight, J., Linderholm, H. W., Fereday, D., Ineson, S., and Hurrell, J. W.: The Summer North Atlantic Oscillation: Past, Present, and Future, https://doi.org/10.1175/2008JCLI2459.1, 2009.

Freund, M. B., Helle, G., Balting, D. F., Ballis, N., Schleser, G. H., and Cubasch, U.: European tree-ring isotopes indicate unusual recent hydroclimate, Commun. Earth Environ., 4, 1–8, https://doi.org/10.1038/s43247-022-00648-7, 2023.

Gebrechorkos, S. H., Sheffield, J., Vicente-Serrano, S. M., Funk, C., Miralles, D. G., Peng, J., Dyer, E., Talib, J., Beck, H. E., Singer, M. B., and Dadson, S. J.: Warming accelerates global drought severity, Nature, 642, 628–635, https://doi.org/10.1038/s41586-025-09047-2, 2025.

Guha-Sapir, D., Hargitt, D., and Hoyois, P.: Thirty years of natural disasters 1974-2003: The numbers, Presses univ. de Louvain, ISBN: 2-930344-71-7, 2004.

~~Guillod, B. P., Orlowsky, B., Miralles, D. G., Teuling, A. J., and Seneviratne, S. I.: Reconciling spatial and temporal soil moisture effects on afternoon rainfall, Nat. Commun., 6, 6443, https://doi.org/10.1038/ncomms7443, 2015.~~

Hamed, K. H.: Trend detection in hydrologic data: The Mann–Kendall trend test under the scaling hypothesis, J. Hydrol., 349, 350–363, https://doi.org/10.1016/j.jhydrol.2007.11.009, 2008.

Hamed, K. H. and Ramachandra Rao, A.: A modified Mann-Kendall trend test for autocorrelated data, J. Hydrol., 204, 182–196, https://doi.org/10.1016/S0022-1694(97)00125-X, 1998.

Hanel, M., Rakovec, O., Markonis, Y., Máca, P., Samaniego, L., Kyselý, J., and Kumar, R.: Revisiting the recent European droughts from a long-term perspective, Sci. Rep., 8, 9499, https://doi.org/10.1038/s41598-018-27464-4, 2018.

Hänsel, S.: Changes in the Characteristics of Dry and Wet Periods in Europe (1851–2015), Atmosphere, 11, 1080, https://doi.org/10.3390/atmos11101080, 2020.

Hänsel, S., Petzold, S., and Matschullat, J.: Precipitation Trend Analysis for Central Eastern Germany 1851–2006, in: Bioclimatology and Natural Hazards, edited by: Střelcová, K., Mátyás, C., Kleidon, A., Lapin, M., Matejka, F., Blaženec, M., Škvarenina, J., and Holécy, J., Springer Netherlands, Dordrecht, 29–38, https://doi.org/10.1007/978-1-4020-8876-6_3, 2009.

Hänsel, S., Ustrnul, Z., Łupikasza, E., and Skalak, P.: Assessing seasonal drought variations and trends over Central Europe, Adv. Water Resour., 127, 53–75, https://doi.org/10.1016/j.advwatres.2019.03.005, 2019.

Hänsel, S., Hoy, A., Brendel, C., and Maugeri, M.: Record summers in Europe: Variations in drought and heavy precipitation during 1901–2018, Int. J. Climatol., 42, 6235–6257, https://doi.org/10.1002/joc.7587, 2022.

van Haren, R., van Oldenborgh, G. J., Lenderink, G., Collins, M., and Hazeleger, W.: SST and circulation trend biases cause an underestimation of European precipitation trends, Clim. Dyn., 40, 1–20, https://doi.org/10.1007/s00382-012-1401-5, 2013.

Hartigan, J. A. and Wong, M. A.: Algorithm AS 136: A K-Means Clustering Algorithm, J. R. Stat. Soc. Ser. C Appl. Stat., 28, 100–108, https://doi.org/10.2307/2346830, 1979.

Hasanean, H. M., Almaashi, A. K., and Abdulhaleem H. Labban: Variability in Global Climatic Circulation Indices and Its Relationship, Atmosphere, 14, 1741, https://doi.org/10.3390/atmos14121741, 2023.

Haslinger, K. and Mayer, K.: Early spring droughts in Central Europe: Indications for atmospheric and oceanic drivers, ~~Atmospheric~~Atmos. Sci. Lett., 24, e1136, https://doi.org/10.1002/asl.1136, 2023.

Haslinger, K., Hofstätter, M., Kroisleitner, C., Schöner, W., Laaha, G., Holawe, F., and Blöschl, G.: Disentangling Drivers of Meteorological Droughts in the European Greater Alpine Region During the Last Two Centuries, J. Geophys. Res. Atmospheres,Atmos., 124, 12404–12425, https://doi.org/10.1029/2018JD029527, 2019.

Helama, S., Meriläinen, J., and Tuomenvirta, H.: Multicentennial megadrought in northern Europe coincided with a global El Niño Southern Oscillation drought pattern during the Medieval Climate Anomaly, Geology, 37, 175–178, https://doi.org/10.1130/G25329A.1, 2009.

Hernandez, A. and Comas-Bru, L.: East Atlantic and Scandinavian patterns, in: Atmospheric Oscillations, Elsevier, 183–202, https://doi.org/10.1016/B978-0-443-15638-0.00009-5, 2025.

Herrera-Lormendez, P., John, A., Douville, H., and Matschullat, J.: Projected changes in synoptic circulations over Europe and their implications for summer precipitation: A CMIP6 perspective, Int. J. Climatol., 43, 3373–3390, https://doi.org/10.1002/joc.8033, 2023.

Hersbach, H., Bell, B., Berrisford, P., Hirahara, S., Horányi, A., Muñoz-Sabater, J., Nicolas, J., Peubey, C., Radu, R., Schepers, D., Simmons, A., Soci, C., Abdalla, S., Abellan, X., Balsamo, G., Bechtold, P., Biavati, G., Bidlot, J., Bonavita, M., De Chiara, G., Dahlgren, P., Dee, D., Diamantakis, M., Dragani, R., Flemming, J., Forbes, R., Fuentes, M., Geer, A., Haimberger, L., Healy, S., Hogan, R. J., Hólm, E., Janisková, M., Keeley, S., Laloyaux, P., Lopez, P., Lupu, C., Radnoti, G., de Rosnay, P., Rozum, I., Vamborg, F., Villaume, S., and Thépaut, J.-N.: The ERA5 global reanalysis, Q. J. R. Meteorol. Soc., 146, 1999–2049, https://doi.org/10.1002/qj.3803, 2020.

Hess, P. and Brezowsky, H.: Katalog der grosswetterlagen Europas, Deutscher Wetterdienst Offenbach am Main, Germany, 1969.

Hoffmann, P. and Spekat, A.: Identification of possible dynamical drivers for long-term changes in temperature and rainfall patterns over Europe, Theor. Appl. Climatol., 143, 177–191, https://doi.org/10.1007/s00704-020-03373-3, 2021.

Hoover, D. L. and Smith, W. K.: The growing threat of multiyear droughts, Science, 387, 246–247, https://doi.org/10.1126/science.adu7419, 2025.

Hurrell, J. W.: Decadal Trends in the North Atlantic Oscillation: Regional Temperatures and Precipitation, Science, 269, 676–679, https://doi.org/10.1126/science.269.5224.676, 1995.

Huang, Y., Weis, J., Vereecken, H., and Hendricks Franssen, H.-J.: Long-term trends in agricultural droughts over Netherlands and Germany: how extreme was the year 2018?, Hydrol. Earth Syst. Sci. Discuss., 1–27, https://doi.org/10.5194/hess-2021-569, 2021.

Hurrell, J. W. and Van Loon, H.: Decadal Variations in Climate Associated with the North Atlantic Oscillation, in: Climatic Change at High Elevation Sites, edited by: Diaz, H. F., Beniston, M., and Bradley, R. S., Springer Netherlands, Dordrecht, 69–94, https://doi.org/10.1007/978-94-015-8905-5_4, 1997.

Huth, R., Beck, C., Philipp, A., Demuzere, M., Ustrnul, Z., Cahynová, M., Kyselý, J., and Tveito, O. E.: Classifications of Atmospheric Circulation Patterns: Recent Advances and Applications, Ann. N. Y. Acad. Sci., 1146, 105–152, https://doi.org/10.1196/annals.1446.019, 2008.

Huth, R., Beck, C., and Kučerová, M.: Synoptic-climatological evaluation of the classifications of atmospheric circulation patterns over Europe, Int. J. Climatol., 36, 2710–2726, https://doi.org/10.1002/joc.4546, 2016.

Ionita, M. and Nagavciuc, V.: Changes in drought features at the European level over the last 120 years, Nat. Hazards Earth Syst. Sci., 21, 1685–1701, https://doi.org/10.5194/nhess-21-1685-2021, 2021.

Ionita, M., Boroneanţ, C., and Chelcea, S.: Seasonal modes of dryness and wetness variability over Europe and their connections with large scale atmospheric circulation and global sea surface temperature, Clim. Dyn., 45, 2803–2829, https://doi.org/10.1007/s00382-015-2508-2, 2015.

Ionita, M., Nagavciuc, V., Kumar, R., and Rakovec, O.: On the curious case of the recent decade, mid-spring precipitation deficit in central Europe, Npj Clim. ~~Atmospheric~~Atmos. Sci., 3, 49, https://doi.org/10.1038/s41612-020-00153-8, 2020.

Ionita, M., Dima, M., Nagavciuc, V., Scholz, P., and Lohmann, G.: Past megadroughts in central Europe were longer, more severe and less warm than modern droughts, Commun. Earth Environ., 2, 61, https://doi.org/10.1038/s43247-021-00130-w, 2021.

~~Ionita, M., Nagavciuc, V., Scholz, P., and Dima, M.: Long-term drought intensification over Europe driven by the weakening trend of the Atlantic Meridional Overturning Circulation, J. Hydrol. Reg. Stud., 42, 101176, https://doi.org/10.1016/j.ejrh.2022.101176, 2022.~~

IPCC: Annex III: Glossary [Planton, S.(Ed.)]. In: Climate Change 2013: The Physical Science Basis. Contribution of Working Group I to the Fifth Assessment Report of the Intergovernmental Panel on Climate Change [Stocker, TF, D. Qin, G.-K. Plattner, M. M. Tignor, S.K. Allen, J. Boschung, A. Nauels, Y. Xia, V. Bex and P.M. Midgley (eds.)]., ~~Camb. Univ. Press Camb. U. K. N. Y. NY~~Cambridge University Press., Cambridge, United Kingdom and New York, NY, USA, 2013.

~~Jacobeit, J., Wanner, H., Luterbacher, J., Beck, C., Philipp, A.,~~Katerji, N. and ~~Sturm, K.: Atmospheric circulation variability in~~Rana, G.: Crop Reference Evapotranspiration: A Discussion of the ~~North Atlantic-European area since~~Concept, Analysis of the ~~mid-seventeenth century, Clim. Dyn., 20, 341–352~~Process and Validation, Water Resour. Manag., 25, 1581–1600, https://doi.org/10.1007/~~s00382-002-0278-0, 2003~~s11269-010-9762-1, 2011.

Kautz, L.-A., Martius, O., Pfahl, S., Pinto, J. G., Ramos, A. M., Sousa, P. M., and Woollings, T.: Atmospheric blocking and weather extremes over the Euro-Atlantic sector – a review, Weather Clim. Dyn., 3, 305–336, https://doi.org/10.5194/wcd-3-305-2022, 2022.

Kendall, M. G.: Rank correlation methods, Griffin, Oxford, England, 1948.

Khaliq, M. N., Ouarda, T. B. M. J., Gachon, P., Sushama, L., and St-Hilaire, A.: Identification of hydrological trends in the presence of serial and cross correlations: A review of selected methods and their application to annual flow regimes of Canadian rivers, J. Hydrol., 368, 117–130, https://doi.org/10.1016/j.jhydrol.2009.01.035, 2009.

Kim, W. M., González-Rojí, S. J., and Raible, C. C.: Extratropical circulation associated with Mediterranean droughts during the Last Millennium in CMIP5 simulations, Clim. Past, 19, 2511–2533, https://doi.org/10.5194/cp-19-2511-2023, 2023.

Kingston, D. G., Stagge, J. H., Tallaksen, L. M., and Hannah, D. M.: European-Scale Drought: Understanding Connections between Atmospheric Circulation and Meteorological Drought Indices, https://doi.org/10.1175/JCLI-D-14-00001.1, 2015.

~~Kornhuber, K., Petoukhov, V., Petri, S., Rahmstorf, S., and Coumou, D.: Evidence for wave resonance as a key mechanism for generating high-amplitude quasi-stationary waves in boreal summer, Clim. Dyn., 49, 1961–1979, https://doi.org/10.1007/s00382-016-3399-6, 2017.~~

Kornhuber, K., Osprey, S., Coumou, D., Petri, S., Petoukhov, V., Rahmstorf, S., and Gray, L.: Extreme weather events in early summer 2018 connected by a recurrent hemispheric wave-7 pattern, Environ. Res. Lett., 14, 054002, https://doi.org/10.1088/1748-9326/ab13bf, 2019.

Kornhuber, K., Coumou, D., Vogel, E., Lesk, C., Donges, J. F., Lehmann, J., and Horton, R. M.: Amplified Rossby waves enhance risk of concurrent heatwaves in major breadbasket regions, Nat. Clim. Change, 10, 48–53, https://doi.org/10.1038/s41558-019-0637-z, 2020.

Lehner, F., Coats, S., Stocker, T. F., Pendergrass, A. G., Sanderson, B. M., Raible, C. C., and Smerdon, J. E.: Projected drought risk in 1.5°C and 2°C warmer climates, Geophys. Res. Lett., 44, 7419–7428, https://doi.org/10.1002/2017GL074117, 2017.

KNMI Climate Explorer: de Bilt: Koninklijk Nederlands Meteorologisch Instituut (KNMI), https://climexp.knmi.nl/start.cgi, 2022.

Lekarkar, K., Rakovec, O., Kumar, R., Dondeyne, S., and van Griensven, A.: SoilReconstructed soil moisture droughts in Belgium duringreveal 2011– 2020 werewas the worst in five decades, EGUsphere, 1–35driest decade since 1970, Hydrol. Earth Syst. Sci., 30, 2817–2835, https://doi.org/10.5194/egusphere-2025-4526, 2025hess-30-2817-2026, 2026.

Lenderink, G., van Meijgaard, E., and Selten, F.: Intense coastal rainfall in the Netherlands in response to high sea surface temperatures: analysis of the event of August 2006 from the perspective of a changing climate, Clim. Dyn., 32, 19–33, https://doi.org/10.1007/s00382-008-0366-x, 2009.

Lhotka, O., Trnka, M., Kyselý, J., Markonis, Y., Balek, J., and Možný, M.: Atmospheric Circulation as a Factor Contributing to Increasing Drought Severity in Central Europe, J. Geophys. Res. Atmospheres,Atmos., 125, e2019JD032269, https://doi.org/10.1029/2019JD032269, 2020.

Lloyd-Hughes, B.: The impracticality of a universal drought definition, Theor. Appl. Climatol., 117, 607–611, https://doi.org/10.1007/s00704-013-1025-7, 2014.

Lüttger, A. B. and Feike, T.: Development of heat and drought related extreme weather events and their effect on winter wheat yields in Germany, Theor. Appl. Climatol., 132, 15–29, https://doi.org/10.1007/s00704-017-2076-y, 2018.

Manise, T. and Vincke, C.: Impacts du climat et des déficits hydriques stationnels sur la croissance radiale du hêtre, du chêne, de l'épicéa et du douglas en Wallonie, For. Wallonne 123 48–57, 2014.

Mann, H. B.: Nonparametric Tests Against Trend, Econometrica, 13, 245–259, https://doi.org/10.2307/1907187, 1945.

Mann, M. E., Rahmstorf, S., Kornhuber, K., Steinman, B. A., Miller, S. K., and Coumou, D.: Influence of Anthropogenic Climate Change on Planetary Wave Resonance and Extreme Weather Events, Sci. Rep., 7, 45242, https://doi.org/10.1038/srep45242, 2017.

Manning, C., Widmann, M., Bevacqua, E., Van Loon, A. F., Maraun, D., and Vrac, M.: Increased probability of compound long-duration dry and hot events in Europe during summer (1950–2013), Environ. Res. Lett., 14, 094006, https://doi.org/10.1088/1748-9326/ab23bf, 2019.

Maslin, M., Ramnath, R. D., Welsh, G. I., and Sisodiya, S. M.: Understanding the health impacts of the climate crisis, Future Healthc. J., 12, 100240, https://doi.org/10.1016/j.fhj.2025.100240, 2025.

Matthews, B. W.: Comparison of the predicted and observed secondary structure of T4 phage lysozyme, Biochim. Biophys. Acta BBA - Protein Struct., 405, 442–451, https://doi.org/https://doi.org/10.1016/0005-2795(75)90109-9, 1975.

Matti, C., Pauling, A., Küttel, M., and Wanner, H.: Winter precipitation trends for two selected European regions over the last 500 years and their possible dynamical background, Theor. Appl. Climatol., 95, 9–26, https://doi.org/10.1007/s00704-007-0361-x, 2009.

McKee, T. B., Doesken, N. J., Kleist, J., and others: The relationship of drought frequency and duration to time scales, in: Proceedings of the 8th Conference on Applied Climatology, 179–183, 1993.

Miralles, D. G., Teuling, A.Mens, M. J. P., van Heerwaarden, C. C.,Rhee, G., Schasfoort, F., and Vilà-Guerau de Arellano, J.: Mega-heatwave temperatures dueKielen, N.: Integrated drought risk assessment to combined soil desiccation and atmospheric heat accumulationsupport adaptive policymaking in the Netherlands, Nat. Geosci., 7, 345–349Hazards Earth Syst. Sci., 22, 1763–1776, https://doi.org/10.1038/ngeo2141, 20145194/nhess-22-1763-2022, 2022.

Miralles, D. G., Gentine, P., Seneviratne, S. I., and Teuling, A. J.: Land–atmospheric feedbacks during droughts and heatwaves: state of the science and current challenges, Ann. N. Y. Acad. Sci., 1436, 19–35, https://doi.org/10.1111/nyas.13912, 2019.

Moberg, A. and Jones, P. D.: Trends in indices for extremes in daily temperature and precipitation in central and western Europe, 1901-99, Int. J. Climatol., 25, 1149–1171, https://doi.org/10.1002/joc.1163, 2005.

Mueller, B. and Seneviratne, S. I.: Hot days induced by precipitation deficits at the global scale, Proc. Natl. Acad. Sci., 109, 12398–12403, https://doi.org/10.1073/pnas.1204330109, 2012.

Muñoz-Sabater, J., Dutra, E., Agustí-Panareda, A., Albergel, C., Arduini, G., Balsamo, G., Boussetta, S., Choulga, M., Harrigan, S., Hersbach, H., Martens, B., Miralles, D. G., Piles, M., Rodríguez-Fernández, N. J., Zsoter, E., Buontempo, C., and Thépaut, J.-N.: ERA5-Land: a state-of-the-art global reanalysis dataset for land applications, Earth Syst. Sci. Data, 13, 4349–4383, https://doi.org/10.5194/essd-13-4349-2021, 2021.

Netherer, S., Panassiti, B., Pennerstorfer, J., and Matthews, B.: Acute Drought Is an Important Driver of Bark Beetle Infestation in Austrian Norway Spruce Stands, Front. For. Glob. Change, 2, https://doi.org/10.3389/ffgc.2019.00039, 2019.

van Mourik, J., Ruijsch, D., van der Wiel, K., Hazeleger, W., and Wanders, N.: Regional drivers and characteristics of multi-year droughts, Weather Clim. Extrem., 48, 100748, https://doi.org/10.1016/j.wace.2025.100748, 2025.

Obasi, G. O. P.: WMO's Rolerole in the International Decadeinternational decade for Natural Disaster Reductionnatural disaster reduction, Bull. Am. Meteorol. Soc., 75, 1655–1661, https://www.jstor.org/stable/26231968, 1994.

Oikonomou, P. D., Karavitis, C. A., Tsesmelis, D. E., Kolokytha, E., and Maia, R.: Drought Characteristics Assessment in Europe over the Past 50 Years, Water Resour. Manag., 34, 4757–4772, https://doi.org/10.1007/s11269-020-02688-0, 2020.

Patakamuri, S. K. and O'Brien, N.: modifiedmk: Modified Versions of Mann Kendall and Spearman's Rho Trend Tests, https://doi.org/10.32614/CRAN.package.modifiedmk, 2017.

Pauling, A., Luterbacher, J., Casty, C., and Wanner, H.: Five hundred years of gridded high-resolution precipitation reconstructions over Europe and the connection to large-scale circulation, Clim. Dyn.,., 26, 387–405, https://doi.org/10.1007/s00382-005-0090-8, 2006.

Penman, H. L.: Natural evaporation from open water, bare soil and grass, Proc. R. Soc. Lond. Math. Phys. Sci., 193, 120–145, https://doi.org/10.1098/rspa.1948.0037, 1948.

Pfister, L., Wilhelm, L., Brugnara, Y., Imfeld, N., and Brönnimann, S.: Weather type reconstruction using machine learning approaches, Weather Clim. Dyn., 6, 571–594, https://doi.org/10.5194/wcd-6-571-2025, 2025.

Philip, S. Y., Kew, S. F., van der Wiel, K., Wanders, N., and Jan van Oldenborgh, G.: Regional differentiation in climate change induced drought trends in the Netherlands, Environ. Res. Lett., 15, 094081, https://doi.org/10.1088/1748-9326/ab97ca, 2020.

Philipp, A., Della-Marta, P. M., Jacobeit, J., Fereday, D. R., Jones, P. D., Moberg, A., and Wanner, H.: Long-Term Variability of Daily North Atlantic–European Pressure Patterns since 1850 Classified by Simulated Annealing Clustering, https://doi.org/10.1175/JCLI4175.1, 2007.

R Core Team: R: A language and environment for statistical computing, R Found. Stat. Comput. Vienna Austria, 2021.

Raible, C. C., Bärenbold, O., and Gómez-navarro, J. J.: Drought indices revisited – improving and testing of drought indices in a simulation of the last two millennia for Europe, Tellus Dyn. Meteorol. Oceanogr., 69, 1287492, https://doi.org/10.1080/16000870.2017.1296226, 2017.

Raposo, V. D. M. B., Costa, V. A. F., and Rodrigues, A. F.: A review of recent developments on drought characterization, propagation, and influential factors, Sci. Total Environ., 898, 165550, https://doi.org/10.1016/j.scitotenv.2023.165550, 2023.

~~Rossi, L., Wens, M., De, M. H., Cotti, D., Sabino, S. A. S., Toreti, A., Maetens, W., Masante, D., Van, L. A., Hagenlocher, M., Rudari, R., Naumann, G., Meroni, M., Avanzi, F., Isabellon, M., and Barbosa, P.: European Drought Risk Atlas, https://doi.org/10.2760/608737, 2023.~~

~~Rouault, G., Candau, J.-N., Lieutier, F., Nageleisen, L.-M., Martin, J.-C., and Warzée, N.: Effects of drought and heat on forest insect populations in relation to the 2003 drought in Western Europe, Ann Sci, 63, 613-624, https://doi.org/10.1051/forest:2006044, 2006.~~

Rousi, E., Selten, F., Rahmstorf, S., and Coumou, D.: Changes in North Atlantic Atmospheric Circulation in a Warmer Climate Favor Winter Flooding and Summer Drought over Europe, J. Clim., 34, 2277–2295, https://doi.org/10.1175/JCLI-D-20-0311.1, 2021.

Ruijsch, D., van Mourik, J., Biemans, H., Hauswirth, S. M., and Wanders, N.: Thrive or Wither: Exploring the Impacts of Multiyear Droughts on Vegetation, J. Geophys. Res. Biogeosciences, 130, e2025JG008992, https://doi.org/10.1029/2025JG008992, 2025.

Savary, O., Ardilouze, C., and Cattiaux, J.: Linking European droughts to year-round weather regimes, ~~EGUsphere, 1–37~~Weather Clim. Dyn., 7, 223–245, https://doi.org/10.5194/~~egusphere-2025-3308, 2025~~wcd-7-223-2026, 2026.

~~Schoofs, J., Vandelanotte, K., Vyver, H. V. de, Sichel, L. V. D., Vandersteene, M., Serras, F., Lipzig, N. P. M. van, and Schaeybroeck, B. V.: Dynamic and thermodynamic contributions to future extreme-rainfall intensification: a case study for Belgium, https://doi.org/10.48550/arXiv.2502.02436, 4 February 2025.~~

van der Schrier, G., Briffa, K. R., Jones, P. D., and Osborn, T. J.: Summer Moisture Variability across Europe, J. Clim., 19, 2818–2834, https://doi.org/10.1175/JCLI3734.1, 2006.

van der Schrier, G., Allan, R. P., Ossó, A., Sousa, P. M., Van de Vyver, H., Van Schaeybroeck, B., Coscarelli, R., Pasqua, A. A., Petrucci, O., Curley, M., Mietus, M., Filipiak, J., Štěpánek, P., Zahradníček, P., Brázdil, R., Řezníčková, L., van den Besselaar, E. J. M., Trigo, R., and Aguilar, E.: The 1921 European drought: impacts, reconstruction and drivers, Clim. Past, 17, 2201–2221, https://doi.org/10.5194/cp-17-2201-2021, 2021.

~~Schumacher, D. L., Zachariah, M., Otto, F., Barnes, C., Philip, S., Kew, S., Vahlberg, M., Singh, R., Heinrich, D., Arrighi, J., van Aalst, M., Hauser, M., Hirschi, M., Bessenbacher, V., Gudmundsson, L., Beaudoing, H. K., Rodell, M., Li, S., Yang, W., Vecchi, G. A., Harrington, L. J., Lehner, F., Balsamo, G., and Seneviratne, S. I.: Detecting the human fingerprint in the summer 2022 western-central European soil drought, Earth Syst. Dyn., 15, 131–154, https://doi.org/10.5194/esd-15-131-2024, 2024.~~

Schwander, M., Rohrer, M., Brönnimann, S., and Malik, A.: Influence of solar variability on the occurrence of central European weather types from 1763 to 2009, Clim. Past, 13, 1199–1212, https://doi.org/10.5194/cp-13-1199-2017, 2017.

Sen, P. K.: Estimates of the Regression Coefficient Based on Kendall's Tau, J. Am. Stat. Assoc., 63, 1379–1389, https://doi.org/10.1080/01621459.1968.10480934, 1968.

Seneviratne, S. I.: Historical drought trends revisited, Nature, 491, 338–339, https://doi.org/10.1038/491338a, 2012.

Seneviratne, S. I., Lüthi, D., Litschi, M., and Schär, C.: Land–atmosphere coupling and climate change in Europe, Nature, 443, 205–209, https://doi.org/10.1038/nature05095, ~~2006a~~2006.

~~Seneviratne, S. I., Koster, R. D., Guo, Z., Dirmeyer, P. A., Kowalczyk, E., Lawrence, D., Liu, P., Mocko, D., Lu, C. H., Oleson, K. W., and Verseghy, D.: Soil Moisture Memory in AGCM Simulations: Analysis of Global Land–Atmosphere Coupling Experiment (GLACE) Data, J. Hydrometeorol., 7, 1090–1112, https://doi.org/10.1175/JHM533.1, 2006b.~~

~~Seneviratne, S. I., Corti, T., Davin, E. L., Hirschi, M., Jaeger, E. B., Lehner, I., Orlowsky, B., and Teuling, A. J.: Investigating soil moisture–climate interactions in a changing climate: A review, Earth-Sci. Rev., 99, 125–161, https://doi.org/10.1016/j.earscirev.2010.02.004, 2010.~~

~~Senf, C. and Seidl, R.: Persistent impacts of the 2018 drought on forest disturbance regimes in Europe, Biogeosciences, 18, 5223–5230, https://doi.org/10.5194/bg-18-5223-2021, 2021.~~

Serras, F., Vandelanotte, K., Borgers, R., Van Schaeybroeck, B~~. V.~~., Termonia, P., Demuzere, M., and van Lipzig, N. P. M~~. V.~~.: Optimizing climate model selection in regional studies using an adaptive weather type based framework: a case study for extreme heat in Belgium, Clim. Dyn., 62, 9927–9949, https://doi.org/10.~~21203/rs.3.rs-4216664/v1, 10 April~~1007/s00382-024-07432-7, 2024.

~~Shaman, J.: The Seasonal Effects of ENSO on European Precipitation: Observational Analysis, J. Clim., 27, 6423–6438, https://doi.org/10.1175/JCLI-D-14-00008.1, 2014.~~

Sheffield, J., Wood, E. F., and Roderick, M. L.: Little change in global drought over the past 60 years, Nature, 491, 435–438, https://doi.org/10.1038/nature11575, 2012.

Simpson, I., Hanna, E., Baker, L., Sun, Y., and Wei, H.-L.: North Atlantic atmospheric circulation indices: Links with summer and winter temperature and precipitation in north-west Europe, including persistence and variability, Int. J. Climatol., 44, 902–922, https://doi.org/10.1002/joc.8364, 2024.

Slivinski, L. C.: Historical Reanalysis: What, How, and Why?, J. Adv. Model. Earth Syst., 10, 1736–1739, https://doi.org/10.1029/2018MS001434, 2018.

Slivinski, L. C., Compo, G. P., Whitaker, J. S., Sardeshmukh, P. D., Giese, B. S., McColl, C., Allan, R., Yin, X., Vose, R., Titchner, H., Kennedy, J., Spencer, L. J., Ashcroft, L., Brönnimann, S., Brunet, M., Camuffo, D., Cornes, R., Cram, T. A., Crouthamel, R., Domínguez-Castro, F., Freeman, J. E., Gergis, J., Hawkins, E., Jones, P. D., Jourdain, S., Kaplan, A., Kubota, H., Blancq, F. L., Lee, T.-C., Lorrey, A., Luterbacher, J., Maugeri, M., Mock, C. J., Moore, G. W. K., Przybylak, R., Pudmenzky, C., Reason, C., Slonosky, V. C., Smith, C. A., Tinz, B., Trewin, B., Valente, M. A., Wang, X. L., Wilkinson, C., Wood, K., and Wyszyński, P.: Towards a more reliable historical reanalysis: Improvements for version 3 of the Twentieth Century Reanalysis system, Q. J. R. Meteorol. Soc., 145, 2876–2908, https://doi.org/10.1002/qj.3598, 2019.

Slivinski, L. C., Compo, G. P., Sardeshmukh, P. D., Whitaker, J. S., McColl, C., Allan, R. J., Brohan, P., Yin, X., Smith, C. A., Spencer, L. J., Vose, R. S., Rohrer, M., Conroy, R. P., Schuster, D. C., Kennedy, J. J., Ashcroft, L., Brönnimann, S., Brunet, M., Camuffo, D., Cornes, R., Cram, T. A., Domínguez-Castro, F., Freeman, J. E., Gergis, J., Hawkins, E., Jones, P. D., Kubota, H., Lee, T. C., Lorrey, A. M., Luterbacher, J., Mock, C. J., Przybylak, R. K., Pudmenzky, C., Slonosky, V. C., Tinz, B., Trewin, B., Wang, X. L., Wilkinson, C., Wood, K., and Wyszyński, P.: An Evaluation of the Performance of the Twentieth Century Reanalysis Version 3, https://doi.org/10.1175/JCLI-D-20-0505.1, 2021.

Soci, C., Hersbach, H., Simmons, A., Poli, P., Bell, B., Berrisford, P., Horányi, A., Muñoz-Sabater, J., Nicolas, J., Radu, R., Schepers, D., Villaume, S., Haimberger, L., Woollen, J., Buontempo, C., and Thépaut, J.-N.: The ERA5 global reanalysis from 1940 to 2022, Q. J. R. Meteorol. Soc., 150, 4014–4048, https://doi.org/10.1002/qj.4803, 2024.

Spinoni, J., Naumann, G., Carrao, H., Barbosa, P., and Vogt, J.: World drought frequency, duration, and severity for 1951–2010, Int. J. Climatol., 34, 2792–2804, https://doi.org/10.1002/joc.3875, 2014.

Spinoni, J., Naumann, G., Vogt, J., and Barbosa, P.: European drought climatologies and trends based on a multi-indicator approach, Glob. Planet. Change, 127, 50–57, https://doi.org/10.1016/j.gloplacha.2015.01.012, 2015.

Spinoni, J., Naumann, G., Vogt, J., and Barbosa, P.: Meteorological Droughts in Europe: Events and Impacts: Past Trends and Future Projections, https://doi.org/10.2788/79637, 2016.

Spinoni, J., Naumann, G., and Vogt, J. V.: Pan-European seasonal trends and recent changes of drought frequency and severity, Glob. Planet. Change, 148, 113–130, https://doi.org/10.1016/j.gloplacha.2016.11.013, 2017.

Spinoni, J., Vogt, J. V., Naumann, G., Barbosa, P., and Dosio, A.: Will drought events become more frequent and severe in Europe?, Int. J. Climatol., 38, 1718–1736, https://doi.org/10.1002/joc.5291, 2018.

Spinoni, J., Barbosa, P., De Jager, A., McCormick, N., Naumann, G., Vogt, J. V., Magni, D., Masante, D., and Mazzeschi, M.: A new global database of meteorological drought events from 1951 to 2016, J. Hydrol. Reg. Stud., 22, 100593, https://doi.org/10.1016/j.ejrh.2019.100593, 2019.

Stagge, J. H., Tallaksen, L. M., Gudmundsson, L., Van Loon, A. F., and Stahl, K.: Candidate Distributions for Climatological Drought Indices (SPI and SPEI), Int. J. Climatol., 35, 4027–4040, https://doi.org/10.1002/joc.4267, 2015.

Stahl, K. and Demuth, S.: Linking streamflow drought to the occurrence of atmospheric circulation patterns, Hydrol. Sci. J., 44, 467–482, https://doi.org/10.1080/02626669909492240, 1999.

Stahl, K., Kohn, I., Blauhut, V., Urquijo, J., De Stefano, L., Acácio, V., Dias, S., Stagge, J. H., Tallaksen, L. M., Kampragou, E., Van Loon, A. F., Barker, L. J., Melsen, L. A., Bifulco, C., Musolino, D., de Carli, A., Massarutto, A., Assimacopoulos, D., and Van Lanen, H. A. J.: Impacts of European drought events: insights from an international database of text-based reports, Nat. Hazards Earth Syst. Sci., 16, 801–819, https://doi.org/10.5194/nhess-16-801-2016, 2016.

Stefanon, M., D’Andrea, F., and Drobinski, P.: Heatwave classification over Europe and the Mediterranean region, Environ. Res. Lett., 7, 014023, https://doi.org/10.1088/1748-9326/7/1/014023, 2012.

Stegehuis, A. I., Vogel, M. M., Vautard, R., Ciais, P., Teuling, A. J., and Seneviratne, S. I.: Early Summer Soil Moisture Contribution to Western European Summer Warming, J. Geophys. Res. ~~Atmospheres,~~Atmos., 126, e2021JD034646, https://doi.org/10.1029/2021JD034646, 2021.

Suarez-Gutierrez, L., Müller, W. A., Li, C., and Marotzke, J.: Dynamical and thermodynamical drivers of variability in European summer heat extremes, Clim. Dyn., 54, 4351–4366, https://doi.org/10.1007/s00382-020-05233-2, 2020.

~~Sutanto, S. J., Vitolo, C., Di Napoli, C., D’Andrea, M., and Van Lanen, H. A. J.: Heatwaves, droughts, and fires: Exploring compound and cascading dry hazards at the pan-European scale, Environ. Int., 134, 105276, https://doi.org/10.1016/j.envint.2019.105276, 2020.~~

Svensson, C. and Hannaford, J.: Oceanic conditions associated with Euro-Atlantic high pressure and UK drought, Environ. Res. Commun., 1, 101001, https://doi.org/10.1088/2515-7620/ab42f7, 2019.

Tapia, C., Abajo, B., Feliu, E., Mendizabal, M., Martinez, J. A., Fernández, J. G., Laburu, T., and Lejarazu, A.: Profiling urban vulnerabilities to climate change: An indicator-based vulnerability assessment for European cities, Ecol. Indic., 78, 142–155, https://doi.org/10.1016/j.ecolind.2017.02.040, 2017.

~~Teuling, A. J.: A hot future for European droughts, Nat. Clim. Change, 8, 364–365, https://doi.org/10.1038/s41558-018-0154-5, 2018.~~

Thornthwaite, C. W.: An Approach toward a Rational Classification of Climate, Geogr. Rev., 38, 55–94, https://doi.org/10.2307/210739, 1948.

Tomas-Burguera, M., Vicente-Serrano, S. M., Peña-Angulo, D., Domínguez-Castro, F., Noguera, I., and El Kenawy, A.: Global Characterization of the Varying Responses of the Standardized Precipitation Evapotranspiration Index to Atmospheric Evaporative Demand, J. Geophys. Res. ~~Atmospheres,~~Atmos., 125, e2020JD033017, https://doi.org/10.1029/2020JD033017, 2020.

Topál, D., Herein, M., and Haszpra, T.: Northern Annular Mode, in: Atmospheric Oscillations, Elsevier, 203–219, https://doi.org/10.1016/B978-0-443-15638-0.00010-1, 2025.

~~Tractenberg, R. E., Yumoto, F., Jin, S., and Morris, J. C.: Sample size requirements for training to a kappa agreement criterion on Clinical Dementia Ratings, Alzheimer Dis. Assoc. Disord., 24, 264–268, https://doi.org/10.1097/WAD.0b013e3181d489e6, 2010.~~

Trenberth, K. E., Dai, A., van der Schrier, G., Jones, P. D., Barichivich, J., Briffa, K. R., and Sheffield, J.: Global warming and changes in drought, Nat. Clim. Change, 4, 17–22, https://doi.org/10.1038/nclimate2067, 2014.

Trnka, M., Kyselý, J., Možný, M., and Dubrovský, M.: Changes in Central-European soil-moisture availability and circulation patterns in 1881–2005, Int. J. Climatol., 29, 655–672, https://doi.org/10.1002/joc.1703, 2009.

~~Trouet, V. and Van Oldenborgh, G. J.: KNMI Climate Explorer: A Web-Based Research Tool for High-Resolution Paleoclimatology, Tree-Ring Res., 69, 3–13, https://doi.org/10.3959/1536-1098-69.1.3, 2013.~~

Tuel, A. and Eltahir, E. A. B.: Mechanisms of European Summer Drying under Climate Change, https://doi.org/10.1175/JCLI-D-20-0968.1, 2021.

Valler, V., Franke, J., Brugnara, Y., Burgdorf, A.-M., Lundstad, E., Hand, R., Samakinwa, E., Lipfert, L., Friedman, A. R., and Brönnimann, S.: ModE-RA - A global monthly paleo-reanalysis of the modern era (1421 to 2008): Set 1420-3_1850-1, https://doi.org/10.26050/WDCC/ModE-RA_s14203-18501, 2023.

Valler, V., Franke, J., Brugnara, Y., Samakinwa, E., Hand, R., Lundstad, E., Burgdorf, A.-M., Lipfert, L., Friedman, A. R., and Brönnimann, S.: ModE-RA: a global monthly paleo-reanalysis of the modern era 1421 to 2008, Sci. Data, 11, 36, https://doi.org/10.1038/s41597-023-02733-8, 2024.

Van Oldenborgh, G. J., Burgers, G., and Tank, A. K.: On the El Niño teleconnection to spring precipitation in Europe, Int. J. Climatol., 20, 565–574, https://doi.org/10.1002/(SICI)1097-0088(200004)20:5~~<565~~%3C565::AID-JOC488~~>3~~%3E3.0.CO;2-5, 2000.

~~Vautard, R., Cattiaux, J., Happé, T., Singh, J., Bonnet, R., Cassou, C., Coumou, D., D'Andrea, F., Faranda, D., Fischer, E., Ribes, A., Sippel, S., and Yiou, P.: Heat extremes in Western Europe increasing faster than simulated due to atmospheric circulation trends, Nat. Commun., 14, 6803, https://doi.org/10.1038/s41467-023-42143-3, 2023.~~

Vicente-Serrano, S. M. and López-Moreno, J. I.: Nonstationary influence of the North Atlantic Oscillation on European precipitation, J. Geophys. Res. ~~Atmospheres,~~Atmos., 113, https://doi.org/10.1029/2008JD010382, 2008.

Vicente-Serrano, S. M., Beguería, S., and López-Moreno, J. I.: A Multiscalar Drought Index Sensitive to Global Warming: The Standardized Precipitation Evapotranspiration Index, J. Clim., 23, 1696–1718, https://doi.org/10.1175/2009JCLI2909.1, 2010.

~~Vicente-Serrano, S. M., Beguería, S., Lorenzo-Lacruz, J., Camarero, J. J., López-Moreno, J. I., Azorin-Molina, C., Revuelto, J., Morán-Tejeda, E., and Sanchez-Lorenzo, A.: Performance of Drought Indices for Ecological, Agricultural, and Hydrological Applications, https://doi.org/10.1175/2012EI000434.1, 2012.~~

Vicente-Serrano, S. M., Domínguez-Castro, F., Murphy, C., Hannaford, J., Reig, F., Peña-Angulo, D., Tramblay, Y., Trigo, R. M., Mac Donald, N., Luna, M. Y., Mc Carthy, M., Van der Schrier, G., Turco, M., Camuffo, D., Noguera, I., García-Herrera, R., Becherini, F., Della Valle, A., Tomas-Burguera, M., and El Kenawy, A.: Long-term variability and trends in meteorological droughts in Western Europe (1851–2018), Int. J. Climatol., 41, https://doi.org/10.1002/joc.6719, 2021.

Vicente-Serrano, S. M., Peña-Angulo, D., Beguería, S., Domínguez-Castro, F., Tomás-Burguera, M., Noguera, I., Gimeno-Sotelo, L., and El Kenawy, A.: Global drought trends and future projections, Philos. Trans. R. Soc. Math. Phys. Eng. Sci., 380, 20210285, https://doi.org/10.1098/rsta.2021.0285, 2022.

~~Vicente-Serrano, S. M., Tramblay, Y., Reig, F., González-Hidalgo, J. C., Beguería, S., Brunetti, M., Kalin, K. C., Patalen, L., Kržič, A., Lionello, P., Lima, M. M., Trigo, R. M., El-Kenawy, A. M., Eddenjal, A., Türkes, M., Koutroulis, A., Manara, V., Maugeri, M., Badi, W., Mathbout, S., Bertalanič, R., Bocheva, L., Dabanli, I., Dumitrescu, A., Dubuisson, B., Sahabi-Abed, S., Abdulla, F., Fayad, A., Hodzic, S., Ivanov, M., Radevski, I., Peña-Angulo, D., Lorenzo-Lacruz, J., Domínguez-Castro, F., Gimeno-Sotelo, L., García-Herrera, R., Franquesa, M., Halifa-Marín, A., Adell-Michavila, M., Noguera, I., Barriopedro, D., Garrido-Perez, J. M., Azorin-Molina, C., Andres-Martin, M., Gimeno, L., Nieto, R., Llasat, M. C., Markonis, Y., Selmi, R., Ben Rached, S., Radovanović, S., Soubeyroux, J.-M., Ribes, A., Saidi, M. E., Bataineh, S., El Khalki, E. M., Robaa, S., Boucetta, A., Alsafadi, K., Mamassis, N., Mohammed, S., Fernández-Duque, B., Cheval, S., Moutia, S., Stevkov, A., Stevkova, S., Luna, M. Y., and Potopová, V.: High temporal variability not trend dominates Mediterranean precipitation, Nature, 639, 658–666, https://doi.org/10.1038/s41586-024-08576-6, 2025.~~

Villani, L., Piemontese, L., Castelli, G., Borgo, A., Ghilain, N., Van Schaeybroeck, B., Lucca, E., Aslam, M. F., Debolini, M., Bouizrou, I., Yimer, E. A., Baudewyn, M., Jaramillo, F., Trabucco, A., van Griensven, A., Penna, D., and Bresci, E.:

Neglecting plant physiology: systematic overestimation of drought projections, Environ. Res. Clim., https://doi.org/10.1088/2752-5295/ae583c, 2026.

Visbeck, M. H., Hurrell, J. W., Polvani, L., and Cullen, H. M.: The North Atlantic Oscillation: Past, present, and future, Proc. Natl. Acad. Sci. U. S. A., 98, 12876–12877, https://doi.org/10.1073/pnas.231391598, 2001.

Vogel, E., Donat, M. G., Alexander, L. V., Meinshausen, M., Ray, D. K., Karoly, D., Meinshausen, N., and Frieler, K.: The effects of climate extremes on global agricultural yields, Environ. Res. Lett., 14, 054010, https://doi.org/10.1088/1748-9326/ab154b, 2019.

~~de Vries, H., Lenderink, G., van der Wiel, K., and van Meijgaard, E.: Quantifying the role of the large-scale circulation on European summer precipitation change, Clim. Dyn., 59, 2871–2886, https://doi.org/10.1007/s00382-022-06250-z, 2022.~~

Wang, Y., Rammig, A., Blickensdörfer, L., Wang, Y., Zhu, X. X., and Buras, A.: Species-specific responses of canopy greenness to the extreme droughts of 2018 and 2022 for four abundant tree species in Germany, Sci. Total Environ., 958, 177938, https://doi.org/10.1016/j.scitotenv.2024.177938, 2025.

~~Webber, H., Lischeid, G., Sommer, M., Finger, R., Nendel, C., Gaiser, T., and Ewert, F.: No perfect storm for crop yield failure in Germany, Environ. Res. Lett., 15, 104012, https://doi.org/10.1088/1748-9326/aba2a4, 2020.~~

~~Wickham, H.: ggplot2, WIREs Comput. Stat., 3, 180–185, https://doi.org/10.1002/wics.147, 2011.~~

van der Wiel, K., Lenderink, G., and de Vries, H.: Physical storylines of future European drought events like 2018 based on ensemble climate modelling, Weather Clim. Extrem., 33, 100350, https://doi.org/10.1016/j.wace.2021.100350, 2021.

van der Wiel, K., Batelaan, T. J., and Wanders, N.: Large increases of multi-year droughts in north-western Europe in a warmer climate, Clim. Dyn., 60, 1781–1800, https://doi.org/10.1007/s00382-022-06373-3, 2023.

World Meteorological Organization: Standardized precipitation index: user guide (M. Svoboda, M. Hayes and D. Wood), WMO-No 1090 Geneva, 2012.

WorldPop: Global 1km Population, , https://doi.org/10.5258/SOTON/WP00647, 2018.

~~Yimer, E. A., De Trift, L., Lobkowicz, I., Villani, L., Nossent, J., and van Griensven, A.: The underexposed nature-based solutions: A critical state-of-art review on drought mitigation, J. Environ. Manage., 352, 119903, https://doi.org/10.1016/j.jenvman.2023.119903, 2024.~~

Xue, H., Goosse, H., Dalaiden, Q., Seftigen, K., Gennaretti, F., and Shi, F.: Scandinavian pattern and temperature changes shape European summer droughts over the past millennium, Nat. Commun., https://doi.org/10.1038/s41467-026-72385-w, 2026.

Yin, Z., Dong, B., Wei, W., and Yang, S.: Anthropogenic Impacts on Amplified Midlatitude European Summer Warming and Rapid Increase of Heatwaves in Recent Decades, Geophys. Res. Lett., 51, e2024GL108982, https://doi.org/10.1029/2024GL108982, 2024.

Zanaga, D., Van De Kerchove, R., Daems, D., De Keersmaecker, W., Brockmann, C., Kirches, G., Wevers, J., Cartus, O., Santoro, M., Fritz, S., and others: ESA WorldCover 10 m 2021 v200, https://doi.org/10.5281/zenodo.7254221, 2022.

Zscheischler, J. and Fischer, E. M.: The record-breaking compound hot and dry 2018 growing season in Germany, Weather Clim. Extrem., 29, 100270, https://doi.org/10.1016/j.wace.2020.100270, 2020.

Zscheischler, J., Martius, O., Westra, S., Bevacqua, E., Raymond, C., Horton, R. M., van den Hurk, B., AghaKouchak, A., Jézéquel, A., Mahecha, M. D., Maraun, D., Ramos, A. M., Ridder, N. N., Thiery, W., and Vignotto, E.: A typology of compound weather and climate events, Nat. Rev. Earth Environ., 1, 333–347, https://doi.org/10.1038/s43017-020-0060-z, 2020.